A STUDY OF THE SYNTHESIS AND CHARACTERISATION OF SOME RUTHENIUM BIS (2,2'-BIPYRIDYL) COMPLEXES.

By

Rachel Keirse, B.Sc. (Hon.)

A Thesis presented to Dublin City University for the Degree of Master of Science.

Supervisor Prof. J.G Vos,

School of Chemical Sciences,

Dublin City University.

July 2002

This work is dedicated to the memory of my mother, Miriam

REFERENCE

I declare that the work described within this thesis is all my own work

Rachel Keirse

Date 26/07/02

Acknowledgements

I would like to thank my supervisor Prof J G Vos, for his support and advice throughout this project

I'd especially like to thank the 'Lads' in the Vos research group and the other postgraduate students in the department

I would also like to thank all the technical staff in the school of chemical sciences, D C U for their help and patience

And last but not least my family and friends on the "outside" for all their help and friendship through the years

Abbreviations

2,2'-bipyridine (bpy)

3-(4-hydroxyphenyl)-5-(pyridin-2-yl)-1,2,4,triazole (4-phenol-ptr)

3-(1-hydroxyphenyl)-5-(pyridin-2-yl)-1,2,4,triazole (1-phenol-ptr)

3-(phenyl)-5-(pyridin-2-yl)-1,2,4,triazole (phenyl-ptr)

2 6 1 4,4'-dimethyl-2,2'-bipyridine (dmb)

2 6 2 4,4'-dicarboxylic acid-2,2'-bipyridine (dcbpy)

2 6 3 4,4'-diethoxycarbonyl-2,2'-bipyridine (decb)

2 6 4 3,5-bis(pyridin-2-yl)-4-amino-1,2,4-triazole (Hbpt)

2 6 5 $[Ru(dcbpy)_2(NCS)_2]\ 2H_2O$

2 6 6 $Ru(decb)_2Cl_2$

2 6 7 $Ru(dcbpy)_2Cl_2$

2 6 8 $[Ru(bpy)_2(dcbpy)][PF_6]_2$

2 6 9 $[Ru(bpy)_3][PF_6]_2$

2 6 10 $[Ru(bpy)_2(bpt)][PF_6]$

2 6 11 $[Ru(decb)_2(4\text{-phenol-ptr})][PF_6]$

2 6 12 $[Ru(decb)_2(1\text{-phenol-ptr})][PF_6]$

2 6 13 $[Ru(decb)_2(phenyl\text{-ptr})][PF_6]$

2 6 14 $[Ru(decb)_2(3\text{-Me-ptr})][PF_6]$

2 6 15 $[Ru(^2H_8\text{-bpy})_2(dcbpy)]$

2 6 16 $[Ru(decb)_2(bpt)][PF_6]$

2 6 17 $[Ru(decb)_2bptRu(bpy)_2](PF_6)_3$

2 6 18 $[Ru(dcbpy)_2(1\text{-phenol-ptr})]$ from $Ru(dcbpy)_2Cl_2$

2 6 19 $[Ru(dcbpy)_2(4\text{-phenol-ptr})]$ from $Ru(dcbpy)_2Cl_2$

2 6 20 $[Ru(dcbpy)_2(phenyl\text{-ptr})]$ from $Ru(dcbpy)_2Cl_2$

2 6 21 $[Ru(dcbpy)_2(4\text{-phenol-ptr})]$ from $[Ru(decb)_2(4\text{-phenol-ptr})]^+$

2 6 22 $[Ru(dcbpy)_2(1\text{-phenol-ptr})]$ from $[Ru(decb)_2(1\text{-phenol-ptr})]^+$

2 6 23 $[Ru(dcbpy)_2bptRu(bpy)_2][PF_6]_3$

Table of Contents

Page

1. Introduction

1.1 Introduction 2

1.2 Light Absorption 3

1.3 Reaction Centres 5

1.4 Water Splitting 7

1.5 Silicon Solar Cells 9

1.6 Absorption and emission properties of ruthenium(II) polypyridyl complexes... 12

1.7 Dye-Sensitised Solar Cells 16

1.7.1 The Cell 17

1.7.2 Nanocrystalline Semiconductors 18

1.7.3 The dye 19

1.7.4 Tuning the performance of the Cell 23

1.8 Scope of the thesis 23

1.9 References 25

2. Experimental Section

Ligands Cited in text 32

Physical measurements 33

2.1 Absorption and Emission Spectroscopy 33

2.2 Chromatographic Techniques 33

2.3 Nuclear Magnetic Resonance Spectroscopy (^{1}H-NMR) 34

2.4 Luminescent Lifetimes measurements 35

2 5 Elemental Analysis 35

2 6 Synthesis and Purification of Ruthenium Complexes and ligands 36

3 Results and Discussion

3 1 Introduction 52

3 2 Synthetic Approach 52

3 3 Analysis of products obtained 53

3 3 1 Column Chromatography 53

3 3 2 HPLC 59

3 4 ^{1}H-NMR 104

3 5 Electronic Properties 117

3 5 1 UV/vis Absorption Spectroscopy 117

3 5 2 Acid-base behaviour 120

3 6 Luminescence 134

3 7 Elemental Analysis 141

4 0 Concluding Remarks 142

4 1 References 144

Appendix I Laser Lifetime Results

Chapter 1

INTRODUCTION

1 1 Introduction

The sun is a sphere of intensely hot gaseous matter lying at an average distance of 1 5 X 10^8 km from the earth It's temperature ranges from approximately 6,000 K at the surface to > 10^6 K in the interior regions [1] The energy content of the sunlight striking the surface of the earth is enormous, almost 7 2 X 10^{20} kcal per year The incident intensity on a unit area of the earth's surface in full sunlight may rise to 8 0 J/cm^2/min i e 6 0 X 10^7 J/m^2/12h day, although on dull days it can fall to one third of this [2] At present consumption levels of primary energy in all forms this solar energy greatly exceeds all mans foreseeable energy requirements With increasing demands on the worlds current, mainly non-renewable, energy resources much attention has been drawn to the use of solar power as a non-polluting, renewable energy resource

The different areas involved in solar power utilisation include photovoltaic silicon crystal-based devices and more recently the study of artificial photosynthetic systems This thesis is mainly concerned with artificial photosynthesis which aims to design systems which are capable of light absorption over a wide spectral range (ultimately leading to efficient charge separation) with components which are capable of high efficiency of solar energy conversion into chemical energy This area of artificial photosynthesis involves the design and use of photochemical molecular devices (PMDs) which consist of assemblies of molecular components capable of performing light induced functions, such as vectorial electron transfer, migration of electronic energy, and switching on/off receptor ability

1 2 Light Absorption

The process of photosynthesis depends on the efficient capture of light quanta by aggregates of pigments forming an antennae system present in photosynthetic tissues An efficient photosynthetic transformation of light requires the absorption of as many photons as possible The antennae system consists of hundreds of pigment molecules (mainly chlorophyll or bacteriochlorophyll and carotenoids) that are anchored to proteins within the photosynthetic membrane and serve a specialised protein complex known as the reaction centre [3]

Higher plants contain two forms of chlorophyll, designated chlorophyll a (chl a) (Figure 1 1) and chlorophyll b (chl b) Chlorophylls contain conjugated tetrapyrole systems where the four central nitrogen atoms are co-ordinated with a Mg^{2+} ion to form an extremely stable essentially planar complex with a long hydrophobic side chain which show high absorptivity with molar extinction coefficients of about 10^5 M ^{1}cm ^{1} at both the long and the short wavelength ends of the visible spectrum [4, 5]

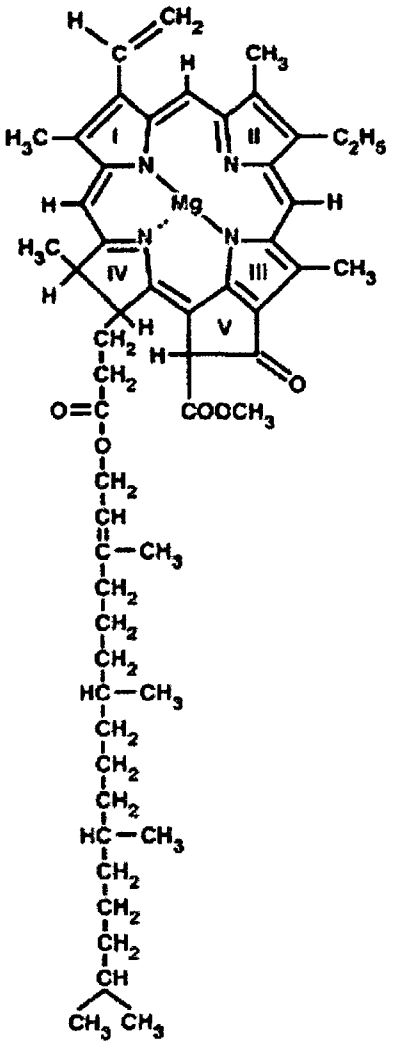

Chlorophyll *a*

Figure 1 1 [6]

In view of the rather low photon density in diffuse sunlight (rate of absorption is less than one photon per pigment molecule per second) and the necessarily rapid charge separation process it is more economical to use the major part (> 98 %) of the chlorophyll molecules to act as antennae devices to collect available photons ('light-harvesting') Chromophores are arranged in spatial proximity with a certain well-defined orientation to enable them to funnel the light energy to the actual reaction

centres with about 95 % efficiency within 10-100 ps. Only a few special forms of chla and bacteriochlorophyll (bchl) form reaction centres in higher plants and photosynthetic bacteria respectively. All other pigments are therefore accessory pigments, forming groups arranged to extend the size of the light-capturing unit, thus acting as antennae for capturing photons [7].

1.3 Reaction Centres

The reaction centres in photosynthesis convert the light energy collected by the antennae system into its chemical form. There are two reaction centres-photosystem I (PS I) and photosystem II (PS II). Photon capture by the antennae light harvesting system and excitation transfer to PS II and PS I provide the energy for oxidation of water and electron movement to acceptors which donate electrons to biochemical processes and for passage of protons into the thylakoid lumen for synthesis of adenosine triphosphate (ATP). In PS I, where oxygen evolution does not take place, oxidised nicotinamide adenine dinucleotide phosphate ($NADP^+$) is reduced to NADPH for use in a series of dark reactions called the Calvin Cycle, in which carbon dioxide is converted into useful fuels such as carbohydrates and sugars. PS II is only present in the thylakoid membrane of chloroplasts of green plants, in algae and in cyanobacteria [8]. Water is oxidised in the active site of PS II at a (probably) tetranuclear manganese cluster (Figure 1.2) [9]. Absorption of light quanta results in the excitation of electrons that are channelled to P680, the reaction centre of PS II. Excitation of the reaction centre P680 of PS II (a chlorophyll pigment with a λ_{max} at 680 nm) is defined as that part of oxygenic photosynthesis catalysing photoinduced

electron transfer of protons from the stromal to the lumen side of the thylakoid membrane [10]

$$2H_2O + 2PQ + 4H \xrightarrow[[Mn]_x]{4h\nu} O_2 + 2PQH_2 + 4H^+$$

PQ = Plastoquinone, PQH_2 = Plastohydroquinone

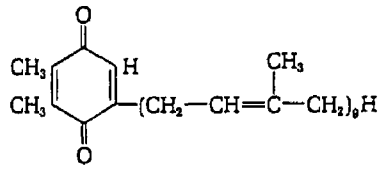

Figure 1 2

Plastoquinone A, which is the most abundant plastoquinone in plants and algae Other plastoquinones differ in the length of the side chain and the nature of the substituents in the quinone ring [5]

From elemental analysis it appears that four manganese centres make up the active site in PS II with Ca^{2+} and Cl^- ions also essential for activity [11] From Joliets observation that O_2 evolution occurs periodically from dark-adapted chloroplasts after irradiation with 4 light flashes [12], Kok has identified five oxidation states in the manganese containing centre of PS II, S_0 - S_4 [13] In each case the absorption of one quantum of light raises the oxidation level by one unit (releasing one electron each time) and drives the system from S_0 to S_4 In the regenerative step S_4 to S_0, O_2 is finally evolved (Figures 1 3 and 1 4)

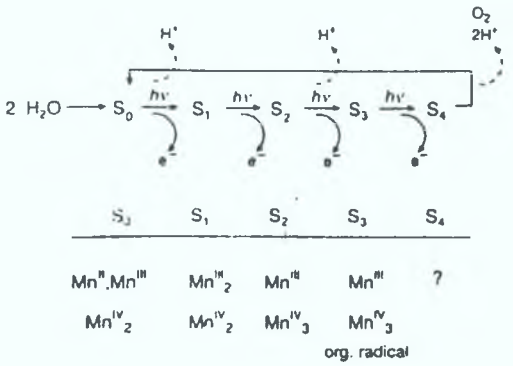

Figure 1.3

Representation of Kok's catalytic cycle. The scheme given at the bottom shows the most likely (according to present information) distribution of the oxidation steps in the tetranuclear manganese cluster in the S_0 to S_4 states of PS II [13].

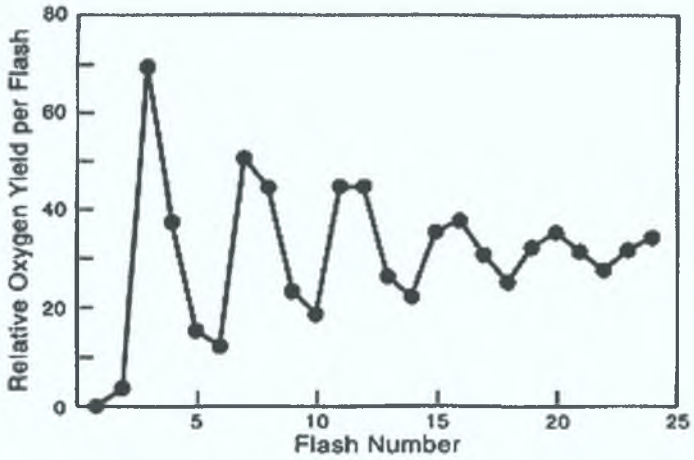

Figure 1.4

Oxygen evolution on illumination of dark-adapted chloroplasts [6].

1.4 Water Splitting:

A main goal in the development of PMDs and in artificial photosynthesis in general is the use of solar photons to split H_2O into hydrogen and oxygen, thereby converting solar energy into electrical energy and providing an energy rich clean fuel source (H_2) from an abundant resource (light and H_2O).

The water splitting reaction as

$$H_2O \xrightarrow{\text{sunlight}} H_2\,(g,\ 1\ atm) + \tfrac{1}{2}O_2\,(g,\ 1\ atm)$$

has a free energy change of $\Delta G^\circ = 237.2$ kJ/mol or 2.46 eV/molecule H_2O. Since two electrons are involved in the reaction this corresponds to 1.23 eV/e which is also the standard emf for the reaction [14]. The photons in the solar spectrum provide sufficient energy to drive this reaction, but the efficiency of the reaction depends upon how the reaction is carried out. It is possible to cause water splitting thermally with light via concentrators and a solar furnace by heating water to 1500-2500 K. However, the efficiency of this process is typically below 2 %, which does not deem it as a viable process for energy conversion [15, 16].

The solar spectrum at sea level extends from the near infrared through to the visible to the near ultraviolet with photon energies up to 3.0 eV [15]. Since water itself does not absorb appreciable radiation within the solar spectrum, one or more light absorbing species (photoconverters or sensitisers) must be used to transduce the radiant energy to chemical or electrical energy in the form of electrons/hole pairs, i.e. to the oxidising and reducing potential needed to drive the reaction.

1 5 Silicon Solar Cells

The major emphasis in industry is to produce solar cells of reasonable performance, with a life expectancy in excess of 20 years, at the lowest possible cost per unit of electrical energy generating capability The conversion of solar radiation into electricity by means of the photovoltaic cell is at present the most sophisticated technical development in solar energy devices The silicon solar cell is still the most efficient and reliable of photovoltaic cells Silicon cells are made from silicon doped with phosphorus (n-type, i e an electron conductor) and silicon doped with boron (p-type, i e a hole conductor), creating a pn junction

Silicon absorbs light throughout the visible region into the infrared and, when it is irradiated, electrons are released from a localised situation, such as a covalent bond (the valence band) into a delocalised situation (the conduction band) The energy needed to separate the electron from the nuclei and create a free conduction electron is known as the bandgap energy (or threshold energy) Eg and in the case of silicon is 1 12 eV This energy gap Eg is the most important physical characteristic of a candidate solar cell semiconductor, since it determines to what fraction of the solar spectrum the semiconductor can respond Therefore the maximum efficiency of a photochemical cell depends upon the band gap of the photoconverter Radiation of energy below Eg is not absorbed while that above Eg is partly lost as heat conversion or intraband thermalisation processes Additional thermodynamic losses occur because the excited state concentration is only a fraction of that of the ground state and because some excited states are lost through radiative decay [17]

The conversion efficiency of a solar cell is the ratio of its output electrical power to the input light power The highest efficiencies are expected from solar cells made from

materials with an Eg value between 1 2 and 1 6 eV (Figure 1 5) The most common solar cells, silicon pn-junction cells have efficiencies ranging between 12 and 17 %

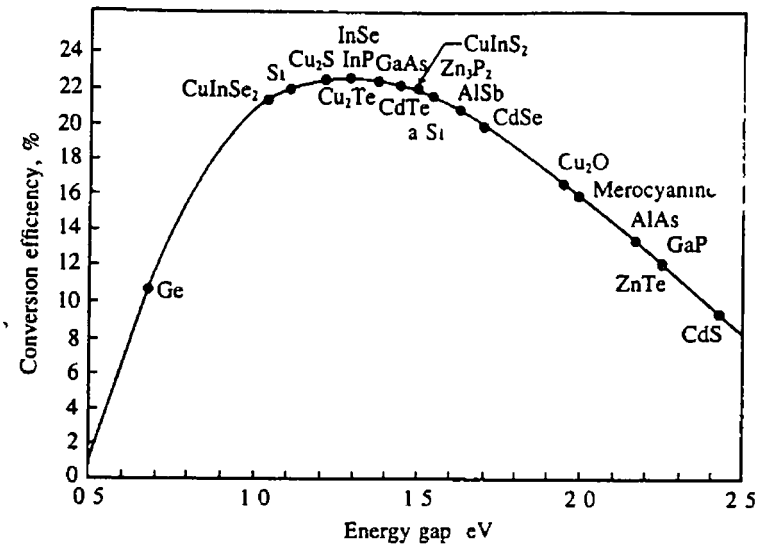

Figure 1 5

Maximum theoretical con version efficiency vs Energy gap for solar cells in AM1 sunlight Crystalline silicon is denoted Si, and amorphous silicon is a-Si [18]

To avoid the premature recombination of electrons and "holes", a semiconductor must be highly pure and defect free The fabrication of this type of cell still presents numerous difficulties, preventing the use of such devices for electricity production on an industrial scale

For present commercial technology, single-crystal and multicrystalline silicon substrates are primarily used and have dominated the market for more than a decade Future developments in the area of solar cell research will no doubt involve the use of thin film technologies that provide an alternative to using high cost high purity silicon wafers In thin film technology, a foreign substrate is used onto which crystalline

silicon material is deposited/grown with a fairly thick layer (in excess of 100 microns) presently required to give adequate quality material in the surface regions in order to achieve reasonable device performance [19] One difficulty in the development of thin films is silicon's weak light absorption, which implies that silicon has to be thick to absorb a reasonable fraction of sunlight, as is the case in developed silicon cell systems However developments in 'light trapping' (confining the light to within regions where all the silicon is active) has changed the dependence Recent demonstrations of 21 5 % efficiency for a thin crystalline silicon solar cell of thickness less than 50 μm, although not using practical processes, demonstrated the ability to achieve high performance through the use of light trapping [20] High efficiencies in a commercially viable thin-film crystalline silicon cell can only be achieved through a design that facilitates near-unity internal quantum efficiencies for all wavelengths of light, which by necessity requires well-passivated surfaces and metal contacts in conjunction with diffusion lengths that are substantially greater than the device dimensions These qualities can only be achieved through the use of a rear reflector or equivalent to ensure that light does not pass out of the active cell volume into inactive regions m the material Additionally light returning within the silicon to the front surface must be prevented from escaping through the use of an appropriate light-trapping scheme [20]

Recent developments in thin film technology have used a laser technique, which allows for the reliable creation of islands of crystalline silicon in a thin amorphous silicon film The laser light causes crystallisation in amorphous films by breaking the bonds in the amorphous material and allowing the atoms to rearrange themselves into a crystalline form The technique developed by Im and co-workers allows for reliable reproducible crystalline silicon growth with sizes of up to 100 μm^2 [21]

1 6 Absorption and Emission Properties of ruthenium(II) polypyridyl complexes

The absorption spectra of ruthenium polypyridyl complexes are dominated by a metal to ligand charge transfer (MLCT) band in the visible region [22] that is largely singlet in character (^{1}MLCT) This means that absorption of a photon promotes an electron from a t_{2g} orbital on the Ru(II) ion to an antibonding π^* orbital on the ligand system [23] An example of a typical energy diagram showing the relevant energy levels for a ruthenium polypyridyl compound is given in Figure 1 6

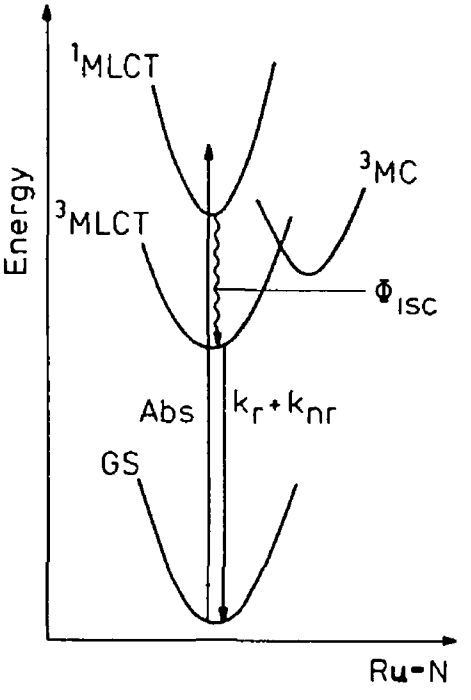

Figure 1 6

Photophysical processes of $[Ru(bpy)_3]^{2+}$ [24]

Intersystem crossing, estimated to occur with a rate of 5 X 10^{-10} s ^{1}, from the ^{1}MLCT to the ^{3}MLCT state then occurs with an efficiency close to one [25] Emission from the triplet state to the ground state (k_r) or radiationless deactivation to the ground state (k_{nr}) can take place [24] However in d^6 transition metal complexes MLCT (and LC)

excited states, being relatively undistorted in comparision to the ground state geometry, undergo slow radiationless decay processes so that they can give rise to luminescence and can be involved in bimolecular reactions [25] Another deactivating pathway is population of the metal centred $3e_g^*$ (^{3}MC) excited state [26] This state is strongly distorted with respect to the ground state nuclear geometry, and upon population, reduces the emission quantum yield by causing rapid radiationless decay, or more destructively, cleavage of a Ru-N bond, leading to photosubstitution (ligand dissociation) [27] Radiationless decay from the ^{3}MC state is rapid despite its triplet character since these are metal centred orbitals and are therefore strongly influenced by spin-orbit coupling [28]

Other electronic transitions occuring in ruthenium polypyridyl complexes include ligand centred transitions from the π-bonding orbital to the π*-antibonding orbital of the ligand These occur at high energies (e g 185 and 285 nm for $[Ru(bpy)_3]^{2+}$) and have high extinction coefficients Promotion of an electron from a metal t_{2g} orbital to an e_g orbital are also possible and these d-d or metal centred transitions give rise to weak absorption bands (322 and 344 nm for $[Ru(bpy)_3)]^{2+}$ [29]

From the electronic transitions of the Ru(II) polypyridyl systems it is clear that the luminescent properties of a complex are related to the energy and the orbital nature of the lowest excited state The energy positions of the MC, MLCT, and LC excited states depend on the ligand field strength, the redox properties of the metal and the ligands and intrinsic properties of the ligands, among other things Therefore the ability to determine the orbital nature of the lowest excited state and thus the design of stable, useful photoactive compounds can be controlled by a judicious choice of ligands

To avoid ligand photodissociation the population of the ^{3}MC state should be prevented [30] The energy of the MC excited states depends on the ligand field strength, which in turn depends on the σ-donor and π-acceptor properties of the ligands, the steric crowding around the metal (that can preclude a sufficiently close approach between metal and ligand), and the bite angle of the polydentate ligands Population of the ^{3}MC state can be prevented/reduced by increasing the energy gap between the ^{3}MLCT and ^{3}MC states, working at low temperatures, addition of sufficient quencher to capture ^{3}MLCT energy before surface crossing to ^{3}MC can occur, among other things The energy of the MLCT excited state depends on the reduction potential of the ligand involved in the MLCT transition, the oxidation potential of the metal in the complex (which is affected by the electron donor and acceptor properties of all the ligands), and by the charge separation caused by the transition Large changes in the excited state energy can be obtained on changing the ligand involved in the MLCT There are a number of parameters to consider in the choice of ligand such as, as mentioned earlier, the reduction potential of the free ligand, the σ-donor ability of the ligand (which is related to the pK_a of the free ligand), π-donor and acceptor properties of the ligand, the charge separation in the excited state (since the coulombic interaction between the hole on the metal and the electron on the ligand decreases with increasing separation distance) and solvent parameters which govern the complex-solvent interaction Preparation of complexes having one bpy with a low energy π* level and more basic bipyridines filling the remaining coordination sites may result in ruthenium polypyridine complexes having ^{3}MC states which are thermally inaccessible from the ^{3}MLCT state Substitution on the ligand aromatic rings offers the opportunity to carry out a fine-tuning of the excited state [31, 32, 33, 34]

Ligands based on the pyridyl triazole systems have strong σ-donor and weak π-acceptor capacities which means that the empty π* orbitals are at a higher energy than the bpy or substituted bpy π* orbitals [35] The strong σ-donor capacities of the ptr based ligand results in larger ligand field splitting making photodecomposition and low emission yields, through population of the ^{3}MC state, unlikely The disadvantage of these ligands is their high level π* orbitals which result in a higher energy being required for the metal to ligand π* charge transfer transition to take place This means that both the absorption and emission spectra will be blue-shifted to higher energies, which means that a smaller amount of the solar spectrum can be absorbed by the complexes [36, 37, 38, 39, 40]

Using ligands which are good π-acceptors such as bpy and bpy substituted analogues results in lower energy electron transfer transitions which allows for absorption well into the red and therefore the harvesting of more of the solar spectrum [41] The disadvantage of good π-acceptor ligands is that they are consequently poor σ-donors and have a small ligand field splitting of the Ru (II) orbitals and after an electron transfer to the excited state, population of the ^{3}MC state can take place with loss of emission yields and possible photodecomposition [42, 43, 44] Using mixed ligand complexes is a solution to the problems listed above as the lowest excited state is still bpy based but the ligand splitting is relatively large with the influence of the ptr-based σ-donor [40, 45]

In this thesis ruthenium complexes which incorporate both good π-acceptor ligands such as dicarboxy- (dcbpy) and diethylester- (decb) substituted bpys [46] which act as chromophore ligands and good σ-donor ligands such as pyridyl-triazole (ptr) based

ligands which act as spectator ligands will be synthesised and their absorption and emission properties along with their acid-base behaviour will be studied

Studies have shown that red shifts in the low energy absorption features of Ru complexes containing both dcbpy and bpy ligands have been observed on protonation of the complexes indicating that the lowest excited state is on the dcbpy ligand [47, 48, 49, 50] Red shifts in the emission spectra and a shortening of the lifetimes also confirms that the d - π^* transition leads to an increase in electron density on the protonation site i e on the dcbpy [51] Ruthenium complexes containing both decb and bpy ligands also show low energy MLCT transitions where the transferred electron resides on the decb ligand [46] From electrochemistry studies it has been shown that the first redox electron is placed into a π^* orbital localised on the ester ring [52] further confirming that in mixed decb / bpy complexes the lowest unoccupied molecular orbit (LUMO) is located on the decb ligand [53] The acid-base properties of the ptr-based ligands were examined in the complexes along with the acid-base properties of the diacid moieties and the base hydrolysis of the diester groups [54]

1 7 Dye-Sensitised Solar Cells

Water splitting using semi-conductor TiO_2 electrodes can be accomplished but with an additional electrical bias However the problem with TiO_2 is that the conduction band is too low (i e at an insufficiently negative potential) to generate hydrogen at a useful rate In addition to this because the TiO_2 band gap is large (3 0 eV for Rutile), only a fraction of the solar light is absorbed and the efficiency of the TiO_2-based cells can never attain the specified 10 % level [13, 55] To overcome the problems of large band gaps and inefficient use of the solar spectrum, sensitisers can be adsorbed onto

the surface of the electrode or particle In these devices, unlike the silicon solar cell, the processes of light absorption and charge separation are differentiated Due to their simple construction, the cells offer the hope of a significant reduction in the cost of solar electricity Recent advances in dye-sensitised cells have used porous TiO_2 electrodes with a very large substrate area [56]

1 7 1 The Cell

Light absorption is performed by a monolayer of dye (the sensitiser, S), which is adsorbed chemically at the semiconductor surface After having being excited by a photon of light (S*), the dye, usually a transition metal complex whose molecular properties are specifically designed for the task, is able to transfer an electron to the semiconductor (e g TiO_2) (the process of 'injection') The electric field inside the bulk material allows extraction of the electron Positive charge is transferred from the dye (S+) to a redox mediator present in the solution ("interception") with which the cell is filled, and thence to the counter electrode Via this last electron transfer, in which the mediator is returned to its reduced state, the circuit is closed The theoretical maximum voltage that such a device could deliver corresponds to the difference between the redox potential of the mediator and the Fermi level of the semiconductor (Figure 1 7) [57, 58]

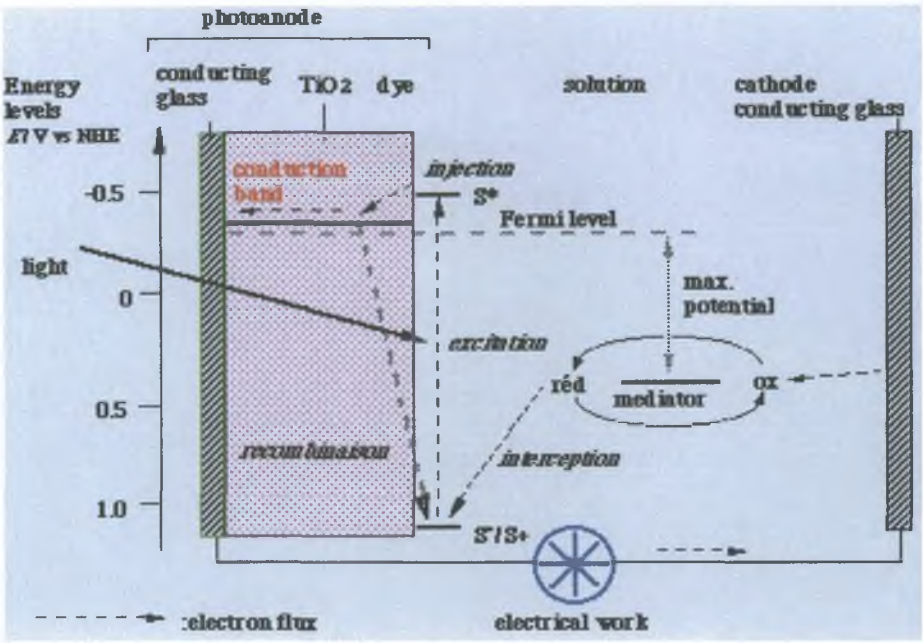

Figure 1.7

Energy scheme for the sensitised nanocrystalline solar cell [59].

1.7.2 'Nanocrystalline' Semiconductors

With a thin film of dye, the quantum efficiency, i.e., the number of electrons injected into the semiconductor per photon absorbed, can be very high. However with a thin dye layer, even in dyes with high extinction coefficients, only a fraction of the incident photons are absorbed, so the overall efficiencies tends to be small. The total absorbance by the dye layer can be increased by increasing its thickness, but in that case, since most of the photons are absorbed away from the interface between semiconductor and solution and must diffuse and migrate to that site before reaction, the quantum efficiency decreases sharply. For normal photosensitised semiconductors only the first monolayer of dye results in efficient electron injection into the semiconductor, but the light harvesting efficiency of a single dye monolayer is very

small In a porous film consisting of nanometer-sized e g TiO_2 particles, the effective surface area can be enhanced 1,000-fold [59] thus making light absorption more efficient with only a dye monolayer on each particle Other materials used in the preparation of the nanoporous electrodes have been investigated including ZnO, CdSe, CdS, WO_3, Fe_2O_3, SnO_2, Nb_2O_5 and Ta_2O_5 [60, 61, 62] but the TiO_2 system has been researched the most extensively [63, 64, 65, 66, 67]

Despite the heterogeneous nature of the semiconducting material, the diffusion of electrons in the bulk matter occurs with almost no energy loss [68] The recombination between the electron which is injected into the conduction band of the semiconductor, and the hole that remains on the oxidised dye is effectively very slow compared to the reduction of the latter by the mediator in solution [69]

Furthermore, electron-hole recombination in the semiconductor which seriously effects the efficiency of classic photovoltaic cells, does not occur in this case, due to the fact that there is no corresponding hole in the valence band for the electron in the conduction band As a result, the efficiency of the cell is not impaired by weak illumination, e g under a cloudy sky, in contrast to what happens with classical systems (e g silicon cells) [75]

1 7 3 The Dye

The dye sensitiser represents a key element of the cell It must be capable of (i) absorbing light over as wide a spectral range as possible, (ii) injecting an electron from its excited state into the conduction band of the semiconductor, and (iii) displaying an excellent stability that allows accomplishment of the dozens of thousands of excitation-oxidation-reduction cycles which must be performed during the required 20 year operational lifetime of the cell

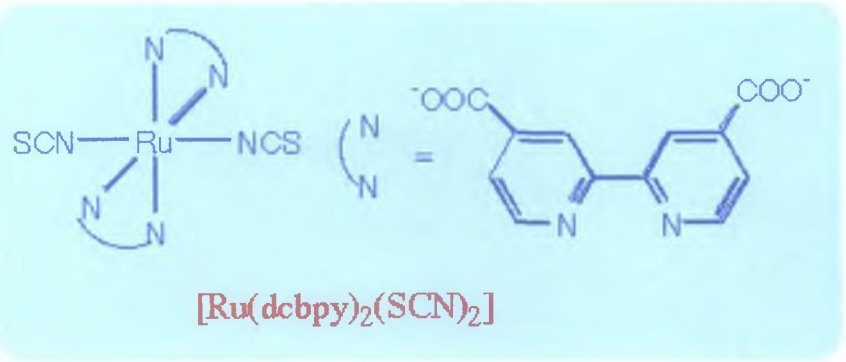

Figure 1.8 [72]

The complex having X as NCS was found to give the greatest efficiencies (Figures 1.9, 1.10). In conjunction with the nanostructured colloidal TiO_2 films and the iodide/triiodide electrolyte this complex converts 10% of AM1.5 solar radiation into electrical energy approaching the performance of polycrystalline silicon photovoltaic cells [73].

The $[Ru(dcbpy)_2(NCS)_2]$ complex has also indicated the presence of S-bound isomers. For a complex containing two ligand sites for substitution, several isomeric -N/-S bound NCS based species are possible. For the reaction of $[Ru(dcbpy)_2Cl_2]$ with thiocyanate cis $[Ru(dcbpy)_2(NCS)_2]$, $[Ru(dcbpy)_2(NCS)(SCN)]$, $[Ru(dcbpy)_2(SCN)_2]$, as well as the two monochloro species $[Ru(dcbpy)_2Cl(NCS)]$ and $[Ru(dcbpy)_2Cl(SCN)]$. However under prolonged reluxing at high temperatures the presence of S-bound thiocyanate can be reduced to approximately 2 % [74, 76, 77]. The formation of isomers poses a problem in the development of the dye-sensitised solar cell as the dye needs to be produced at reproducibly pure levels in a stable form [78].

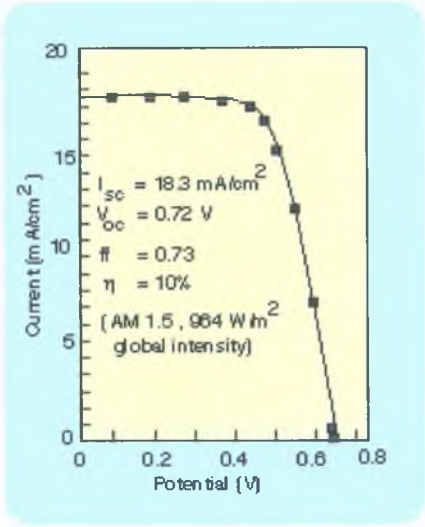

Figure 1.9

Voltage current characteristics of a nanocrystalline cell sensitised with

$[Ru(dcbpy)_2(SCN)_2]$ [72]

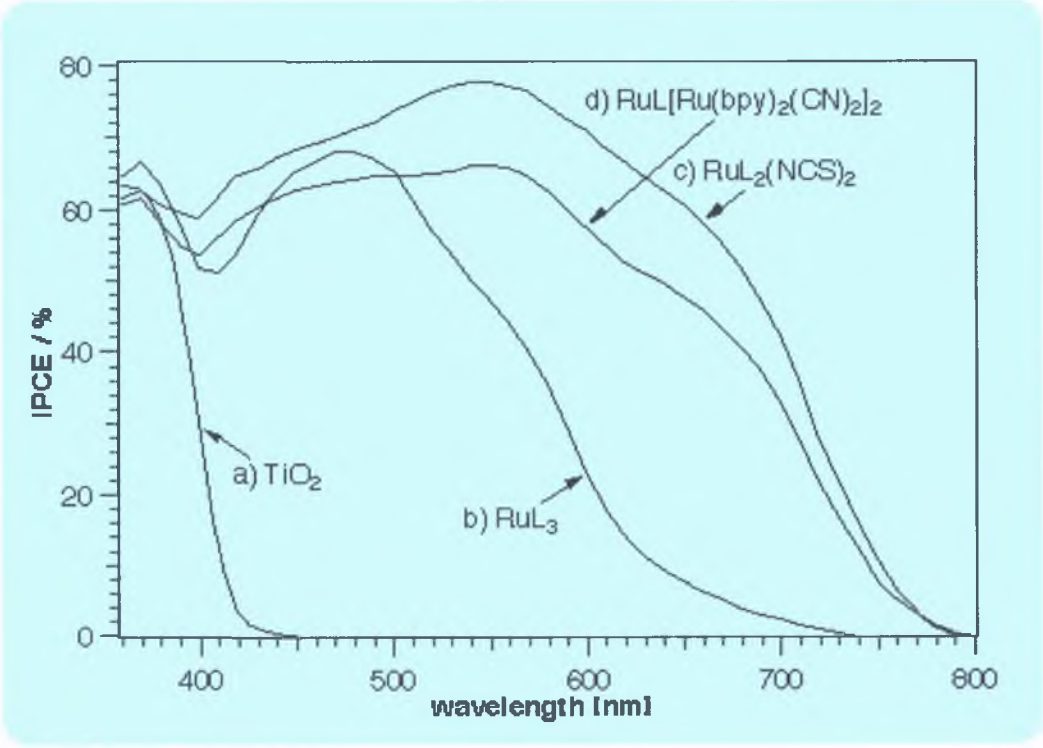

Figure 1.10

Action spectrum of nanocrystalline cells sensitised with complexes as indicated [72].

The most promising solar cells to date are based on ruthenium(II), osmium(II) and rhenium(I) polypyridyl compounds as dyes These transition metal complexes display high absorptivity of visible light among other things The Ru polypyridyl complexes are the most extensively studied potential solar cell sensitisers

Very promising results have been obtained from ruthenium complexes where at least one of the ligands was 4,4'dicarboxy-2,2'bipyridine and TiO_2 nanocrystalline semiconductors The carboxylates serve to attach the ruthenium complex to the surface of the semiconductor oxide and to establish good electronic coupling between the π^* orbital of the electronically excited complex and the 3d wave function manifold of the TiO_2 film (the orbital manifold of the conduction band) [70] As a result of the strong orbital coupling ultrafast electron injection from the excited complex into the semiconductor occurs at near unity quantum yield

The substitution of the bipyridyl with the carboxylate groups also lowers the energy of the π^* orbital of the ligand (due to the electron withdrawing -COOH) which results in a larger visible light harvesting capacity than e g tris bipyridyl Ru(II) analogues (i e higher absorption into the red) Since the electronic transition of the dye is of metal to ligand charge transfer (MLCT) character the excitation energy is channelled into the right ligand (dcbpy) i e the one from which electron injection into the conduction band takes place

The best performing sensitisers to date are those of the cis-X_2 bis(4,4'-dicarboxy-2,2'-bipyridine) ruthenium(II) family, where X= Cl , Br , I , CN or NCS (Figure 1 8) [71]

1.7.4 Tuning the Performance of the Cell

(I)

The maximum voltage produced by the system depends on the redox potential of the dissolved mediator The couple that gives the best efficiency, iodide-trnodide, is far from having the optimal potential Almost 500 mV are "lost" in this case [79, 80, 81, 82, 83]

(II)

Continuing work on the ruthenium dye sensitisers is being carried out to increase the efficiency of the solar cell when exposed to sunlight One area of development to increase the efficiencies of solar cells is to extend the sensitisers spectral absorption towards the infrared, which represents almost half of the radiative flux incident on the earth's surface The dyes currently employed already perform the photon-electron conversion efficiently over a good part of the visible spectrum, however beyond 800 nm their efficiency falls to zero

1 8 Scope of the thesis

The central aim of this thesis is to develop synthetic and purification methods for the preparation of ruthenium polypyridyl complexes based on 4,4'-dicarboxy-2,2'-bipyridine Although such compounds have been described in the literature, no well-described methods for their synthesis and purification exist

As already pointed out in the introduction carboxy-bpy ligands are important building blocks for the design of dye sensitised solar cells The development of effective synthetic procedures is therefore important

In the work two different approaches will be taken, one based on the direct synthesis of carboxy containing complexes, the other on an indirect synthetic pathway via ester precursors

The characterisation of the products obtained has been carried out using UV/vis, emission and ^{1}H-NMR spectroscopy Of interest in these studies is also the dependence of the electronic properties of the compounds on the pH of the solution

1 9· References

[1] C Kutal, J Chem Ed , 60, 1983, 882

[2] C P Whittingham, The Mechanism of Photosynthesis, J Wiley, New York, 1977

[3] D O Hall, K K Rao, Photosynthesis, 3rd edition, Edward Arnold London, 1984

[4] E Rabinowitch, Govindjee, Photosynthesis, 3rd edition, John Wiley & sons New York, 1975

[5] A L Leninger, Biochemistry, 2nd edition, 1975, Worth Publishers Inc , 587

[6] J Whitmarsh and Govindjee, Photosynthesis, Encyclopaedia for Applied Physics, 13, 1995, 513-532

[7] R Hill, C P Whittingham, Photosynthesis, 2nd edition, Methuen & Co ltd , London, 1977

[8] R P F Gregory, Biochemistry of Photosynthesis, 2nd edition, John Wiley London, 1989

[9] X Tang, D W Randall, D A Force, B A Diner,R D Brit, J Am Chem Soc 118, 1996, 7638

[10] Coyle, Hill, Roberts, Light, Chemical change and life, The Open University Press, Milton Keynes (England), 1982

[11] K Wieghardt, Angew Chem Int Ed Engl , 28, 1989, 1153

[12] P Joliot, A Joliot, B Bourges, G Barbieri, Photochem Photobiol , 14, 1971, 287

[13] B Kok, B Forbush, M McGloin, Photochem Photobiol , 11, 1970, 457

[14] A J Bard, M A Fox, Acc Chem Res , 28, 1995, 141

[15] C Elievant, Solar Energy Mater , 24, 1991, 413

[16] M D Archer, J R Bolton, J Phys Chem , 94,1990,8028

[17] C Hu , R M White, Solar Cells, McGraw-Hill, 1983

[18] D Thorp, P Campbell, S R Wenham, Progress in Photovoltaics, Research and Applications, 4, 1996, 205

[19] S R Wenham, M A Green, Progress in Photovoltaics, Research and Applications, 4, 1996, 3

[20] R F Service, Science, 279, 1998,1300

[21] D V Pinnick, B Durham, Inorg Chem , 23, 1984, 3840

[22] E A Seddon, K R Seddon, "The Chemistry of Ruthenium", Elsevier Science Publisher BV , Amsterdam, 1984

[23] A Juris, V Balzani, F Barigelleti, S Campagna, P Belser, Coord Chem Rev , 84, 1988, 85

[24] J Demas, G Crosby, J Am Chem Soc , 93, 1971, 2840

[25] X Xu, K Shreder, B L Iverson, J A Bard, J Am Chem Soc , 118, 1996, 3656

[26] J Van Houten, J Am Chem Soc , 98, 1976, 4853

[27] J Van Houten, Inorg Chem , 17, 1978, 3381

[28] T J Meyer, J Am Chem Soc , 104, 1982, 4803

[29] K Kalyanasundaram, Coord Chem Rev , 46, 1982, 159

[30] J V Casper, T J Meyer, Inorg Chem , 22,1983, 2444

[31] M Kropf, E Joselevich, H Durr, I Willner, J Am Chem Soc , 118, 1996, 655

[32] S L Larson, C M Elliot, D F Kelley, Inorg Chem , 35, 1996, 2070

[33] S Serroni, S Campagna, G Denti, T Keyes, J G Vos, Inorg Chem , 35, 1996, 4513

[34] P V Kamat, I Bedja, S Hotchandani, L K Patterson, J Phys Chem , 100, 1996, 4900

[35] B D J R Fennema, R Hage, J G Haasnoot, J Reedijk, J G Vos, Inorg Chim Acta, 171, 1990, 223

[36] R Hage, J G Haasnoot, J Reedijk, R Wang, E M Ryan, J G Vos, A L Speck, A J M Duisenberg, Inorg Chim Acta , 174, 1990, 77

[37] G Giuffrida, G Calogero, G Guglielmo, V Ricevuto, M Ciano, S Campagna, Inorg Chem , 23, 1993, 1179

[38] R Hage, R Prins, J G Haasnoot, J Reedijk, J G Vos, J Chem Soc , Dalton Trans , 1987, 1389

[39] J M de Wolf, R Hage, J G Haasnoot, J Reedijk, J G Vos, New J Chem , 15, 1991, 501

[40] H A Nieuwenhuis, J G Haasnot, R Hage, J Reedijk, T L Snoeck, D J Stufkens, J G Vos, Inorg Chem , 30, 1991, 48

[41] S Ernst, W Kaim, Inorg Chem , 28, 1989, 1520

[42] R Hage, J G Haasnoot, H A Nieuwenhuis, J Reedijk, R Wang, J G Vos, J Chem Soc , Dalton Trans , 1991, 3271

[43] G F Strousse, P A Anderson, J R Schoonover, T J Meyer, F R Keene, Inorg Chem , 31, 1992, 3004

[44] R J Crutchley, A B P Lever, J Am Chem Soc , 102, 1980, 7128

[45] F Barigelletti, A Juris, V Balzani, P Belser, A von Zelewsky, Inorg Chem , 26, 1987, 4115

[46] J Ferguson, A W H Mau, W H F Sasse, Chem Phys Let , 68, 1979, 21

[47] P J Giordano, C R Bock, M S Wrighton, L V Interrante, R F X Williams, J Am Chem Soc , 99, 1977, 3187

[48] P A Lay, W H Sasse, Inorg Chem , 23, 1984, 4123

[49] A Launikoms, P A Lay, A W H Mau, A M Sargeson, W H F Sasse, Aust J Chem , 39, 1986, 1053

[50] T Shimidzu, T Iyoda, K Izaki, J Phys Chem , 89, 1985, 642

[51] V Balzani, N Sabbatini, F Scandola, Chem Rev , 86, 1986, 319

[52] M K DeArmond, Y Ohsawa, S Sprouse, S King, K W Hanck, R J Watts, J Phys Chem , 91, 1987, 4686

[53] C M Elliot, E Hershenhart, J Am Chem Soc , 104, 1982, 7579

[54] G Sprintschnik, H W Sprintschnik, P P Kirsch, D D Whitten, J Am Chem Soc , 99, 1977, 4947

[55] N Vlachopoulos, P Liska, J Augustynski, M Gratzel, J Am Chem Soc , 110, 1988, 1216

[56] I Desilvestro, M Gratzel, L Kavau, I Moser, J Augustynski, J Am Chem Soc , 107, 1985, 2988

[57] M Gratzel, P Liska, Photoelectrochemical cells and process for making same, U S Patent, 1992, 5, 084, 365

[58] K Kalyanasundaram, M Gratzel, M Nazeeruddin, J Chem Soc , Dalton trans , 1991, 343

[59] A Hagfeldt, M Gratzel , Chem Reviews, 95, 1995, 49

[60] G Redmond, D Fitzmaurice, M Gratzel, Chem Mater , 6, 1994, 686

[61] T J Meyer, G J Meyer, B W Pfennig, J R Schoonover, C J Timpson, J F Wall, C Kobusch, X Chen, B M Peek, C G Wall, W Ou, B W Erickson, C A Bignozzi, Inorg Chem , 33,1994, 3952

[62] K Hashimoto, M Hiramoto, T Sakata, H Muraki, H Takemura, M Fugihira, J Phys Chem , 91, 1987, 6198

[63] R Argazzi, C Bignozzi, T A Heimer, F Castellano, G J Meyer, J Am Chem Soc , 117, 1995, 11815

[64] B O'Regan, J Moser, M Anderson, M Gratzel, J Phys Chem , 94, 1990, 8720

[65] M A Ryan, E C Fitzgerald, M T Spilter, J Phys Chem , 93, 1989, 6150

[66] A Kay, M Gratzel, J Phys Chem , 97, 1993, 6272

[67] J Kiwi, E Borgarello, E Pelizzetti, M Visca, M Gratzel, Angew Chem Int Ed Engl , 19, 1980, 646

[68] S Sodergren, A Hagfeldt, J Olsson, SE Lindquist, J Phys Chem , 98, 1994, 5552

[69] K K Rao, D O Hall, N Vlachopoulos, M Gratzel, M C W Evans, M Seibert, J Photochem Photobiol B , 5, 1990, 379

[70] P Liska, N Vlachopoulos, M K Nazeeruddin, P Comte, M Gratzel, J Am Chem Soc , 110, 1988, 3686

[71] M K Nazeeruddin, A Kay, I Rodicio, R Humphry-Baker, E Muller, P Liska, N Vlachopoulos, M Gratzel, J Am Chem Soc , 115, 1993, 6382

[72] M K Nazeeruddin, P Liska, J Moser, N Vlachopoulos, M Gratzel, Helvetica Chimica Acta, 73, 1990, 1788

[73] B O'Regan, M Gratzel, Nature, 353, 1991, 737

[74] O Kohle, S Ruile, M Gratzel, Inorg Chem , 35, 1996, 4779

[75] S A Haque, Y Tachibana, R L Willis, J E Moser, M Gratzel, D R Klug, J R Durrant, J Phys Chem B, 104(3), 2000, 538

[76] M Gratzel, Inorg Chem , 35(16), 1996, 4779

[77] M Gratzel, Chemistry of Materials, 10(9),1998, 2533

[78] M K Nazeeruddın, S M Zakeeruddın, R Humphry-Baker, M Jırousek, P Lıska, N Vlachopoulos, V Shklover, C-H Fıscher, M Gratzel, Inorg Chem , 38(26), 1999, 6298

[79] S Pelet, J E Moser, M Gratzel, J Phys Chem B, 104(8), 2000, 1791

[80] I Rıess, J Phys Chem B, 104(9), 2000, 2053

[81] M K Nazeeruddın, M Amırnasr, P Comte, J R Mackay, A J McQuıllan, R Hourıet, M Gratzel, Langmuır, 16(22), 2000, 8525

[82] C A Kelly, F Farzad, D W Thompson, J M Stıpkala, G J Meyer, Langmuır, 15(20), 1999, 7047

[83] G J Meyer, J Phys Chem B, 102(39), 1998, 7577

Chapter 2

EXPERIMENTAL SECTION

Ligands Cited in Text

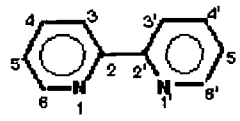

2,2'-bipyridine
(bpy)

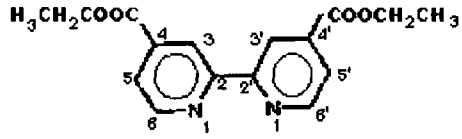

4,4'diethyester-2,2'bipyridine
(decb)

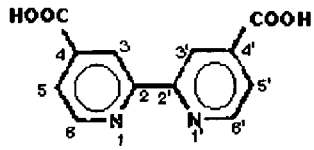

4 4'-dicarboxy-2,2'-bipyridine
(dcbpy)

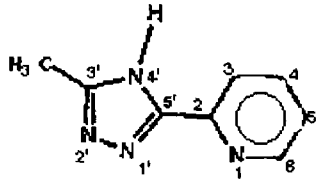

3-methyl-5-(pyridin-2-yl)-1,2,4-triazole
(3-Me-ptr)

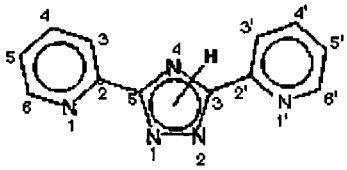

3,5-bis(pyridin-2-yl)-1,2,4-triazole
(Hbpt)

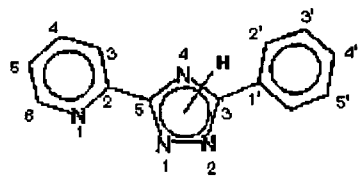

3-(phenyl)-5-(pyridin-2-yl)-1 2,4-triazole
(phenyl-ptr)

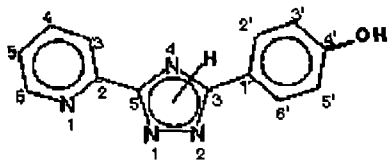

3-(4-hydroxyphenyl)-5-(pyridin-2-yl)
-1,2,4-triazole
(4-phenol-ptr)

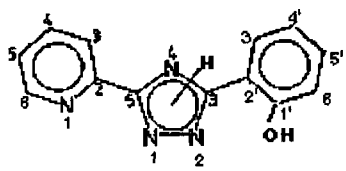

3-(1 hydroxyphenyl)-5-(pyridin-2-yl)
-1,2,4-triazole
(1-phenol-ptr)

Physical Measurements

2 1 Absorption and Emission Spectroscopy

UV-vis spectra were obtained on a Shimadzu UV-240 spectrometer Emission spectra were obtained at room temperature using a Perkin-Elmer LS50 luminescence spectrometer equipped with a red sensitive Hamamatsu R928 detector with an emission and excitation slit width of 10 nm The results obtained were not corrected for photomultiplier response For pH studies the samples to be measured were first dissolved in ca 1 cm^3 acetonitrile (HPLC grade) and then added to 150 - 200 cm^3 of Britton-Robinson buffer (0 04 M H_3BO_3, 0 04 M H_3PO_4, 0 04 M H_3CCOOH) or Phosphate buffer (0 1 M Na_2HPO_4 + 0 1 M NaH_2PO_4) in the case of the diester complexes The pH of the solutions was adjusted with concentrated sulphuric acid or concentrated sodium hydroxide solution and measured using a Corning 240 digital pH meter

2 2 Chromatographic Techniques

Analytical High Performance Liquid Chromatography (HPLC)

Analytical HPLC experiments were carried out using a system which consisted of a Waters pump model 6000 A, a 990 photodiode array detector, an NEC APC III computer and a 20 µl injector loop The columns used were a µPartisil SCX (cation)

radial PAK cartridge and a SAX (anion) cartridge (8 mm x 100 mm) for the dicarboxy complexes The detection wavelength used was 280 nm which corresponds to the high absorbency $\pi \rightarrow \pi^*$ transitions in the ruthenium complexes studied The mobile phase for the SAX column was 50 50 acetonitrile water with 0 025 M phosphate buffer, pH = 7 (0 025 M Na_2HPO_4/NaH_2PO_4) The mobile phase for the SCX column was 80 20 acetonitrile water with 0 8 - 1 2 M lithium perchlorate depending on the charge of the compounds to be separated All mobile phases were filtered using a Sartorious

0 45 μm disposable filter and deaerated using a sonic bath for 30 min The chromatographic system was allowed to equilibrate for approximately one hour prior to any sample injection

Semi-Preparative HPLC

Semi-Preparative HPLC experiments were carried out using a system which consisted of a Waters pump model 6000 A, a 1 cm^3 injection loop and a Magnum 9 Partisil cation exchange column (10 mm x 25 cm) The mobile phase used for separation of mononuclear/dinuclear ruthenium complexes was 80 20 acetonitrile water with 0 12 M potassium nitrate, all mobile phases were filtered and deaerated as above

All chromatography was carried out in HPLC grade solvents

2 3 Nuclear Magnetic Resonance Spectroscopy (^{1}H-NMR)

All the ^{1}H-NMR spectra were obtained using a Bruker AC 400 MHz spectrometer For dicarboxy substituted complexes measurements were usually carried out in

D_2O/NaOD or occasionally d_6-DMSO and a drop of NaOD (Na + D_2O) All other complexes were measured in d_6-DMSO or d_6-acetone and ligands in d_6-DMSO All chemical shifts are relative to TMS

2.4 Luminescent Lifetimes measurements

The lifetime measurements were carried out using a Q-switched Nd-YAG spectrum laser system Samples were dissolved in analytical grade acetonitrile at room temperature and deaerated with N_2 for 30 min prior to measurement Lifetime data were analysed using a non-linear least squares fit to exponential decay with a baseline correction Room temperature measurements in 1 cm Pyrex luminescence cells were used, approximately 10 µl trifluoroacetic acid or diethylamine were added to about 10 cm^3 sample solution to ensure protonation/deprotonation The lifetime errors are estimated to be less than 10 %

2.5 Elemental Analysis

Elemental analysis on C, H and N were carried out at the Microanalytical Laboratory of the University College Dublin (UCD) The CHN analyser used is an Exador analytical CE440

2 6 Synthesis and Purification of Ruthenium Complexes and ligands

The synthesis of the ligands and the various synthetic approaches taken to the synthesis of the complexes are described below Unless otherwise stated, all starting materials and solvents were of commercial grade

The following ligands were synthesised according to modified literature methods and are known compounds

2 6 1 4,4'-dimethyl-2,2'-bipyridine (dmb) [1, 2]

This compound was prepared as an intermediate for the synthesis of 4,4'-dicarboxylic acid-2,2'-bipyridine

100 cm^3 of 4-Picoline and 3 6 g Palladium/Charcoal were heated at reflux temperature for 5 days, after which time the solution was cooled and filtered Unreacted Picoline was distilled off and the remaining few cm^3 were diluted in acetone

Pd/C remaimng was washed with acetone and all acetone fractions were combined Water was added to solution to crash out the dmb and the resulting white solid was recrystallised 3 x times from acetone/water (80/20 v/v)

Yield 5 % ^{1}H-NMR (d_6-DMSO) H^3,$H^{3'}$ 8 68 (s), H^5,$H^{5'}$ 7 38 (d), H^6,$H^{6'}$ 7 82 (d)

2 6 2. 4,4'-dicarboxylic acid-2,2'-bipyridine (dcbpy)

Method 1 (modification on literature methods [3, 1, 4, 5]

To 5 0 g of finely ground dmb 15 g of potassium permanganate in 150 cm^3 water was added in 3 x 5 g lots The solution was heated at reflux temperature for 12 h On

cooling the MnO_2 solid was filtered off and washed with diethylether and water The filtrates were combined and unreacted dmb was extracted into the diethylether The pH of the aqueous extract was lowered to pH=1 2 with dilute hydrochloric acid and the dcbpy precipitate was filtered off

The precipitate was then heated at reflux temperature in 50% nitric acid for 8 h to ensure complete oxidation of methyl groups On cooling, water was added slowly to the solution and the resulting precipitate was filtered off and washed with water The diacid was purified further by dissolution in aqueous sodium bicarbonate, followed by precipitation with dilute HCl

Due to the repeatedly low yield of the reaction above (approx 45 – 50 %) the synthesis of dcbpy was also carried out using potassium dichromate as the oxidising agent from the method of Morgen and Oki [6]

Method 2 [1]

To a stirring solution of sulphuric acid (98%, 125 cm^3) 4 81 g (26 12 mmol) of dmb was added With efficient stirring, 24 15 g (8 21 mmol) of potassium dichromate was added in small portions such that the temperature remained between 70 and 80 °C Occasional cooling in an ice bath was necessary during the addition of potassium dichromate After all the dichromate was added the reaction was stirred at room temperature until the temperature fell below 40 °C The deep green reaction mixture was poured into approximately 100 cm^3 of ice water The resulting solid was filtered off and washed with copious amounts of water The light yellow solid was then refluxed in 50 % nitric acid for 4 h On cooling aqueous sodium bicarbonate was added and the resulting precipitate was filtered off, washed with water (2 x 20 cm^3),

acetone (2 x 20 cm^3) and allowed to dry giving 5 35 g (21 89 mmol) of fine white solid Yield 84 % ^{1}H-NMR ($NaOD/D_2O$) H^3,$H^{3'}$ 8 27 (s), H^5,$H^{5'}$ 7 73-7 75 (d), H^6,$H^{6'}$ 8 64-8 66 (d)

2 6 3 4,4'-diethoxycarbonyl-2,2'-bipyridine (decb) [3], [7]

The diethyl ester of dcbpy was prepared by existing literature methods (Fischer Esterification) [9, 13] and obtained as colourless crystals

1 00 g (4 09 mmol) of dcbpy, 60 cm^3 dry ethanol and 17 cm^3 conc sulphuric acid were heated at reflux temperature for 21 h, after which time the excess ethanol was distilled off 40 cm^3 of chloroform was added to the remaining solution and the mixture was treated with aqueous sodium bicarbonate The solution was extracted with chloroform (3 x 50 cm^3) and the combined organic layers were dried over magnesium sulphate and evaporated to dryness, resulting in a colourless crystalline solid The decb was recrystallised from chloroform/Petroleum ether (40-60), (50/50 v/v) From the aqueous layer the unreacted or partially reacted diacid was recovered by acidification of the solution

Yield 21 % ^{1}H-NMR ($CDCl_3$) H^3, $H^{3'}$ 8 96 (s), H^6, $H^{6'}$ 8 88 (d), H^5, H^5 7 93 (d), CH_2 4 44-4 48 (q), CH_3 1 44-1 47 (t)

2 6 4 3,5-bis(pyridin-2-yl)-4-amino-1,2,4-triazole (Hbpt) [18]

Method 1

3 02 g 3,5-bis(pyridin-2-yl)-4-amino-1,2,4-triazole was heated in 40 cm^3 nitric acid (5M) to boiling point for 3 min after which time the solution was cooled to 0 °C and 6 02 g sodium nitrite was added, resulting in the evolution of ammonia and a white

precipitate forming The solution was stirred for 15 mm to dissolve the precipitate, heated to boiling for 5 mm and allowed to cool before ammonia was added to precipitate out the product Yield 75%

Method 2

5 23 g of 2-cyanopyridine (50 25 mmol), 20 cm^3 sodium methoxide solution (MeONa - 25% wt solution in methanol) and 40 cm^3 methanol were refluxed for 1h, after which time the clear solution turned red On cooling 1 4 cm^3 hydrazine monohydrate was added and the solution was heated at reflux temperature for 1h, resulting in a dark red solution The methanol was removed and the solution was heated in ethylene glycol at 120 °C for 1 h On cooling approx 10 cm^3 2 M HCl was added and the solution was neutralised with NaOH, resulting in a fine yellow precipitate Product was recrystallised from ethanol/methanol Yield 22 % ^{1}H-NMR (d_6-DMSO) H^3, $H^{3'}$ 8 18 (d), H^4, $H^{4'}$ 8 05(dd), H^5, $H^{5'}$ 7 50 (dd), H^6, $H^{6'}$ 8 65 (d)

Ruthenium complexes containing both dcbpy and decb ligands

2 6 5· [Ru(dcbpy)$_2$(NCS)$_2$] 2H$_2$O [9]

0 30 g (0 428 mmol) Ru(dcbpy)$_2$Cl$_2$ 2H$_2$O was dissolved in 30 cm^3 dimethylforamide, under reduced light To this solution 0 38 g $NaHCO_3$ dissolved in 10 cm^3 H_2O was added to deprotonate the dicarboxy groups 1 77 g (17 12 mmol, x 40 excess) of potassium thiocyanate was dissolved in 3 cm^3 H_2O and added to the above solution The reaction mixture was heated with stirring at reflux temperature under N_2 atmosphere and reduced light for 5 hr The solvent was removed under reduced pressure and 4 cm^3 H_2O added to the product mixture The solution was filtered and

the pH of the filtrate was lowered to 2 5 with dilute perchloric acid and refrigerated for three days The resulting dark red crystalline solid was collected on a medium frit sintered glass filter (size 3) and washed with copious amounts of H_2O and 4 x 20 cm^3 acetone/diethylether (1 10 v/v) Yield 68 % ^{1}H-NMR (NaOD/D_2O) H^6 9 68 (d), H3 9 17 (s), $H^{3'}$ 9 01 (s), $H^{6'}$ 8 43 (d), H^5 8 03 (d), $H^{5'}$ 7 67 (d)

The following ruthenium complexes were prepared according to modified literature methods $Ru(bpy)_2Cl_2$ was used as synthesised previously according to literature methods [10]

2 6.6. $Ru(decb)_2Cl_2$ [1]

To 0 47 g (1 799 mmol) $Ru(III)Cl_3\ 3H_2O$ in 100 cm^3 ethanol/water (90/10) 1 08 g (3 60 mmol) decb was added slowly with stirring The solution was refluxed for 9 h On cooling, the solution was filtered and the solvent evaporated off The product was recrystallised from ethanol/ethylacetate and the final product was washed with 3 x 40 cm^3 diethylether, 2 x 20 cm^3 H_2O, 4 x 20 cm^3 ethylacetate Yield 60 % ^{1}H-NMR ($CDCl_3$) H^6 10 47 (d), H^3 8 81 (s), $H^{3'}$ 8 63 (s), $H^{6'}$ 8 15 (d) H^5 7 68 (d), H^5 7 48 (d)

2 6 7 $Ru(dcbpy)_2Cl_2$ [11]

To 1 3 g (4 97 mmol) $RuCl_3\ 3H_2O$ in 100 cm^3 DMF, 2 6 g (10 65 mmol) dcbpy was added over time and the solution was heated at reflux temperature under nitrogen for 8h After cooling the solution was filtered to remove any $Ru(dcbpy)_3$ present Most of the DMF was taken off under vacuum and cis-$Ru(dcbpy)Cl_2$ was precipitated in a

stirring solution of 4 1 diethylether acetone The solution was filtered and the product was washed with diethylether and dried in vacuo Yield 82 % ^{1}H-NMR (d_6-DMSO) H^6 9 68 (d), H^3 8 67 (s), $H^{3'}$ 8 48 (s), $H^{6'}$ 7 83 (d) H^5 7 35 (d), $H^{5'}$ 7 10 (d)

2.6 8 $[Ru(bpy)_2(dcbpy)][PF_6]_2$ [12]

Method 1

1 94 g (4 70 mmol) $Ru(bpy)_2Cl_2$ and 1 15 g (4 70 mmol) dcbpy were heated at reflux temperature in 100 cm^3 methanol/water (80 20 v/v) for 5 h After reflux most of the solvent was removed, the solution was made acidic and aqueous NH_4PF_6 was added The resulting precipitate was filtered off and washed with 4 x 20 cm^3 water and 2 x 10 cm^3 diethylether

Method 2

As above, After heating the solution at reflux temperature and subsequent removal of most of the solvent, the solution was filtered and the product was precipitated by lowering the pH of the filtrate to approximately 1 90 (i e no NH_4PF_6 added and all the dcbpy groups are therefore fully protonated) Yield 72 % ^{1}H-NMR (d_6-acetone + CF_3COOH)

bpy protons H^3,$H^{3'}$ (4H) 8 82, H^4,H^4 (4H) 8 18–8 23 (m), H^5,$H^{5'}$ (4H) 7 52-7 60 (2 x dd), H^6,$H^{6'}$ (4H) 8 02–8 07 (2 x d)

dcbpy protons H^3 9 26 (s), H^5 7 95 (d), H^6 8 28 (d)

2 6.9. $[Ru(bpy)_3][PF_6]_2$ [13]

0 5 g (1 03 mmol) $Ru(bpy)_2Cl_2$ and 0 16 g (1 03 mmol) bpy in 100 cm^3 methanol/H_2O (80/20 v/v) were heated at reflux temperature for 6 h after which time the solvent was

removed under reduced pressure The resulting solid was reconstituted in 5 cm^3 H_2O and aqueous NH_4PF_6 was added The precipitate was filtered off and washed with H_2O and diethylether Yield 72 % ^{1}H-NMR (d_6-DMSO) H^3 8 90 (d), H^4 8 12 (m), H^5 7 53 (m), H^6 7 71 (d)

2 6 10. [Ru(bpy)$_2$(bpt)][PF$_6$] [8]

0 89 g (4 0 mmol) 3,5-bis(pyridin-2-yl)-1,2,4-triazole was dissolved in 100 cm^3 methanol/water (70/30) and heated at reflux temperature for 30 minutes or until all the ligand was dissolved Cis-[Ru(bpy)$_2$Cl$_2$] 2H_2O was added in small portions to the dissolved ligand and the solution was refluxed for a further 5 h The hot solution was filtered and evaporated to dryness after which 10 cm^3 water, 1 drop of ammonia and aqueous NH_4PF_6 was added slowly with stirring The resulting precipitate was filtered off and purified as described below to remove any trace amounts of the dimer [Ru(bpy)$_2$)$_2$(bpt)](PF$_6$)$_3$

Method 1

Purification was carried out using a semi-preparative analytical HPLC system [14, 15] The mobile phase used was 80 20 acetonitrile water and 0 12 M KNO_3 After collection of the fractions from both the monomer and the dimer, the solvent was evaporated off Acetone was added to the solid and the solutions were filtered to remove the KNO_3 present The acetone was evaporated off and the products were redissolved in water Aqueous NH_4PF_6 was added and the resulting precipitates were filtered and recrystallised from acetone/H_2O

Method 2

A method of purification by column chromatography was developed as a more efficient method of separation

The monomer and dimers were separated using gradient elution on neutral alumina The mobile phase used was acetonitrile/methanol, with a gradual increase in methanol concentration from 0-100% The monomer eluted first and the dimer elutes with the increasing polarity of the mobile phase

^{1}H-NMR (d_6-DMSO)

bpt protons H^3 8 23 (d), $H^{4'}$ 8 01 (dd), $H^{5'}$ 7 26 (dd), ,$H^{6'}$ 7 74 (d), H^3 8 06 (d), H^4 7 74 (dd), H^5 7 20 (dd), H^6 8 45 (d)

bpy protons H^3 8 68-8 8 (d), H^4 7 8-8 18 (dd), H^5 7 41-7 63 (dd), H^6 7 95-8 10 (d)

New complexes synthesised

The ligands 4-phenol-ptr, 1-phenol-ptr, 3-Me-ptr and phenyl-ptr which were used had been synthesised previously according to literature methods [8]

2.6.11 [Ru(decb)$_2$(4-phenol-ptr)][PF$_6$]

355 0 mg (0 4 mmol) Ru(decb)$_2$Cl$_2$ and 109 5 mg (0 4 mmol) 4-phenol-ptr were refluxed in 90 cm^3 ethanol/water (80/10 v/v) for 8h On cooling the solution was filtered and the solvent was removed under vacuum The resulting solid was redissolved in 10 cm^3 water and the precipitate filtered (2 6 11a ^{1}H-NMR impure) Aqueous NH_4PF_6 was added to the filtrate and the precipitate was filtered off (2 6 11b) 2 6 11b was redissolved in ethyl acetate and filtered, removing any unreacted Ru(decb)$_2$Cl$_2$ The product obtained from the filtrate was washed with

2 x 40 cm^3 diethylether Yield 60 % CHN Found C, 28 43, H, 3 02, N, 8 64, $C_{45}H_{43}F_6N_8O_9PRu$ requires C, 49 87, H, 3 81, N, 10 34

^{1}H-NMR of $[Ru(decb)_2(4\text{-phenol-ptr})][PF_6]$ (d_6-acetone)

decb protons H^3H^3 (4H) 9 27-9 22 (m), H^6 (2H) 8 36 (d), H^5 (2H) 8 05-8 0 (d), H^6 (2H) 7 95-7 93 (d), H^5 (2H) 7 78 (d), CH_2 4 41 (q), CH_3 1 33 (t), OH 11 67 (s)

4-phenol-ptr protons H^3 8 51 (d), H^4 8 19 (dd), H^5 7 47 (dd), H^6 8 30 (d), $H^{2'}$ 8 44 (d), $H^{3'}H^5$ 6 87 (d), $H^{6'}$ 7 85 (d)

Free ligand 4-phenol-ptr (d_6-DMSO) H^3 8 12 (d), H^4 7 96 (dd), H^5 7 50 (dd), H^6 8 68 (d), $H^{2'}$ & $H^{6'}$ 7 90 (d), $H^{3'}$ & $H^{5'}$ 6 88 (d), OH 11 42 (s)

2.6 12 $[Ru(decb)_2(1\text{-phenol-ptr})][PF_6]$

336 5 mg (0 4 mmol) $Ru(decb)_2Cl_2$ and 103 8 mg (0 4 mmol) 1-phenol-ptr were refluxed in 90 cm^3 ethanol/water (80/10 v/v) for 8h The product was purified and isolated as described for $[Ru(decb)_2$ 4-phenol-ptr$][PF_6]$ (2 6 11) Yield 58 % CHN Found C, 54 56, H, 4 98, N, 9 78, $C_{45}H_{43}F_6N_8O_9PRu$ requires C, 49 87, H, 3 81, N, 10 34

^{1}H-NMR of $[Ru(decb)_2(1\text{-phenol-ptr})][PF_6]$ (d_6-acetone)

decb protons H^3H^3 (4H) 9 31-9 26 (m), H^6 (2H) 8 46-8 39 (m), $H^{6'}$ & H^5H^5 (6H) 8 02-7 9 (m), CH_2 (q) 4 83-4 46, CH_3 (t) 1 39-1 37, OH (s) 11 79

1-phenol-ptr protons H^3 8 63 (d), H^4 8 22 (dd), H^5 7 50 (dd), H^6 8 34 (d), $H^{3'}$ 8 56 (d), $H^{4'}$ 6 92 - 6 98 (m), $H^{5'}$ 7 34 (dd), $H^{6'}$ 6 92 -6 98 (m)

Free ligand 1-phenol-ptr (d_6-DMSO) H^3 8 19 (d), $H^{3'}$ & H^4 8 01-8 06 (m), H^6 8 74 (d), H^5 7 36 (dd), $H^{4'}$ & $H^{6'}$ 7 02-6 96 (m), $H^{5'}$ 7 55 (dd), OH 11 12 (s)

2 6 13 [Ru(decb)$_2$(phenyl-ptr)][PF$_6$]

118 6 mg (0 15 mmol) Ru(decb)Cl$_2$ and 34 1 mg (0 15 mmol) phenyl-ptr were heated at reflux temperature in 60 cm^3 methanol/water (50/10 v/v) for 6 h The product was purified and isolated as described for [Ru(decb)$_2$ 4-phenol-ptr][PF$_6$] (2 6 11) Yield 50 % CHN Found C, 40 77, H, 3 57, N, 8 43, $C_{45}H_{41}F_6O_8N_8PRu$ requires C, 50 61, H, 3 87, N, 10 49

^{1}H-NMR of [Ru(decb)$_2$(phenyl-ptr)][PF$_6$] (d$_6$-acetone)

decb protons H^{3}H$^{3'}$ (4H) 9 23-9 18 (m), H^6 (2H) 8 26 (m), H^{5}H$^{5'}$ & H$^{6'}$ (6H) 8 02-7 92 (m)

phenyl-ptr protons H^3 8 39 (d), H^4 8 16 (dd), H^5 7 17 (dd), H^6 8 20 (d), H$^{2'}$ 8 32 (d), H$^{5'}$ & H$^{3'}$ 6 76 (m), H^4 7 12 (dd), H^6 7 75 (d)

Free ligand phenyl-ptr (d$_6$-DMSO) H^3 8 32 (d), H^4 7 93 (dd), H^5 7 20 (dd), H^6 8 64 (d), H^2 & H$^{6'}$ 7 86 (m), H^4 7 10 (dd), H^3 & H$^{5'}$ 6 75 (m)

2 6 14. [Ru(decb)$_2$(3-Me-ptr)][PF$_6$]

To 0 14 g (0 89 mmol) 3-Me-ptr dissolved in 80 cm^3 methanol/water (70 10 v/v), 0 25 g (0 33 mmol) Ru(decb)$_2$Cl$_2$ was added slowly over 1 5 h The solution was heated at reflux temperature for 3 h The product was purified and isolated as described for [Ru(decb)$_2$ 4-phenol-ptr][PF$_6$] (2 6 11) Yield 55 % CHN Found C, 39 38, H, 3 36, N, 9 96, $C_{40}H_{39}F_6N_8O_8PRu$ requires C, 47 74, H, 3 91, N, 11 15

^{1}H-NMR of [Ru(decb)$_2$(3-Me-ptr)][PF$_6$] (d$_6$-acetone)

decb protons H^{3}H$^{3'}$ (4H) 9 39-9 26 (m), H^{6}H^6 (4H) 8 46 – 8 39 (m),

H^{5}H^5 (4H) 8 02 – 7 9 (m), CH$_2$ 4 40 (m), CH$_3$ 1 44 (m)

3-Me-ptr protons H^3 8 63 (d), H^4 8 19 (dd), H^5 7 59 (dd), H^6 8 21 (d), CH$_3$ 2 91 (s)

Free Ligand 3-Me-ptr ($CDCl_3$) H^3 8 23 (d), H^4 7 92 (dd), H^5 7 50 (dd), H^6 8 70 (d), CH_3 2 53 (s)

For complexes 2 6 11 to 2 6 14 numerous solvents were used in an attempt to purify the complexes by recrystallisation It was found that by dissolution of the PF_6 product in ethylacetate undissolved material was noted as present When this was filtered off a pure product was isolated from the filtrate which was washed with diethylether until the washings were colourless

2 6 15 [Ru($^2H_8$-bpy)$_2$(dcbpy)]

The Ru($^2H_8$-bpy)$_2Cl_2$ complex was synthesised according to literature methods used for the undeuterated Ru(bpy)$_2Cl_2$ [10] The deuterated bpy was synthesised by typically adding 3 g (0 19 mol) 2,2'-bipyridyl to 30 cm^3 D_2O (99 % deuterated) and allowing the reaction mixture to react in the presence of a H-D exchange catalyst Pd/C (Aldrich, 10 % Pd) in a Teflon-coated steel high pressure reactor at 200 °C for 8 days For complete deuteriation the isolated product was subjected to the same procedure with fresh D_2O for a week [16] The [Ru($^2H_8$-bpy)$_2$(dcbpy)] complex was then synthesised using the same method as the undeuterated [Ru(bpy)$_2$(dcbpy)] (2 6 8)

Yield 72 % ^{1}H-NMR of [Ru($^2H_8$-bpy)$_2$(dcbpy)] (d_6-acetone + CF_3COOH) H^3 8 75 (s), H^6 7 77 (d), H^5 7 45 (d)

Attempted syntheses of the following complexes The reaction products of all the attempted syntheses were examined by HPLC

2 6 16 [Ru(decb)$_2$(bpt)][PF$_6$]

0 58 g bpt was dissolved in 100 cm^3 methanol/H_2O (90/10 v/v) To this was added 1 00 g (1 29 mmol) Ru(decb)Cl_2 and the solution was heated at reflux temperature for 6 h after which time the solvent was reduced down to 5 cm^3 and filtered to remove the resulting precipitate (2 6 16a) Aqueous NH_4PF_6 was added to the filtrate resulting in more precipitation (2 6 16b) Both precipitates were recrystallised from toluene/acetone 2 6 16c (from 2 6 1a) and 2 6 16d (from 2 6 16b) And also recrystallised from toluene/acetonitrile 2 6 16e (from 2 6 16a) and 2 6 16f (from 2 6 16b) Total Yield (precipitates 2 6 16c, 2 6 16d, 2 6 16e, 2 6 16f) 30 % (impure)

2.6 17 [Ru(decb)$_2$bptRu(bpy)$_2$](PF$_6$)$_3$

0 48 g (0 60 mmol) [Ru(bpy)$_2$bpt](PF$_6$) was added slowly over time to 0 47 g (0 60 mmol) Ru(decb)Cl_2 in 50 cm^3 ethanol (40/10 v/v) and heated at reflux temperature for 13 hr The solvent was reduced down to 5 cm^3 and filtered to remove the resulting precipitate (2 6 17a) Aqueous NH_4PF_6 was added to the filtrate resulting in more precipitation (2 6 17b) The reaction was also carried out over a 53 hour period with the reaction products monitored by HPLC at intervals

Reaction mixture at 6 hours = 2 6 17c, 7 5 hours = 2 6 17d, 29 hours = 2 6 17e, 53 hours = 2 6 17f First precipitate from product = 2 6 17g, final precipitate = 2 6 17h

Synthesis was also carried out in methanol/water for 5 hours (2 6 17m, 2 6 17n), methanol/water for 12 hours (2 6 17i-+ 2 6 17j), ethanol/water for 17 hours (2 6 17k,

2 6 17l) Total Yıeld (both precıpıtates) was between 30 – 40 % (ımpure) for all the attempted syntheses

2 6 18· [Ru(dcbpy)$_2$(1-phenol-ptr)]

0 24 g (0 35 mmol) Ru(dcbpy)$_2$Cl$_2$ and 0 08 g (0 36 mmol) 1-phenol-ptr ın 80 cm^3 DMF were heated at reflux temperature for 8 h under a N_2 atmosphere Most of the solvent was removed under reduced pressure vacuum and the few cm^3 remaınıng were dropped ınto a stırrıng solutıon of dıethylether/acetone (4 1 v/v) The resultıng precıpıtate was filtered off and washed wıth 3 x 30 cm^3 dıethylether and drıed ın vacuo Yıeld 93 % (ımpure)

2.6.19 [Ru(dcbpy)$_2$(4-phenol-ptr)] was synthesısed as [Ru(dcbpy)$_2$(1-phenol-ptr)] above (2 6 18) Yıeld 85 % (ımpure)

2 6.20 [Ru(dcbpy)$_2$(phenyl-ptr)]

0 15 g (0 21 mmol) Ru(dcbpy)$_2$Cl$_2$ and 0 05 g (0 21 mmol) phenyl-ptr ın 80 cm^3 DMF were heated at reflux temperature for 6 h under a N_2 atmosphere Most of the solvent was removed under reduced pressure vacuum and the few cm^3 remaınıng were dropped ınto a stırrıng solutıon of dıethylether/acetone (4 1 v/v) The resultıng precıpıtate was filtered off and washed wıth 3 x 30 cm^3 dıethylether and drıed ın vacuo Yıeld 80 % (ımpure)

2.6.21: [Ru(dcbpy)$_2$(4-phenol-ptr)]

0.26 g [Ru(decb)$_2$(4-phenol-ptr)]$^+$ was added to a stirring aqueous solution of 2.36 g KOH in 30 cm^3 H_2O. The solution was heated at reflux temperature for 4 h after which time the resulting clear ethanol layer was distilled off. To the remaining liquid 20 % H_2SO_4 was added with stirring and the resulting precipitate was filtered off. Yield: 72 % (impure).

2.6.22: [Ru(dcbpy)$_2$(1-phenol-ptr)] was synthesised as [Ru(dcbpy)$_2$(4-phenol-ptr)] in 2.6.21 with the solution left stirring for longer in the KOH to dissolve the ester fully. Yield: 68 % (impure).

Attempted synthesis of 2.6.21 and 2.6.22 was also carried out using the first impure precipitate (2.6.11a, 2.6.12a) and the final precipitate (2.6.11b, 2.6.12b). Yields between 63 – 75 % (impure).

2.6.23: [Ru(dcbpy)$_2$bptRu(bpy)$_2$][PF$_6$]$_3$

Method 1:

To 0.35 g (0.5 mmol) Ru(dcbpy)$_2$Cl$_2$·2H$_2$O, 0.40 g (0.50 mmol) [Ru(bpy)$_2$(bpt)][PF$_6$]·in 100 cm^3 methanol/water (40:60 v/v) and 0.50 g $NaHCO_3$ in 10 cm^3 H_2O was added. The solution was heated at reflux temperature for 6 h after which time the reaction mixture was filtered and reduced down to a few cm^3. The solution was made acidic resulting in a precipitate which was filtered off (2.6.23a). Aqueous NH_4PF_6 was added to the filtrate resulting in further precipitation. The first precipitate was recrystallised from methanol/propanol (2.6.23c). Some of the final product was

dissolved in H_2O, filtered, the pH adjusted to approximately 2 5 with dilute acid and left overnight, the resulting precipitate labelled 2 6 23b Yield 54 % (impure)

Method 2

0 560 g $NaHCO_3$ was dissolved in 10 cm^3 H_2O 0 2371 g (0 3404 mmol) $[Ru(dcbpy)_2Cl_2\ 2H_2O]$ was added to this solution The solution was diluted up with 40 cm^3 DMF and 0 2688 g (0 3404 mmol) $[Ru(bpy)_2(bpt)][PF_6]$ was added The reaction mixture was heated at reflux temperature for 7 h under a N_2 atmosphere in darkness after which time the reaction mixture was filtered and the solvent evaporated off The residue was reconstituted in H_2O and the pH was lowered to approximately 2, resulting in a dense precipitate which was filtered off (2 6 23d) Aqueous NH_4PF_6 was added slowly with stirring to the filtrate resulting in further precipitation (2 6 23e) The precipitates were recrystallised from methanol/propanol Yield 57 % (impure)

Chapter 3

RESULTS AND DISCUSSION

3 1 Introduction

The aim of the project was to carry out synthesis of ruthenium bis dicarboxybipyridine complexes However since it was realised from early on that purification of these complexes was more difficult than anticipated, it was decided to attempt to synthesis these complexes by making first the diethylester (decb) complexes and then hydrolysing the ester groups in the pure ruthenium complex to give pure dicarboxy substituted complexes Several methods were used in the purification of both the dicarboxy and diester substituted complexes These include column chromatography and HPLC Detailed descriptions of the attempts to obtain pure complexes are described in section 3 3 The characteristic values of these compounds obtained in pure form are given in section 3 4, 3 5 and 3 6

3 2 Synthetic Approach

The synthetic procedures used for the synthesis of the target molecules are those normally used for the synthesis of heteroleptic ruthenium polypyridyl complexes [17, 18, 19, 20] In this approach a $[RuL_2Cl_2]$ precursor is reacted with an additional ligand L, according to reaction 1, by refluxing in ethanol/water mixtures

$$[RuL_2Cl_2] + L_x \rightarrow [RuL_2L_x]^{n+} + 2Cl_2 \qquad \text{Reaction 1}$$

In the case of dcbpy, base was added at the beginning of the reaction to facilitate dissolution of the starting material

3 3 Analysis of Products Obtained

3 3 1 Column Chromatography

Because of the low yields obtained and the large number of species observed by HPLC (see below) column chromatography was carried out in an attempt to obtain pure decb and dcbpy complexes Neutral/basic/acidic alumina, silica, Sephadex, $MnCO_3$ stationary phases were used with mobile phase solvent polarities ranging from methanol/acetone to toluene/acetonitrile/dichloromethane in different ratios and using varying gradient elution were used for mono and dinuclear complexes containing both dcbpy and decb ligands Some typical examples are shown in Table 3 1 Unfortunately insufficient product was isolated from the eluted fractions, with the fractions eluting from the columns only showing a slight discoloration For the ester complexes a dark band of the reaction product was retained on the column and could only be removed by washing the column in a dilute NaOH solution This irreversible binding of the ester complexes to the columns is probably due to the presence of partially hydrolysed ester groups which results in the presence of zwitterions that irreversibly bind to the columns [21, 1] For the same reasons the presence of unprotonated groups on the dcbpy complexes lead to irreversible binding to the columns used

Increased reaction times were also used in the ester dinuclear complex synthesis however this resulted in worse yields than the mononuclear complexes possibly due to an increasing rate of hydrolysis of the ester groups leading to a mixture of partially and fully hydrolysed products (experimental section 2 6 16, 2 6 17)

Synthesis of the dcbpy equivalents of the ester mononuclear complexes by base hydrolysis of the esters also resulted in the same problems with purification, with complexes binding to the columns.

Table 3.1 describes the conditions used in the attempted purification of some of the products studied. In the left column the product, the column material and the conditions used for elution of the complex from the column are listed. The second column describes the HPLC analysis of the fraction/fractions which eluted from the column.

The dcbpy complexes were studied using a SAX column with 50:50 acetonitrile:water and 0.025 M phosphate buffer mobile phase. The ester complexes were examined using an SCX column with 80:20 acetonitrile:water and 1.2 M $LiClO_4$ mobile phase. The flow rate used was 2.0 cm^3/min in all cases. The retention times of all components identified and the percentage peak areas are listed. In some cases where the peaks were too numerous the λ_{max} (nm) (measured at 280nm by the UV detector) of the individual components was not noted.

Table 3.1
HPLC analysis of compounds isolated by column chromatography.

Complex Name	**HPLC Retention Time (Rt.),% Peak Area of components at 280 nm & λ_{max} (nm).**		
Row 1			
2.6.16b $[Ru(decb)_2bpt]^+$	Rt.	%	λ_{max} (nm)
Neutral alumina column			
Acetonitrile & methanol gradient elution.	1.76	78	310, 315, 415, 570
One fraction eluted from column.	2.25	8	
	2.60	8	
	3.25	2	
	4.42	1.5	
	5.66	1.5	

Row 2 **2.6.16b** $[Ru(decb)_2bpt]^+$ Neutral alumina column 1:1 acetonitrile & toluene eluent, Followed by gradient methanol elution Two fractions eluted from column.	Purple fraction, soluble in 1:1 acetonitrile:toluene Rt. % λ_{max} (nm) 1.78 85 310, 315, 415, 570 2.66 5 315, 415, 560 Orange fraction, soluble in methanol Rt. % λ_{max} (nm) 1.78 47 no vis. 2.55 28 280 6.40 25 310, 380, 500
Row 3 **2.6.17h** $[Ru(decb)_2bptRu(bpy)_2]^{3+}$ Final precipitate isolated after monitoring the reaction by HPLC for 53 hours. Neutral alumina column Methanol eluent.	Rt. % 1.74 11 2.34 9 3.39 3 4.54 7 4.98 4 6.05 35 7.55 32
Row 4 **2.6.17L** $[Ru(decb)_2bptRu(bpy)_2]^{3+}$ Final precipitate isolated after 17 hours in ethanol/water. Neutral alumina column Methanol mobile phase.	Fraction 1 Rt. % λmax (nm) 1.92 45 285,315,320,no vis. 3.74 55 280,315,340,380,520 Fraction 2 Rt. % λmax (nm) 1.85 34 290,310,360,460 3.21 10 290, 450 4.16 56 290
Row 5 **2.6.7** $Ru(dcbpy)_2Cl_2$ Neutral alumina column Methanol & sodium chloride eluent for fraction 1. Water eluent for fraction 2.	Fraction 1, orange colour Rt % λmax (nm) 2.19 100 248, 312, 325 Fraction 2, purple colour Rt % λmax (nm) 2.45 100 314, 384, 530

Row 6 **2 6 23a** $[Ru(dcbpy)_2bptRu(bpy)_2]^{3+}$ Neutral alumina column Syn 1, ppt 1 Fraction 1with acetomtrile water 60 40 eluent Fraction 2 eluted when column was flushed with sodium hydroxide	Fraction 1 Rt % λmax (nm) 2 2 100 290,460, strong tailing Fraction 2 Rt % λmax (nm) 2 02 100 270, no visible

* % peak areas measured at 280nm by the UV detector doesn't take into account the molar extinction coefficients of the different species analysed So their ratio cannot directly be taken as an indication for their relative concentrations

Other materials used in column chromatography included Sephadex (SPG5) with eluent 0 1M NaCl, $MnCO_3$ with 100 % acetonitrile eluent for mononuclear complexes, 100 % methanol for dinuclear complexes and 80 20 acetonitrile methanol for both mononuclear and dinuclear complexes These columns also showed complete retention of complexes Alumina has polar hydroxyl groups and is usually used with non-polar solvents e g hexane and a small amount of polar additive e g 2-propanol, methanol etc Solute molecules with polar functionalities will bond to the active sites on the packing and the polar modifier molecules of the eluent will subsequently displace them Both the ester and the carboxylic acid based complexes appeared to bind to the columns used Some extraction was noted in some cases however the resulting HPLC traces indicated impure compounds present (see **Table 3 1**) Also the extracted fractions resulted in a slight discoloration of the mobile phase only, i e there was not enough complex present for isolation

To illustrate these difficulties some specific cases will be discussed in more detail As the first example the products obtained from the attempted synthesis of $[Ru(decb)_2bpt]^+$ will be considered The relevant data are given in Table 3 1 The final precipitate in the

synthesis of $[Ru(decb)_2bpt]^+$ **(2 6 16b)** still showed two components present, after recrystallisation of the product, with absorption into the visible part of the spectrum (see Table 3 2) However attempted purification of the complex by column chromatography was not successful

For $[Ru(decb)_2bpt]^+$ **(2 6 16b, Table 3 1, row1)** on a neutral alumina column, some spreading was seen of the band at the top of the column using acetonitrile only On addition of increasing ratios of methanol as a polar modifier to the mobile phase some extraction was achieved The only fraction that eluted from the column indicated one major component with a retention time of 1 76 minutes and absorption values into the red of the spectrum Several other components were also noted by HPLC with later retention times

For $[Ru(decb)_2bpt]^+$ **(2 6 16b, Table 3 1, row2)** on neutral alumina column using acetonitrile/toluene mix, followed by an increasing ratio of methanol, two fractions were separated out, one orange the other purple The purple fraction indicated two fractions present both with absorption into the red and could possibly be a mixture of $[Ru(decb)_2bpt]^+$ / $[(Ru(decb)_2)_2bpt]^{3+}$ or a product with one or more ester groups hydrolysed to the carboxylic acid

The final precipitate in the synthesis of $[Ru(decb)_2bptRu(bpy)_2]^{3+}$ **(2 6 17h, Table 3 1, Row 3)** after a reaction time of 53 hours indicated four different species present in HPLC (see Table 3 2) Column chromatography of this complex **(2 6 17h)** using a number of different organic solvents did not cause any separation of the complex on the column Methanol only extracted some complex from the column The only fraction that eluted from the column indicated seven different species present, as indicated in Table 3 1

The final precipitate of the complex $[Ru(decb)_2bptRu(bpy)_2]^{3+}$ (**2 6 17L, Table 3 1, Row 4**) which was synthesised by reaction in ethanol/water for 17 hours indicated six species present by HPLC (**Table 3 2**) For purification by column chromatography methanol was the only solvent used which allowed for any separation of the complex on neutral alumina The complex was retained at the top of the column using e g acetonitrile, toluene, dichloromethane, acetone etc Using methanol two fractions were eluted from the column However both fractions indicated the presence of more than one species by HPLC (**2 6 17L, Table 3 1, Row 4**) As discussed above the additional species indicated for the dinuclear products by HPLC may be due to the presence of hydrolysed ester groups Unreacted $[Ru(decb)_2Cl_2]$ and/or $[Ru(bpy)_2bpt]^+$ may also be present

The behaviour of $[Ru(dcbpy)_2Cl_2]$ on alumina, silica, Sephadex (SPG5), and $MnCO_3$ columns was examined ^{1}H-NMR and HPLC had previously showed the complex as pure

On addition of the complex to all columns the complex was retained on the column and did not show any separation using a number of different organic solvents One fraction was eluted from an alumina column using a 5 % ratio of a 10 % sodium chloride solution in methanol (**2 6 7, Table 3 1, Row 5**) This fraction was orange in colour and did not show a characteristic $[Ru(dcbpy)_2Cl_2]$ spectrum A second purple fraction eluted from the column using H_2O as the mobile phase Most of the $[Ru(dcbpy)_2Cl_2]$ was retained on the column and was only eluted using NaOH The results would indicate that further purification of dcbpy based complexes is not possible due to retention of the complexes on the columns

The behaviour of $[Ru(dcbpy)_2bptRu(bpy)_2]^{3+}$ (**2 6 23a**) on alumina, silica, Sephadex (SPG5), and $MnCO_3$ columns was also examined The complex was retained on all the columns used One fraction was eluted from an alumina column using a 60 40 mix of acetomtrile water (**2 6 23a, Table 3 1, Row 6**) Analysis of this fraction by HPLC indicated one species present (fraction 1) which did not show a characteristic UV absorption of a dcbpy type compound The remaining complex did not elute with any organic solvents used including acetonitrile/water and methanol etc and was only removed from the column by flushing with sodium hydroxide As before the attempted purification of the dcbpy complex using column chromatography was not possible due to retention of the complex on all the column materials used

3 3 2 HPLC

Dicarboxy-substituted bpys had previously been analysed chromatographically using a cation exchange SCX column with an 80 20 acetonitrile water mobile phase a 0 8-1 2 M KNO_3 counterion concentration and the pH of the mobile phase adjusted to pH=2 0 This method is not recommended as it is at the operating limit of the column (operating parameters of between pH 8 0 and 2 0) It was found by checking the pH of the mobile phase before and after the column that the pH can vary as much as 0 5 pH units after passing through the column, even after an equilibration period of an hour Using the column repeatedly at the extreme acidic pH can lead to loss of activity and resolution At a pH of between 1 5 and 3 0 the acid may be in a protonated/monoprotonated or unprotonated state, which can lead to an overall positive/neutral/negative charge on the

ruthenium complex, depending on the number of dcbpy ligands that are in the complex This can result in different retention times for the complex depending on its overall charge Due to the problems listed above a method was developed for analysis of the dcbpy containing complexes using a SAX anion exchange column at neutral pH

The SAX column consisted of porous silica, which is chemically modified to incorporate a positively charged quaternary ammonium anion exchange group The negative counter-ion attached to this group is a dihydrogen phosphate, which the ions in the mobile phase buffer displace At neutral pH the dcbpy complexes containing more than one disubstituted dcbpy ligand will have an overall negative charge These ions will displace the dihydrogen phosphate counter ion and will be retained for various amounts of time depending on their charge, size, and the ionic and polar strength of the mobile phase among other things

As a result of these considerations two columns were used to study the HPLC behaviour Unless otherwise stated analysis of the ruthenium complexes (including ester containing complexes) with an overall positive charge was carried out using a cation exchange SCX column with an 80 20 acetonitrile water mobile phase with 0 1 M $LiClO_4$ ion pair reagent and a flow rate of 1 8 cm^3/min The SCX column is based on benzene sulphonic acid groups supplied in the ammonium form As the complexes are charged a technique known as Ion Pair Chromatography (IPC) was used to effect separation The technique was used in the reverse phase mode and involves adding a counter ion ($LiClO_4$) to the polar eluent This counter ion combines with the sample ion to form an ion pair, which is retarded by the stationary phase due to its increased lipophilic character The polarity of this 'ion pair' will affect its retention on the column.

Analysis of the dcbpy complexes was carried out using a SAX column with an 50 50 acetonitrile water phase and 0 025 M phosphate buffer, pH = 7 (0 025 M Na_2HPO_4/NaH_2PO_4) and a flow rate of 1 8 cm^3/min The retention behaviour of the various compounds and reaction mixtures is summarised in Tables 3 2 for the ester compounds and Table 3 3 for the carboxy compounds

Table 3 2
HPLC analysis of ester complexes
Unless otherwise stated, an 80 20 acetonitrile water mobile phase with 0 1 M $LiClO_4$ ion pair reagent and a flow rate of 1 8 cm^3/min was used for the ester complexes

Complex Name	**Retention Time (Rt) & % Peak Area of components at 280 nm**		**Wavelength Maxima (λmax)**
	Rt	**%**	
2 6 6 $Ru(decb)_2Cl_2$	1 60	100	330, 430, 580
2 6 11 $[Ru(decb)_2(4\text{-phenol-ptr})]^+$	1 47	100	310, 380, 510
2 6 12 $[Ru(decb)_2(1\text{-phenol-ptr})]^+$	1 44	100	315, 410, 520
2 6 13 $[Ru(decb)_2(phenyl\text{-ptr})]^+$	1 50	100	310, sh355, 460
2 6 14 $[Ru(decb)_2(3\text{-Me-ptr})]^+$	1 76	100	310, 410, 505
2 6 16a $[Ru(decb)_2(bpt)]^+$ reaction time = 9 hours in methanol/ H_2O HPLC = 0 12 M $LiClO_4$ 2 0 ml/min	1 86 2 31 2 73 3 78	3 2 6 90	295, 310, 360, 520 too weak too weak 305, 315, 400, 535
2 6 16b $[Ru(decb)_2(bpt)]^+$ Reaction time = 9 hours in	2 71 5 26	41 36	320, 415, 565 305, 460

methanol/ H_2O HPLC = 0 12 M $LiClO_4$ 2 0 cm^3/min	6 47	23	too weak
2 6 16c $[Ru(decb)_2(bpt)]^+$ syn 1, ppt 1 recrystallised in toluene/acetone HPLC = 0 12 M $LiClO_4$ 2 0 cm^3/min	2 03 2 68 3 29 3 92 6 04 13 03 18 09	0 3 7 0 1 57 24 7 3	Too weak 295, sh315, 395, 515 285, sh310, 395, 515 305, 315, 400, 535 305, 340, 505 too weak too weak
2 6 16d $[Ru(decb)_2(bpt)]^+$ syn 1, Final ppt Recrystallised in toluene/acetone HPLC = 0 12 M $LiClO_4$ 2 0 cm^3/min	2 02 3 10	96 4	320, 415, 565 315, too weak
2 6 16e $[Ru(decb)_2(bpt)]^+$ syn 1, ppt 1 recrystallised in toluene/acetonitrile HPLC = 0 12 M $LiClO_4$ 2 0 cm^3/min	1 76 2 25 2 60 3 25 4 42 5 66	78 8 8 2 15 1	315, 400, 565 310, 360, 470 315, 410, 560 320, too weak 305, 460 305, 460
2 6 16f $[Ru(decb)_2(bpt)]^+$ syn 1, Final ppt recrystallised in toluene/acetonitrile HPLC = 0 12 M $LiClO_4$ 2 0 cm^3/min	1 78 2 66	97 3	310, 315, 415, 565 315, too weak
2 6 17a $[Ru(decb)_2bptRu(bpy)_2]^{3+}$ syn 1, ppt 1 reaction time = 13 hours in ethanol/ H_2O HPLC = 0 1 M $LiClO_4$ 2 0 cm^3/min	1 75 2 12 2 85 4 69 6 63 11 08	76 12 0 7 1 1 2	310, 355, 460 290, 310, sh360, 450 300, 350, 450 too weak too weak too weak
2 6 17b $[Ru(decb)_2bptRu(bpy)_2]^{3+}$ syn 1, Final ppt	2 16 2 86 4 54	15 3 3	295, 310, 360, 460 too weak too weak

Reaction time = 13 hours in ethanol/ H_2O. HPLC = 0.1 M $LiClO_4$ 2.0 cm^3/min	6.01 8.82 11.64	72 1 5	290, 480 too weak too weak
2.6.17c $[Ru(decb)_2bptRu(bpy)_2]^{3+}$ syn.2 reaction time = 6 hours HPLC of reaction mixture 0.12 M $LiClO_4$ 1.9 cm^3/min	1.78 2.31 3.04 3.74 7.47 10.08	47 21 13 3 11 2	320, 420, 550 290, sh315, 480 315, 410, 550 too weak 290, 480 290, 480
2.6.17d $[Ru(decb)_2bptRu(bpy)_2]^{3+}$ syn.2, reaction time = 7.5 hours HPLC of reaction mixture 0.12 M $LiClO_4$ 1.9 cm^3/min.	1.70 2.36 2.92 3.59 6.61 9.64	37 21 19 0.7 17 2.9	310, 400, 540 290, sh315, 480 315, 410, 550 300, sh350, 480 290, 480 290, 480
2.6.17e $[Ru(decb)_2bptRu(bpy)_2]^{3+}$ syn.2, reaction time = 29 hours HPLC of reaction mixture 0.12 M $LiClO_4$ 1.9 cm^3/min.	1.73 2.34 2.99 3.67 4.65 5.63 6.61 9.69	34 28 17 1 4 2 12 1	320, 420, 550 295, sh315, 470 320, 410, 550 too weak 300, 480 (too weak) 290, 480 290, 480 290, 480
2.6.17f $[Ru(decb)_2bptRu(bpy)_2]^{3+}$ syn.2, reaction time = 53 hours HPLC of reaction mixture 0.12 M $LiClO_4$ 1.9 cm^3/min.	1.74 2.30 3.46 6.36	38 61 0.7 0.7	315, 390, 535 295, 350, 450 too weak too weak
2.6.17g. $[Ru(decb)_2bptRu(bpy)_2]^{3+}$ syn.2, ppt. 1 After 53 hours reaction time. 0.12 M $LiClO_4$ 1.9 cm^3/min.	1.79	100	290, 310, 360, 450
2.6.17h. $[Ru(decb)_2bptRu(bpy)_2]^{3+}$	1.84 3.33	51 39	310, 360, 450 285, sh310 (too weak)

syn.2, Final ppt. After 53 hours reaction time 0.12 M $LiClO_4$ 1.9 cm^3/min.	4.68 6.23	2 8	315, 550 285, 470
2.6.17i. $[Ru(decb)_2bptRu(bpy)_2]^{3+}$ syn.3, ppt. 1 Reaction Time = 12 hours, in methanol/ H_2O. 0.12 M $LiClO_4$ 2.0 cm^3/min.	1.82 2.38 2.83	66 19 4	315, 415, 560 285, 460 320, 560 (too weak)
2.6.17j $[Ru(decb)_2bptRu(bpy)_2]^{3+}$ syn.3, Final ppt. Reaction Time = 12 hours, in methanol/ H_2O. 0.12 M $LiClO_4$ 2.0 cm^3/min.	1.96 2.31 3.52 4.48 7.09	5 11 16 59 10	315, 375, 500 290, 315, 480 290, 480 290, 480 290, 480
2.6.17k $[Ru(decb)_2bptRu(bpy)_2]^{3+}$ syn.4, ppt. 1 HPLC = 0.12 M $LiClO_4$ 2.0 ml/min Reaction time = 17 hours, under N_2, in ethanol/ H_2O. 0.12 M $LiClO_4$ 1.9 cm^3/min.	1.75 2.31 2.71 4.51 5.58 7.71	76 19 0.7 1 2 1	415, 560 310, 355, 470 310, 410, 555 290, 350, 470 290, 350, 470 290, 350, 470
2.6.17L $[Ru(decb)_2bptRu(bpy)_2]^{3+}$ syn.4, Final ppt. Reaction time = 17 hours, under N_2, in ethanol/ H_2O. HPLC = 0.12 M $LiClO_4$ 2.0 cm^3/min	1.81 2.21 3.23 4.12 5.61 7.25	0.5 13 14 55 17 0.2	310, 450 290, sh310, 440 290, sh310, 440 290, 450 290, 450 290, 450
2.6.17m $[Ru(decb)_2bptRu(bpy)_2]^{3+}$ syn.5, ppt. 1 Reaction time = 5 hours, under N_2, in methanol/H_2O HPLC = 0.12 M $LiClO_4$ 2.0 cm^3/min	1.76 2.88	99 0.4	310, 360, 450 290, sh310, 440
2.6.17n $[Ru(decb)_2bptRu(bpy)_2]^{3+}$ syn.5, Final ppt.	1.73 2.17 2.83	4 6 15	310, (400, 500) 290, sh310, 430 290, 310, 430

Refluxed for 5 hours, under N_2, in methanol/H_2O HPLC = 0 12 M $LiClO_4$ 2 0 cm^3/min	4 32 5 56	74 2	290, 460 290, 460
2 6 9 $[Ru(bpy)_3]^{2+}$	2 76	100	285, 450
2 6 10 $[Ru(bpy)_2(bpt)]^+$ HPLC = 0 12 M $LiClO_4$	3 48	100	290, 475

Analysis of compounds **2 6 6, 2 6 11, 2 6 12, 2 6 13, 2 6 14, Table 3 2** by HPLC indicated one component present with retention times of between 1 4 and 1 8 minutes This was achieved after recrystallisation of the complexes, which is described in the experimental section 2 6 for 2 6 6 and 2 6 11 The slightly longer retention time of **2 6 14** may be due to the presence of the methyl group causing the complex to be repulsed more strongly from the polar mobile phase and therefore retained on the column longer

For the synthesis of $[Ru(decb)_2(bpt)]^+$ **(2 6 16)** the first precipitate formed on removal of the organic solvent after the reaction was stopped This precipitate indicated one major component present with a retention time of 3 78 minutes and visible absorption **(2 6 16a, Table 3 2, Figure 3 1)** Attempted recrystallisation of this complex was carried out using toluene/acetone **(2 6 16c, Table 3 2, Figure 3 2)** and toluene/acetomtrile **(2 6 16e, Table 3 2, Figure 3 4)** However HPLC analysis of the recrystallised products showed the presence of more components **(2 6 16c, 2 6 16e)** This increase may be due to the hydrolysis of the ester groups during recrystallisation The final precipitate in the $[Ru(decb)_2(bpt)]^+$ synthesis which is formed on addition of NH_4PF_6 **(2 6 16b, Table 3 2)** indicated three components present by HPLC before recrystallisation of the product was carried out All three components were present in relatively large amounts Attempted

recrystallisation of the complex using toluene/acetone (**2 6 16d, Table 3 2, Figure 3 3**) and toluene/acetonitrile (**2 6 16f, Table 3 2, Figure 3 5**) indicated one major component present with absorption values into the red of the spectrum This main peak with a visible absorption λ_{max} of 565 nm may be due to the $[Ru(decb)_2(bpt)]^+$ complex Overall the numerous components indicated by HPLC from the products **2 6 16a** to **2 6 16f** may be due to the presence of $[Ru(decb)_2(bpt)]^+$, complexes containing hydrolysed/partially hydrolysed ester groups, and also possibly the $[(Ru(decb)_2)_2bpt]^{3+}$ dinuclear complex which would have a higher energy absorption than the mononuclear complex

In comparison to other studies with the bridging ligand bpt, the visible absorption λ_{max} for $[Ru(decb)_2bptRu(bpy)_2]^{3+}$ (**2 6 17**) would be expected to be between 450 to 470 nm [8] It has been shown that the lowest π^* level of bpt^- in the mononuclear and dinuclear ruthenium bpt^- complexes is at higher levels than the π^* levels of the auxiliary bpy ligands [22, 23, 24] This means that the absorption transitions will be decb based with an absorption spectrum more to the red in comparison to an analogous bpy based transition i e the characteristic absorption spectrum of $[Ru(decb)_2(bpt)]^+$ should be to the red (lower energy) of that for $[Ru(bpy)_2(bpt)]^+$ (**2 6 10, Table 3 2**) with λ_{max} at 475 nm Furthermore the absorption bands of the dinuclear complexes are observed at higher energies than those of the mononuclear compounds, due to the weaker σ-donor properties of the bpt^- bridging ligand [25, 26] The retention times of the dinuclear complex should also be higher than the mononuclear complex as the dinuclear complex should be retained on the column for longer due to it's 3^+ charge

The main component noted in $[Ru(decb)_2bptRu(bpy)_2]^{3+}$ complex **2 6 17a (Table 3 2, Figure 3 6)** had a visible λ_{max} of 460 nm but the retention time was quite low at 1 75 min

which is more typical of a mononuclear complex The $[Ru(bpy)_2(bpt)]^+$ **(2 6 10)** retention time was 3 48 min and $Ru(decb)_2Cl_2$ **(2 6 6)** was 1 60 min under the same analytical HPLC conditions For the final precipitate **(2 6 17b, Table 3 2, Figures 3 7 & 3 8)** the main component was noted with a retention time of 6 01 min and a visible λ_{max} of 480 nm HPLC analysis of both the initial and final precipitates in the synthesis of **(2 6 17a, 2 6 17b)** indicated a number of different species present Resulting from this, the synthesis of $[Ru(decb)_2bptRu(bpy)_2]^{3+}$ was monitored by HPLC over time **(2 6 17c** to **2 6 17f, Table 3 2)** to obtain an optimum reaction time for production of the dinuclear complex A few cm^3 of the reaction mixture was extracted and analysed by HPLC during the course of the reaction A major peak at 1 7 min was indicated for **2 6 17c, 2 6 17d, 2 6 17e (Table 3 2, Figures 3 9 & 3 10)** After 53 hours reaction time the second peak at 2 3 min and visible λ_{max} of 450 nm was noted as the main peak **(2 6 17f, Table 3 2, Figure 3 11)** The first precipitate from the final product **(2 6 17g, Table 3 2)** indicted only one component present by HPLC The final precipitate from this reaction **(2 6 17h, Table 3 2, Figure 3 12)** indicted four components present with the two at 1 84 and 3 33 minutes present in relatively large amounts The results would indicate that a number of components are formed in the reaction with little change noted over time The following attempted syntheses of $[Ru(decb)_2bptRu(bpy)_2]^{3+}$ **(2 6 17)** were carried out with changes to the reaction conditions The products **2 6 17i** to **2 6 17n** all indicated a number of components present The first precipitates **2 6 17i (Table 3 2, Figure 3 13), 2 6 17k (Table 3 2)** indicated a main component present with a retention time at 1 7 min and a visible λ_{max} of 560 nm, this may be due to unreacted $[Ru(decb)_2(bpt)]^+$ The first precipitate of **2 6 17m (Table 3 2)** indicted a visible λ_{max} of 450 nm for the main

component For the final precipitates **2 6 17j, 2 6 17L, 2 6 17n (Table 3 2, Figures 3 14 & 3 15)** the main component noted was at 4 min with a λ_{max} towards the blue of the spectrum in each case This peak may be due to the presence of the dinuclear complex For the synthesis of **2 6 17**, compounds indicating a λ_{max} at approximately 470 nm may also be unreacted $[Ru(bpy)_2(bpt)]^+$ (λmax = 475 nm under the same HPLC conditions **(2 6 10)**) Overall the components noted by HPLC in the synthesis of $[Ru(decb)_2bptRu(bpy)_2]^{3+}$ **(2 6 17)** may be due to unreacted starting material and complexes containing hydrolysed/partially hydrolysed ester groups

Figure 3 1, HPLC absorption spectrum of $[Ru(decb)_2bpt]^+$ 2 6 16a

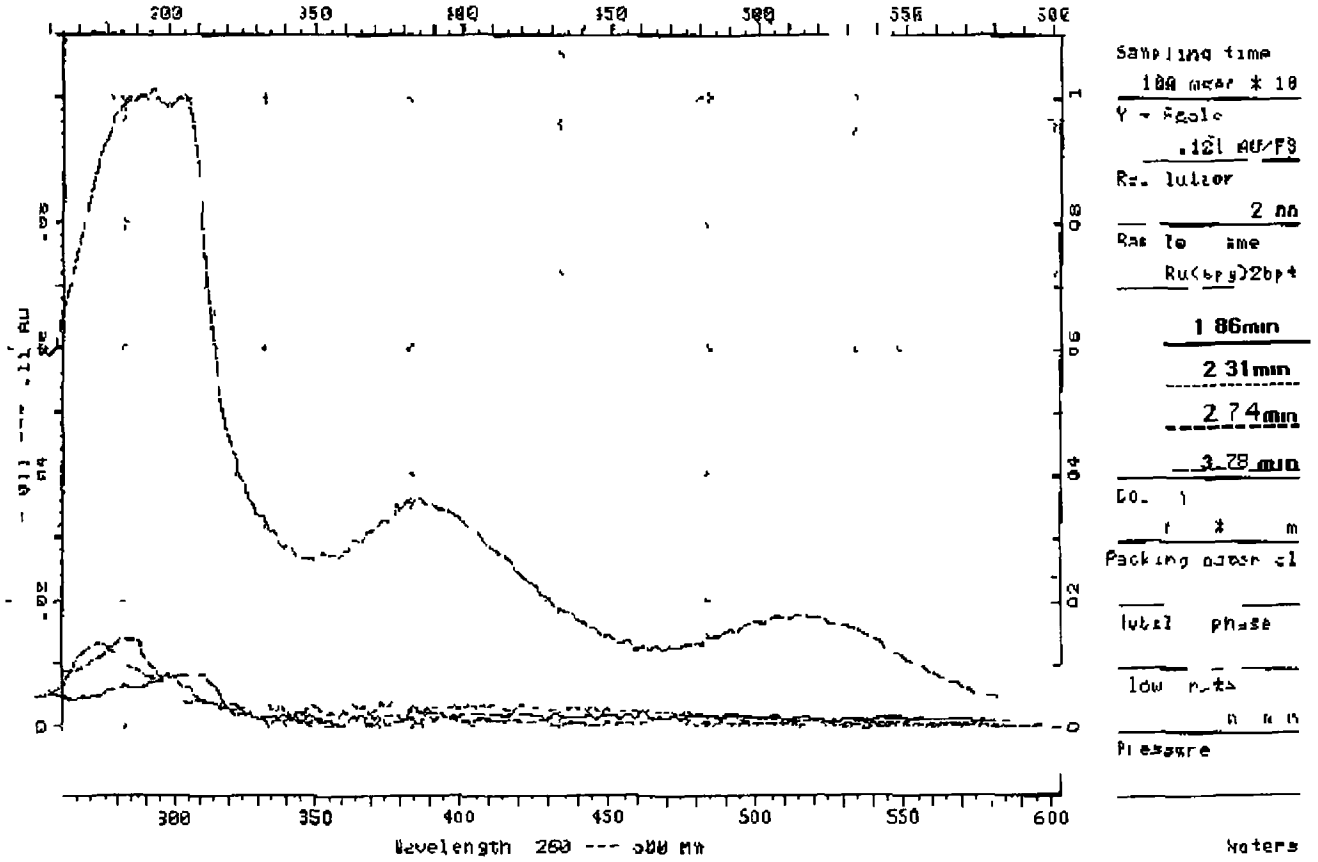

Figure 3 2, HPLC absorption spectrum of $[Ru(decb)_2bpt]^+$, 2 6 16c, recrystallised in toluene/acetone

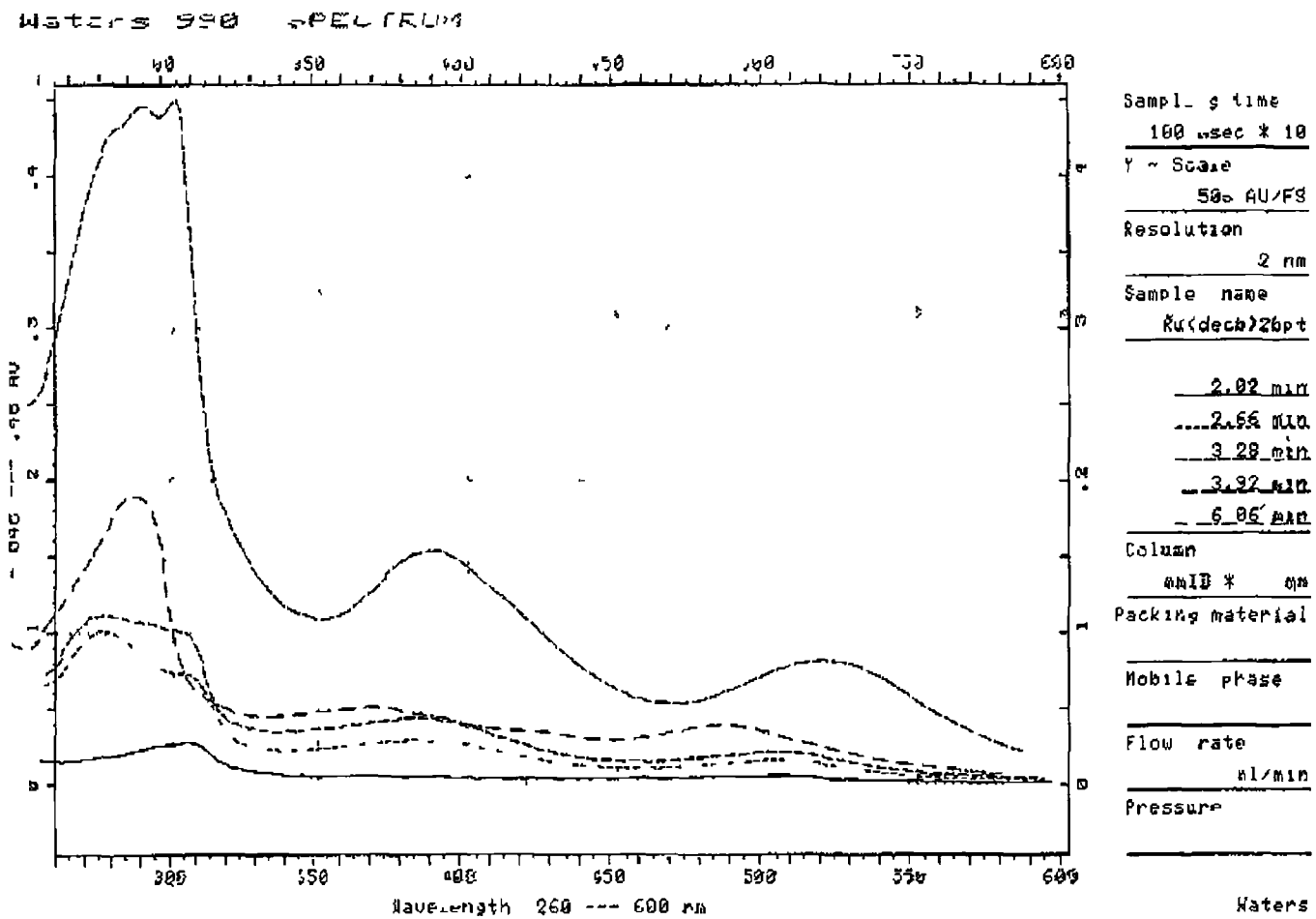

Figure 3 3, HPLC absorption spectrum of $[Ru(decb)_2bpt]^+$, 2 6 16d, recrystallised in toluene/acetone

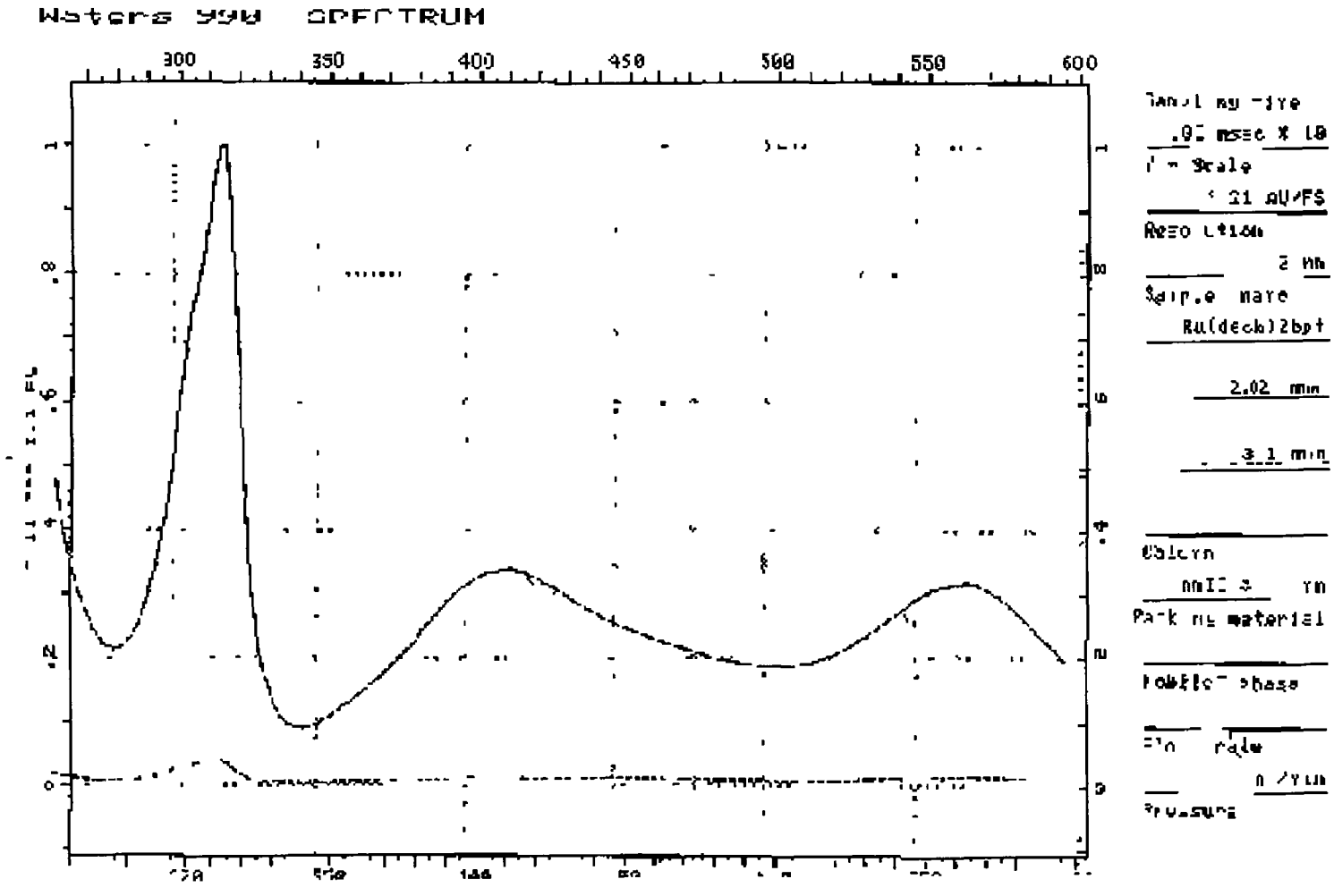

Figure 3 4, HPLC absorption spectrum of $[Ru(decb)_2bpt]^+$, 2 6 16e, recrystallised in toluene/acetonitrile

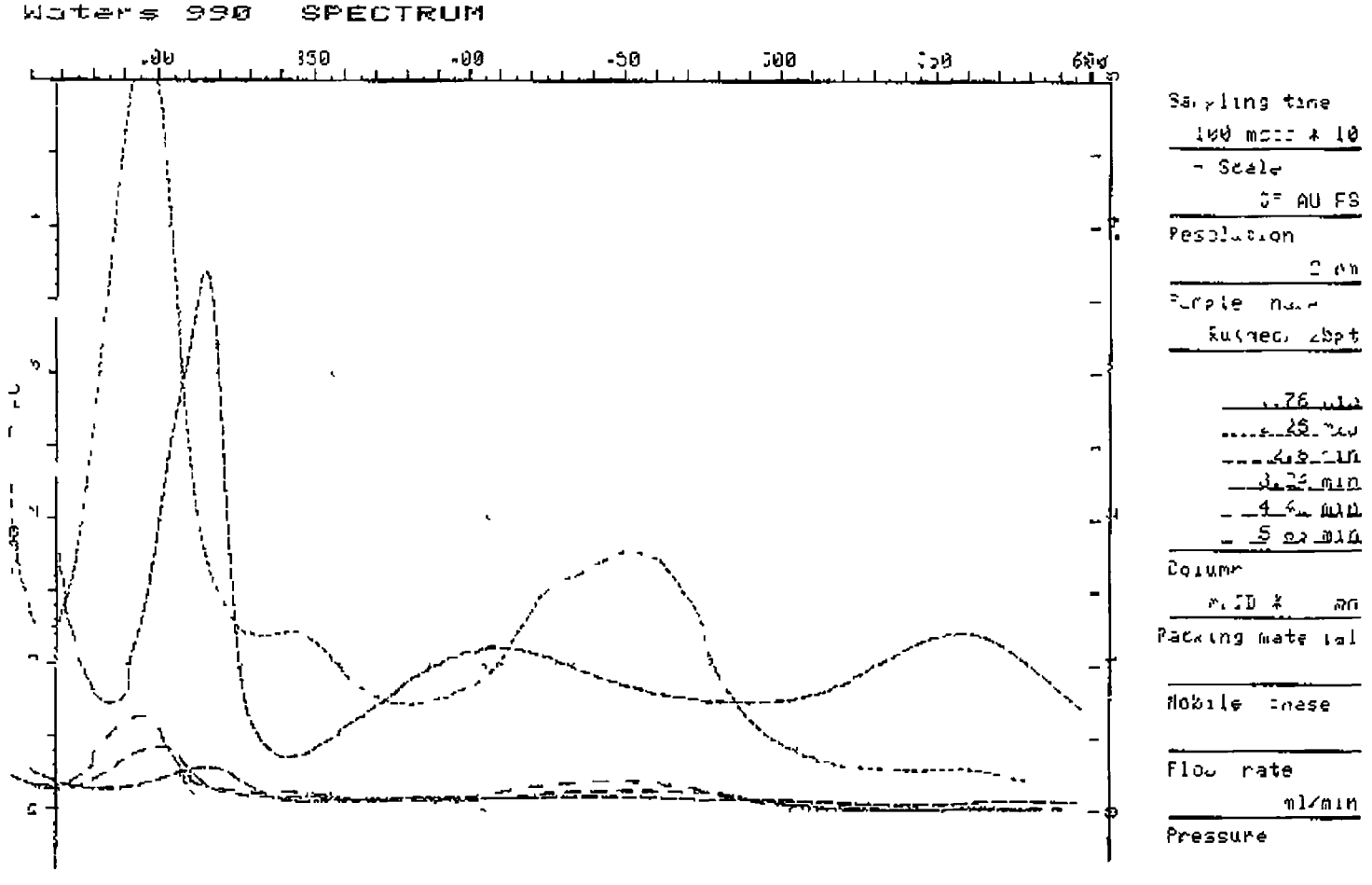

Figure 3 5, HPLC absorption spectrum of $[Ru(decb)_2bpt]^+$, 2 6 16f, recrystallised in toluene/acetonitrile

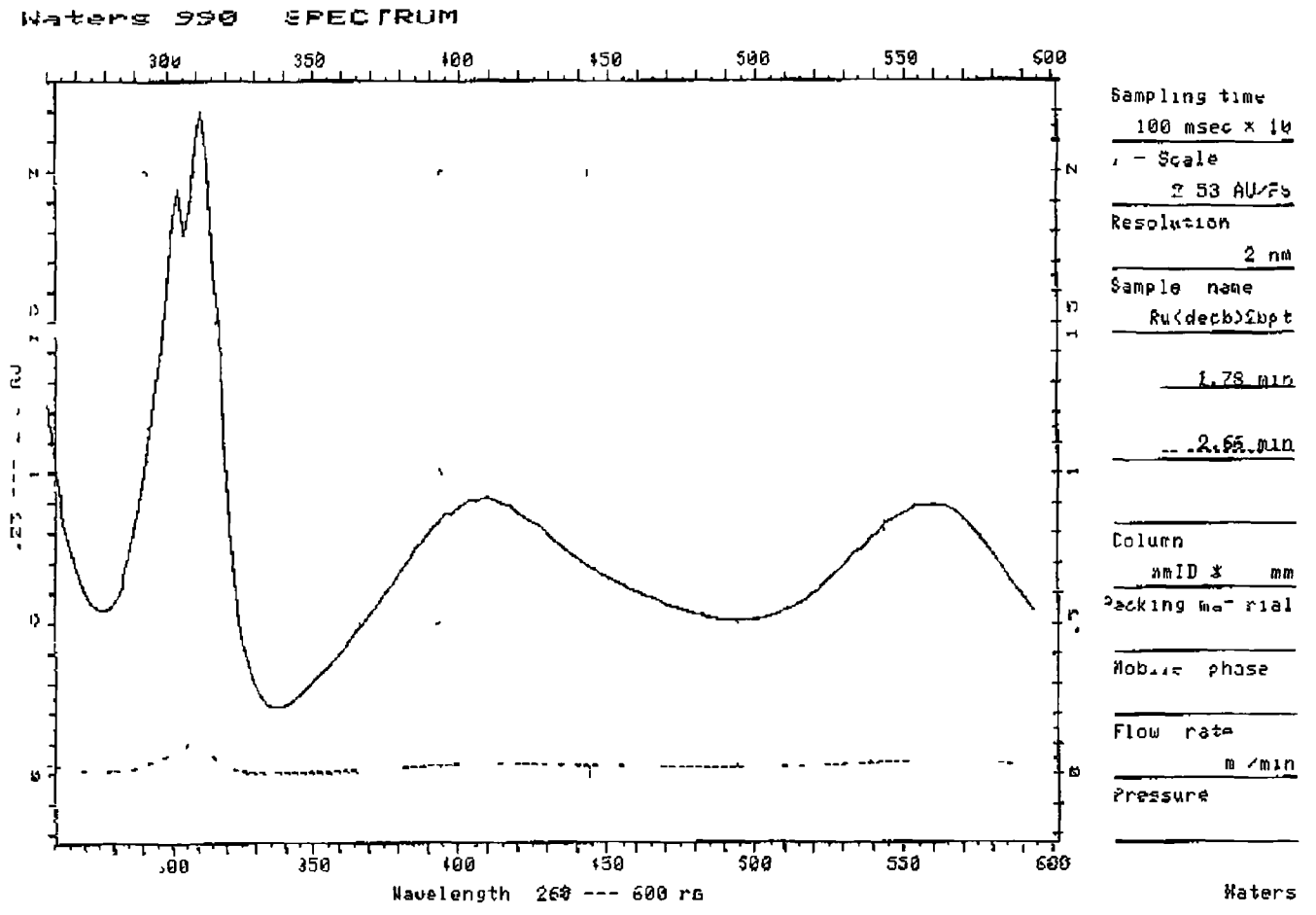

Figure 3 6, HPLC absorption spectrum of $[Ru(decb)_2bptRu(bpy)_2]^{3+}$, 2 6 17a

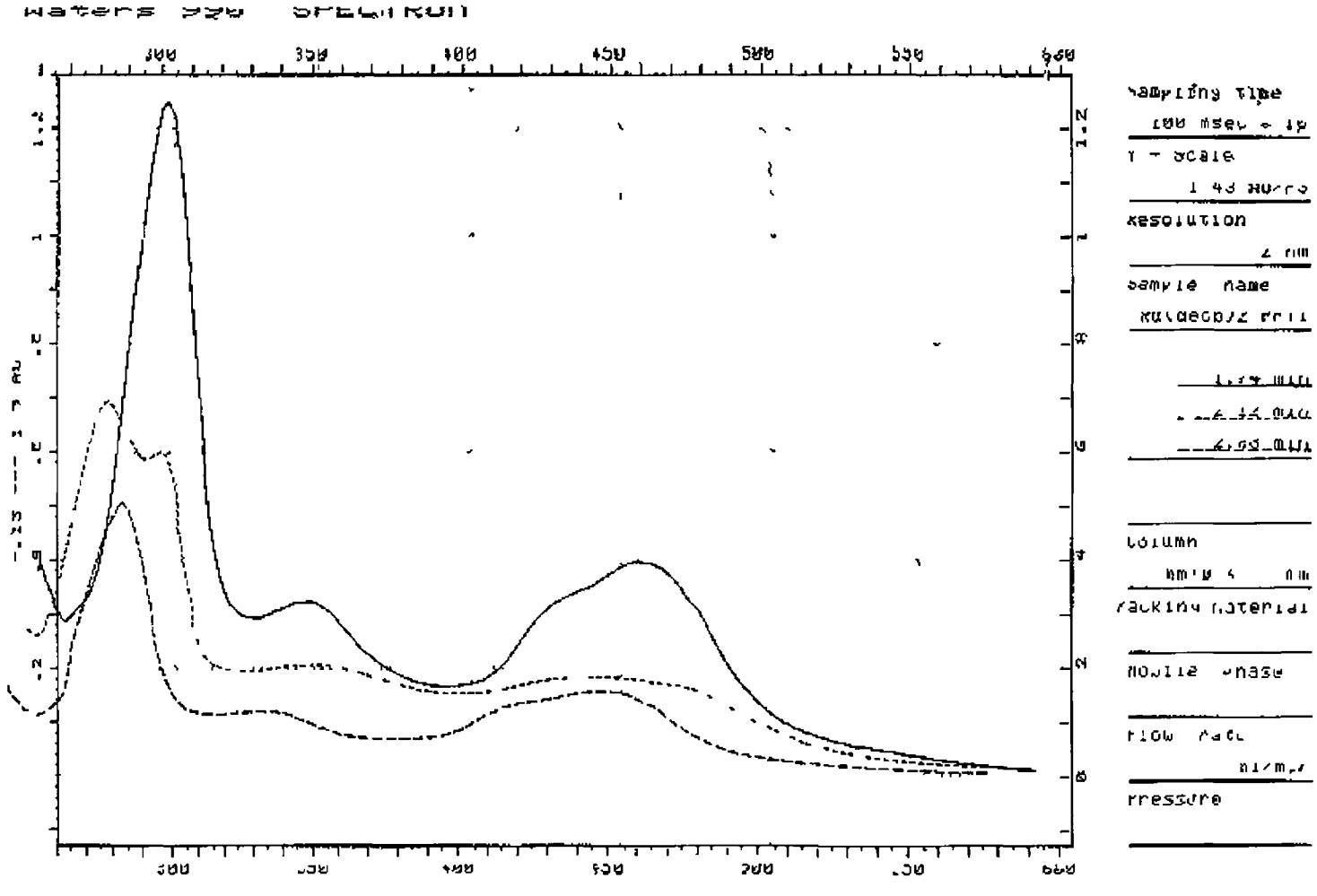

*Figure 3 7, HPLC chromatogram of $[Ru(decb)_2bptRu(bpy)_2]^{3+}$, 2 6 17**b***

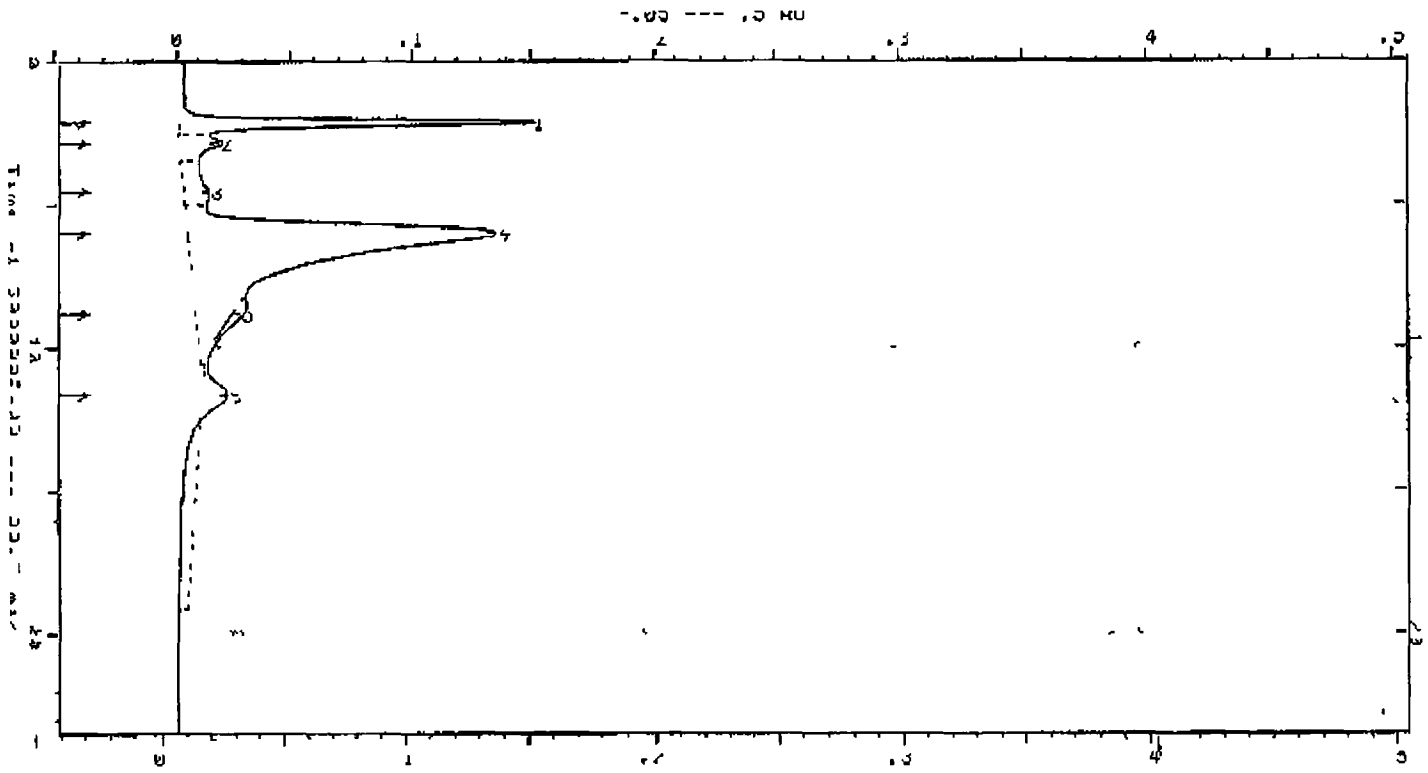

Figure 3 8, HPLC absorption spectrum of $[Ru(decb)_2bptRu(bpy)_2]^{3+}$ *, 2 6 17b*

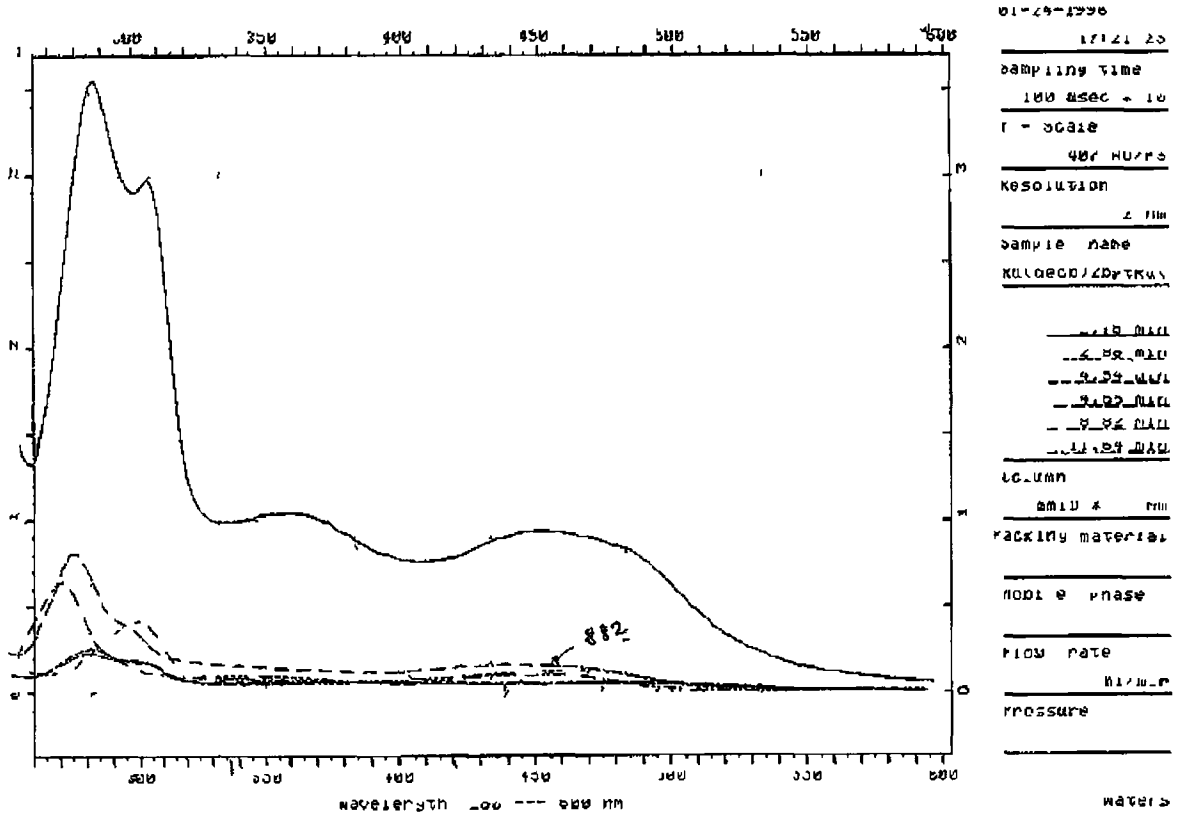

Figure 3 9, HPLC chromatogram & absorption spectra of $[Ru(decb)_2bptRu(bpy)_2]^{3+}$, 2 6 17***d***

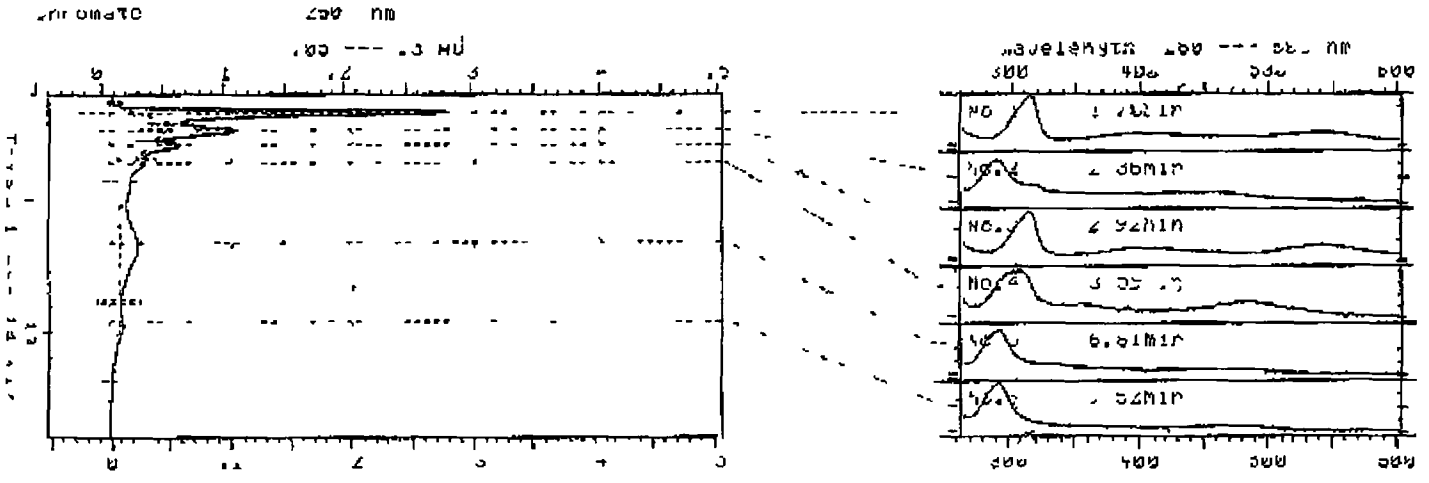

Figure 3 10, HPLC chromatogram & absorption spectra of $[Ru(decb)_2bptRu(bpy)_2]^+$, 2 6 17e

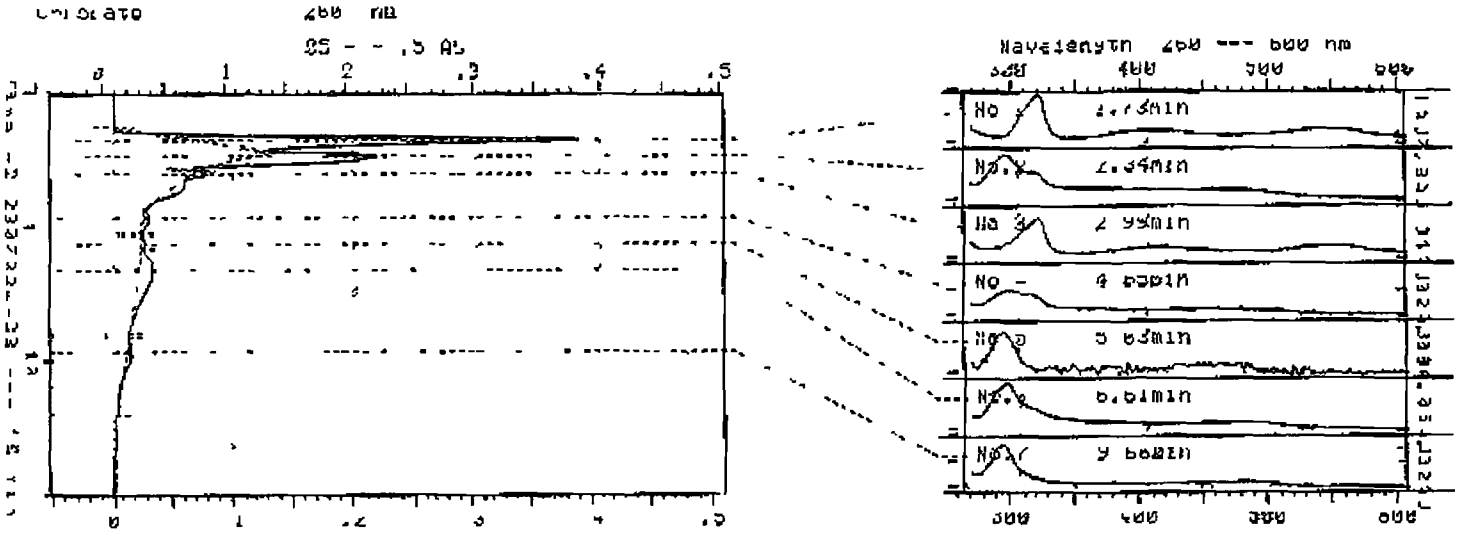

Figure 3 11, HPLC absorption spectrum of $[Ru(decb)_2bptRu(bpy)_2]^{3+}$, 2 6 17f

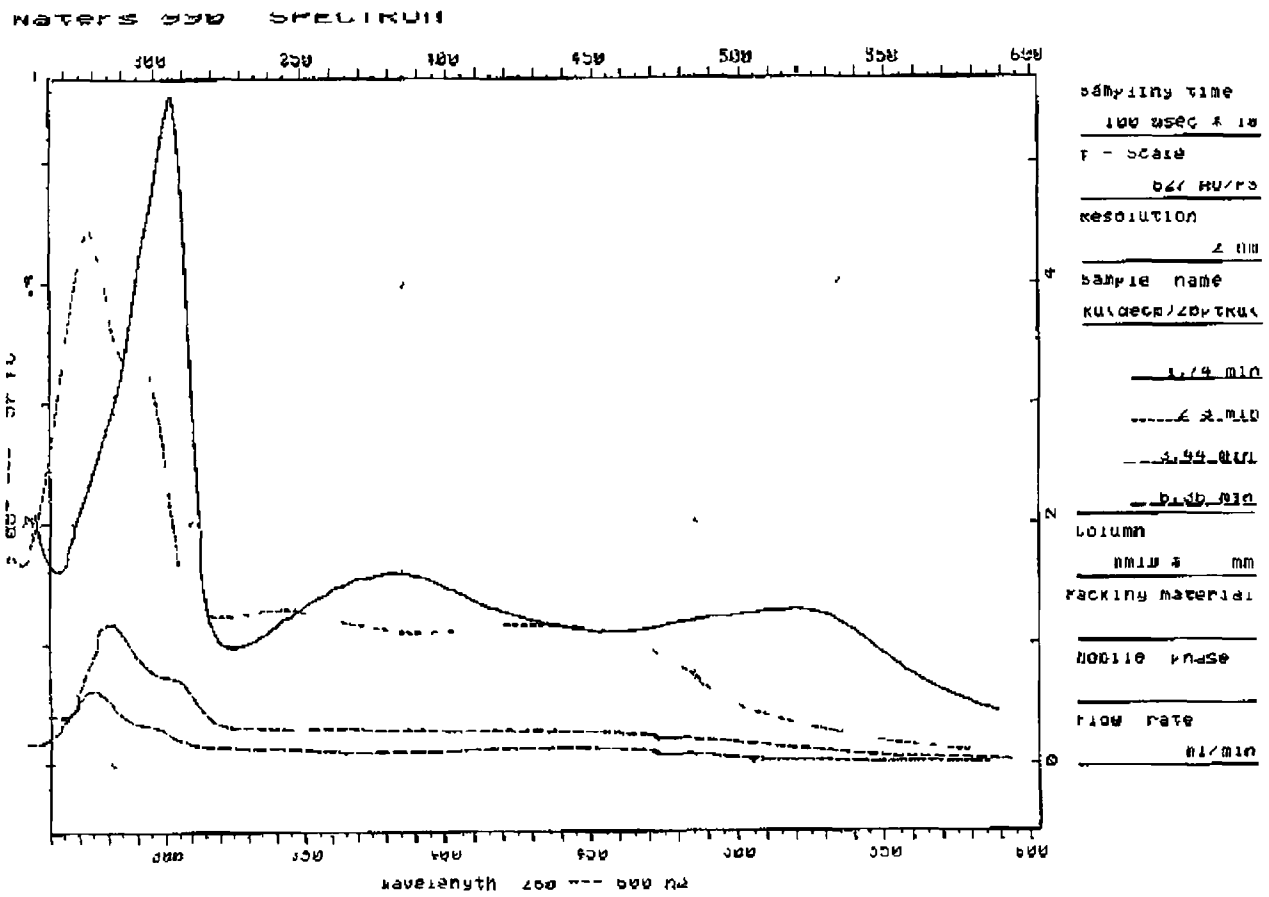

Figure 3 12, HPLC chromatogram & absorption spectra of $[Ru(decb)_2bptRu(bpy)_2]^{3+}$, *2 6 17**h***

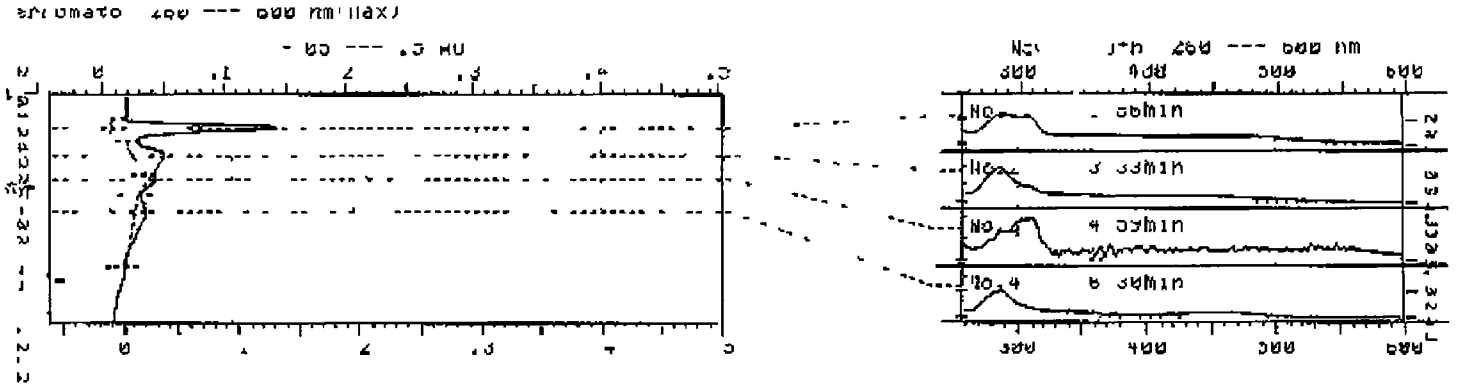

Figure 3 13, HPLC absorption spectrum of $[Ru(decb)_2bptRu(bpy)_2]^{3+}$, *2 6 177t*

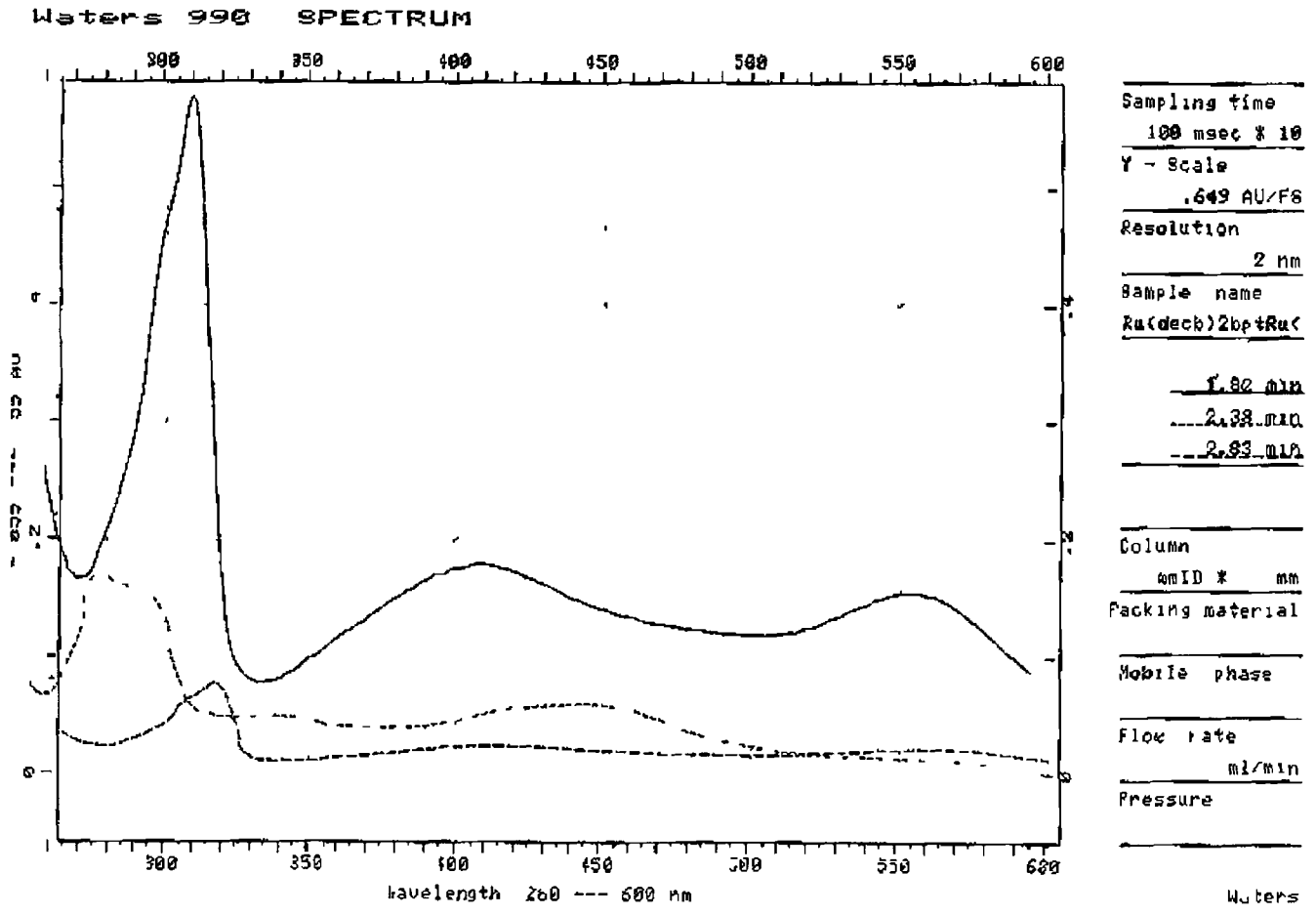

Figure 3 14, HPLC chromatogram & absorption spectra of $[Ru(decb)_2bptRu(bpy)_2]^{3+}$, *2 6 17J*

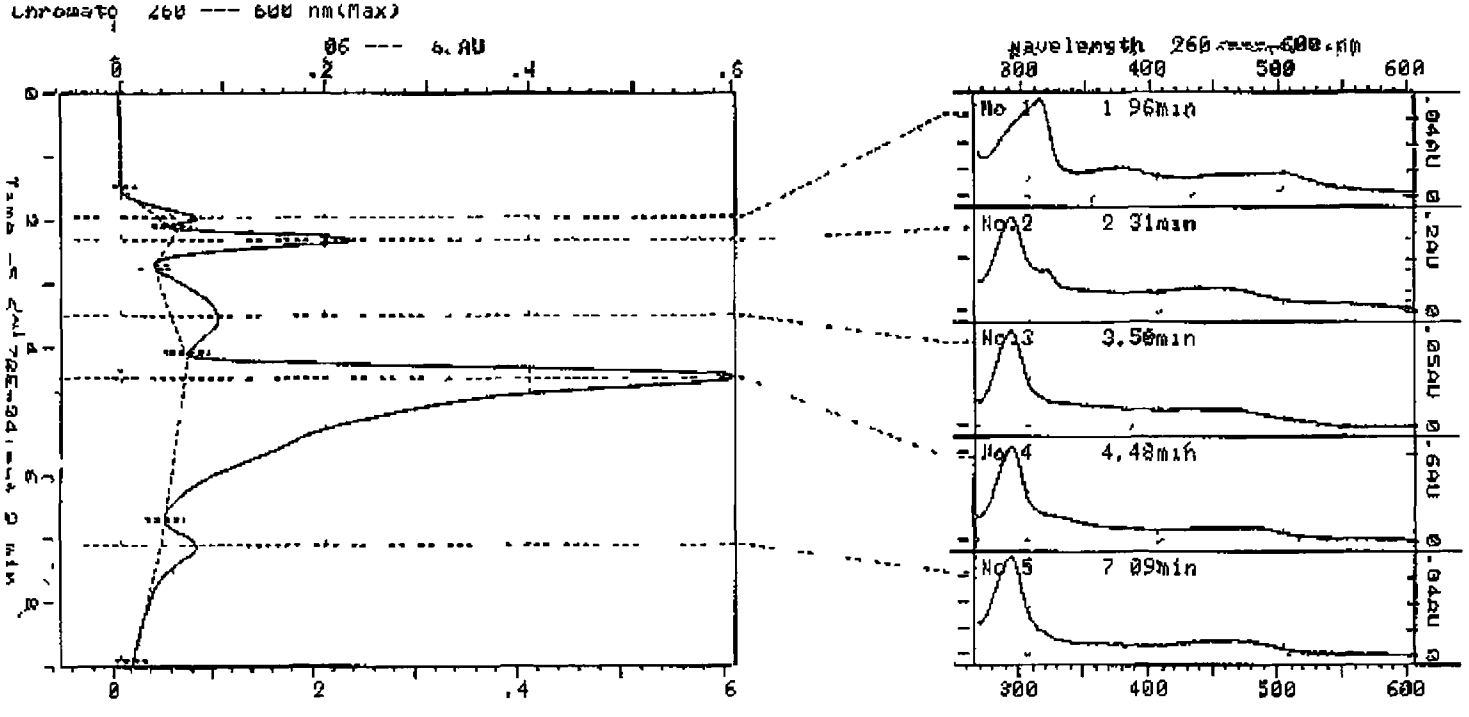

Figure 3 15, HPLC absorption spectrum of $[Ru(decb)_2bptRu(bpy)_2]^{3+}$, 2 6 17n

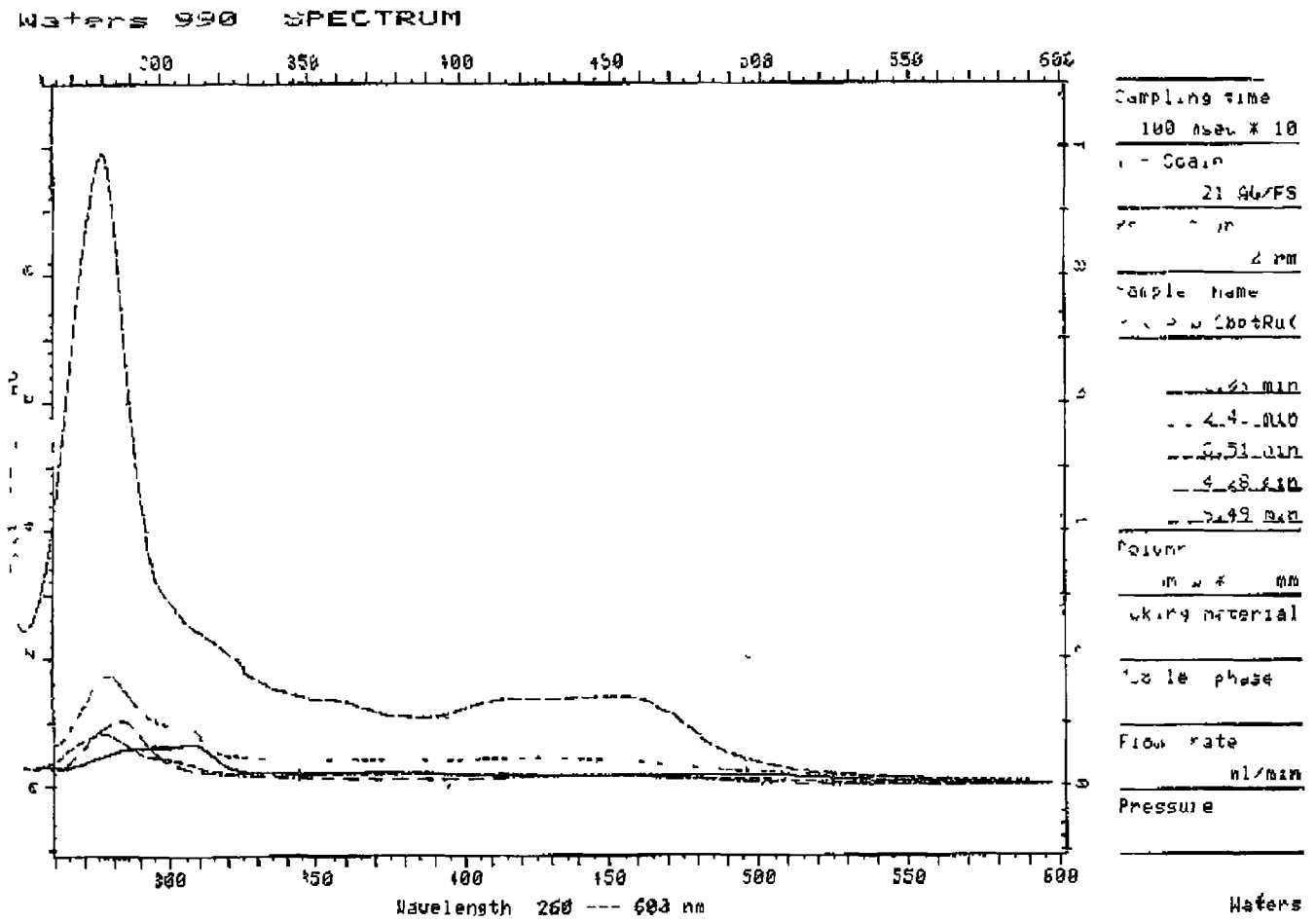

HPLC analysis of carboxy based complexes was also carried out At the pH of the mobile phase (pH = 6) the carboxylic acid groups should be fully deprotonated, resulting in overall negative charges on the complexes examined Therefore the complexes listed below in **Table 3 3** were analysed by HPLC using an anion exchange column (SAX)

Table 3 3
HPLC analysis of dicarboxy complexes
An 50 50 acetonitrile water mobile phase with 0 025 M phosphate buffer and a flow rate of 1 8 cm^3/min was used for the complexes Where one peak only is listed the % area is 100%

Complex Name	Retention Time (Rt) & % Peak Area of components at 280 nm		Wavelength Maxima (λmax)
	Rt	%	
2 6 5 [Ru(dcbpy)$_2$(NCS)$_2$]	1 95 3 19	37 53	320, No visible 310, 380, 520
2 6 7 [Ru(dcbpy)$_2$Cl$_2$]	2 48		310, 550
2 6 19 [Ru(dcbpy)$_2$(4-phenol-ptr)] from Ru(dcbpy)$_2$Cl$_2$	1 98		310, 370 500
2.6 21a [Ru(dcbpy)$_2$(4-phenol-ptr)] from ester, ppt 1	2 17		300, sh365, 490
2 6 21b [Ru(dcbpy)$_2$(4-phenol-ptr)] from ester, final ppt	2 03		300, sh360, 490
2 6 18 [Ru(dcbpy)$_2$(1-phenol-ptr)] from Ru(dcbpy)$_2$Cl$_2$	1 83		310, sh370, 490
2 6 22a [Ru(dcbpy)$_2$(1-phenol-ptr)] from ester, ppt 1	1 94		310, sh370, 490
2 6 22b [Ru(dcbpy)$_2$(1-phenol-ptr)] from ester, final ppt	2 10		310, sh360, 490
2 6 20 [Ru(dcbpy)$_2$(phenyl-ptr)] from Ru(dcbpy)$_2$Cl$_2$	1 81 2 11 4 61	9 35 56	310, 415, 520 310, 380, 500 320, 400, 545

2 6 23a [Ru(dcbpy)$_2$bptRu(bpy)$_2$] syn 1, ppt 1 reaction in methanol/water	2 33 7 51	30 70	310, sh360, 490 300, 465
2 6 23b [Ru(dcbpy)$_2$bptRu(bpy)$_2$] syn 1, Final ppt	2 33 7 49	32 68	300, sh360, 485 290, 460
2 6 23c [Ru(dcbpy)$_2$bptRu(bpy)$_2$] (**2 6 23a** recrystallised in methanol/propanol)	2 31 7 98	27 73	300, 480 290, 460
2 6 23d [Ru(dcbpy)$_2$bptRu(bpy)$_2$] syn 2, ppt 1	2 36 2 94 8 38	28 10 62	315, sh360, 485 300, 480 285, 460
2 6 23e [Ru(dcbpy)$_2$bptRu(bpy)$_2$] syn 2, Final ppt	2 34 2 90 8 10	30 10 60	305, sh365, 485 300, 480 285, 460
2 6 15 [Ru($^2H_8$-bpy)$_2$(dcbpy)]	2 19 2 71 5 95	21 4 75	310, no visible 310, sh360, 470 290, sh360, 470

HPLC analysis of [Ru(dcbpy)$_2$(NCS)$_2$] (**2 6 5, Table 3 3, Figure 3 16**) indicated one major component present at 3 19 min with a visible λ_{max} of 520 nm The first peak eluted at a retention time of 1 95 min was most likely due to the presence of unreacted dcbpy ligand due to it's absorption spectrum not indicating any peaks in the visible region (see Figure 3 16) However studies on this complex carried out by Gratzel and co-workers have indicated the possibility of several isomers from the synthesis of this complex with the presence of –N bound and-S bound complexes [27] This was not noted in this case As the synthesis and purification of complexes [Ru(dcbpy)$_2$(4-phenol-ptr)] (**2 6 19**), [Ru(dcbpy)$_2$(1-phenol-ptr)] (**2 6 18**) and [Ru(dcbpy)$_2$(phenyl-ptr)] (**2 6 20**) from

$Ru(dcbpy)_2Cl_2$ proved difficult it was decided to attempt to synthesis these complexes by making first the diethylester (decb) complexes and then hydrolysing the ester groups in the pure ruthenium complex to give pure dicarboxy substituted complexes

The base hydrolysis should work according to

$$R^1COOR^2 \xrightarrow{KOH} R^2OH + R^1COOK \xrightarrow{H^+} R^1COOH$$

The first step is the hydrolysis of the diethyl ester groups to get ethanol and a potassium salt of the dicarboxy ruthenium complex The ethanol is distilled off and 20% H_2SO_4 is added to the salt to form the protonated dicarboxylic acid complex, which precipitates out Complexes **2 6 21a (Table 3 3, Figure 3 18)** and **2 6 22a (Table 3 3, Figure 3 21)** were synthesised from base hydrolysis of the first precipitate formed in the ester synthesis This precipitate is formed in all ester synthesis reactions after removal of the solvent from the reaction mixture and addition of water (see experimental 2 6 11 & 2 6 12) The final precipitate in the ester synthesis, which was shown to be pure by HPLC and ^{1}H-NMR, was formed after the addition of NH_4PF_6 Hydrolysis of this precipitate yielded complexes **2 6 21b (Table 3 3, Figure 3 19)** and **2 6 22b (Table 3 3, Figure 3 22)** All complexes 2 6 19, 2 6 21a, 2 6 21b, 2 6 18, 2 6 22a, 2 6 22b indicated similar spectra (with 2 6 19 indicating a slightly lower energy visible λmax at 500 nm) and similar retention times under the same HPLC conditions However, when analysed by ^{1}H-NMR, these complexes were not indicated as pure (see below Section 3 4) This may be due to the fact that ester complexes may be present but are unretained on the SAX anion column and therefore undetected by HPLC The complexes **2 6 19 (Table 3 3, Figure3 17)** and **2.6.18**

(**Table 3 3, Figure 3 20**) were synthesised directly from the $[Ru(dcbpy)_2Cl_2]$ and indicated only one peak in HPLC but were impure when examined by ^{1}H-NMR

$[Ru(dcbpy)_2(phenyl\text{-}ptr)]$ (**2 6 20, Table 3 3, Figure 2 6 23**) was synthesised from $[Ru(dcbpy)_2Cl_2]$ only and indicated three components present, the main component showing a retention time of 4 61 min The peaks noted may be due to the presence of unreacted $[Ru(dcbpy)_2Cl_2]$ and possibly also $[Ru(dcbpy)_2ClH_2O]$ or a complex containing one or more sodium salts of the carboxy groups, formed during synthesis of the dichloride

Both the first and final precipitates in the synthesis of $[Ru(dcbpy)_2bptRu(bpy)_2]$ 2 6 23a, 2 6 23b, 2 6 23c (**Table 3 3, Figures 3 24, 3 25, 3 26, 3 27 3 28**) and 2 6 23d, 2 6 23e (**Table 3 3, Figures 3 29, 3 30**) appear to be the same in each case, with similar retention times and absorption spectra noted This could indicate that the same complexes are precipitating out both before and after addition of NH_4PF_6 The first precipitate is formed on lowering the pH without addition of NH_4PF_6 (**2 6 23a, 2 6 23d**) This should result in precipitation of the dinuclear complex with a neutral overall charge on protonation of the carboxy groups Unreacted $[Ru(dcbpy)_2Cl_2]$ may also precipitate The final precipitate is formed on addition of NH_4PF_6 at the already lowered pH (**2 6 23b, 2 6 23e**) The product isolated should be dinuclear only with the possibility of unreacted $[Ru(bpy)_2(bpt)]^+$ also precipitating out However due to the overall positive charge on the $[Ru(bpy)_2(bpt)]^+$ this complex should not be retained on the anion exchange column The lowest energy transition in the dinuclear complex should be the Ru → dcbpy π^* transition which should result in an absorption peak more into the red in comparison to Ru → bpy π^* based

transitions Therefore the peaks noted at a retention time of 2 3 minutes may possibly be due to the presence of the $[Ru(dcbpy)_2bptRu(bpy)_2]$ dinuclear or unreacted $[Ru(dcbpy)_2Cl_2]$, which has a retention time of 2 48 minutes under the same HPLC conditions **(2 6 7, Table 3 3)** However in the case of the dichloride the λmax at 480 to 490 nm is at a higher energy than expected for $[Ru(dcbpy)_2Cl_2]$ (λ_{max} = 550 nm for $[Ru(dcbpy)_2Cl_2]$)

The charge on the deprotonated dinuclear complex should be 1^- with the charge on the $[Ru(dcbpy)_2Cl_2]$ 2^- at the pH of the mobile phase, which would indicate longer retention times for the mononuclear complex However the larger dinuclear molecules, although they have a lower negative charge than the mononuclear complexes will be more hydrophobic in nature which should result in longer retention on the column (due to the polar nature of the mobile phase) The presence of $[Ru(dcbpy)_2ClH_2O]$ is also a possibility In the synthesis reaction $NaHCO_3$ is added to deprotonate the carboxy groups on the $[Ru(dcbpy)_2Cl_2]$ and allow for complete dissolution of the complex The formation of sodium salts of one or more of the carboxylic acid groups is a possibility and may account for some of the impurities present

Analysis of $[Ru(dcbpy)_2bptRu(bpy)_2]$ **(2 6 23c, Table 3 3, Figure 3 28)** which was isolated from recrystallisng complex **2 6 23a** in methanol/propanol indicated two components present with similar spectra as complex **2 6 23a**, indicating that the attempted recrystallisation was not of any benefit in increasing the purity of the complex **2 6 23a** Changing the synthesis conditions for **2 6 23d (Table 3 3, Figure 3 29)** and **2 6 23e (Table 3 3, Figure 3 30)** still resulted in impure products with two main peaks noted at retention times of 2 min and 8 min

HPLC analysis of [Ru($^2H_8$-bpy)$_2$(dcbpy)] **(2 6 15, Table 3 3, Figure 3 31)** indicated a fairly pure complex with the main peak at 5 95 minutes showing a relative % area of 75 % and a visible λ_{max} of 470 nm The peak at 2 19 min did not show any absorption in the visible region of the spectrum and is most likely due to the presence of free dcbpy ligand The small peak at 2 71 minutes and visible λ_{max} of 470 nm could be due to the presence of unreacted of [Ru($^2H_8$-bpy)$_2$Cl$_2$] or undeuteriated [Ru(bpy)$_2$Cl$_2$]

Figure 3 16, HPLC chromatogram & absorption spectra of $[Ru(dcbpy)_2(NCS)_2]$, 2 6 5

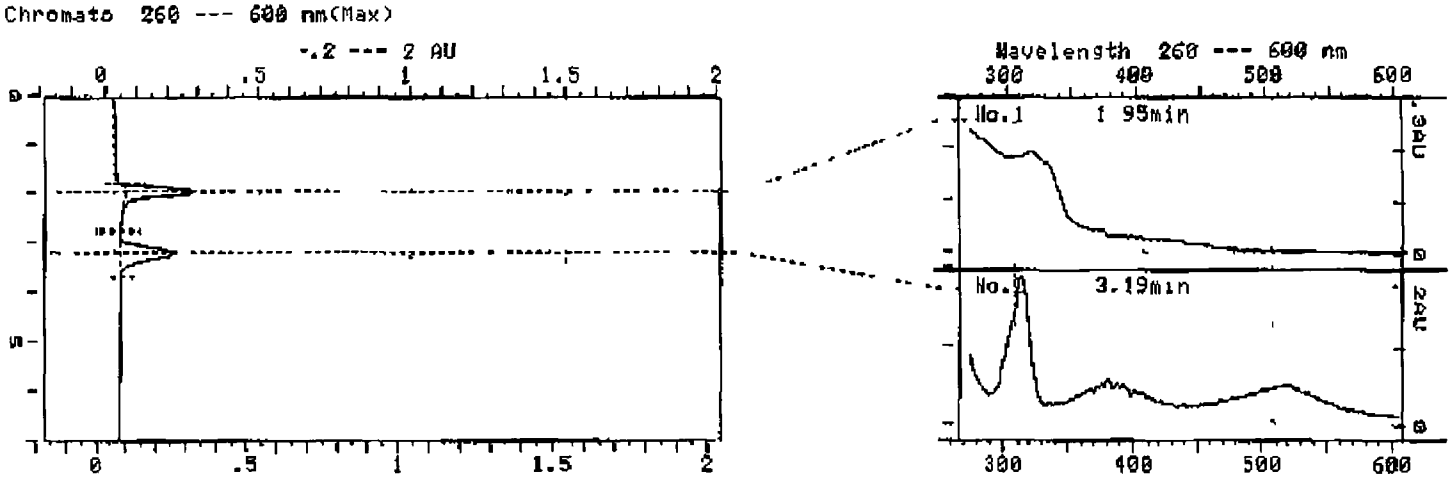

Figure 3 17, HPLC chromatogram & absorption spectra of [Ru(dcbpy)$_2$(4-phenol-ptr)] from Ru(dcbpy)$_2$Cl$_2$, 2 6 19

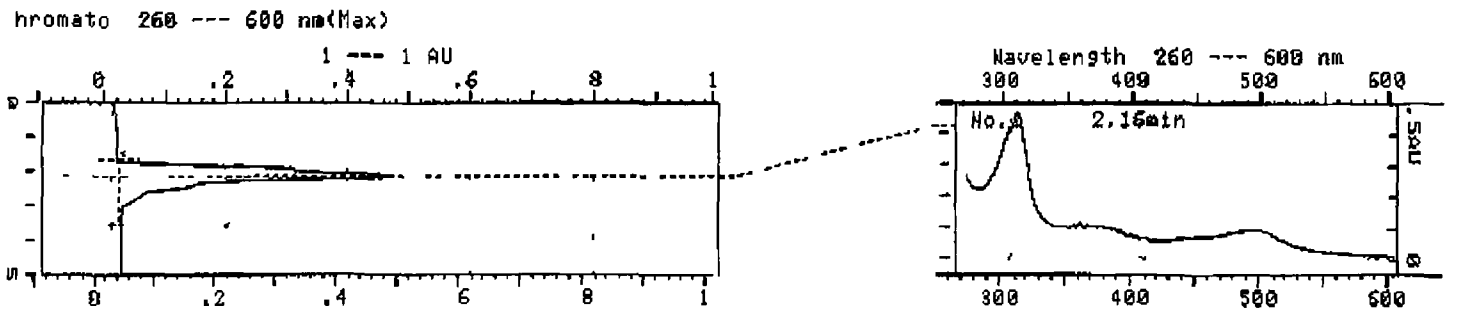

Figure 3 18, HPLC chromatogram & absorption spectra of [Ru(dcbpy)$_2$(4-phenol-ptr)] from ester, 1st ppt, 2 6 21a

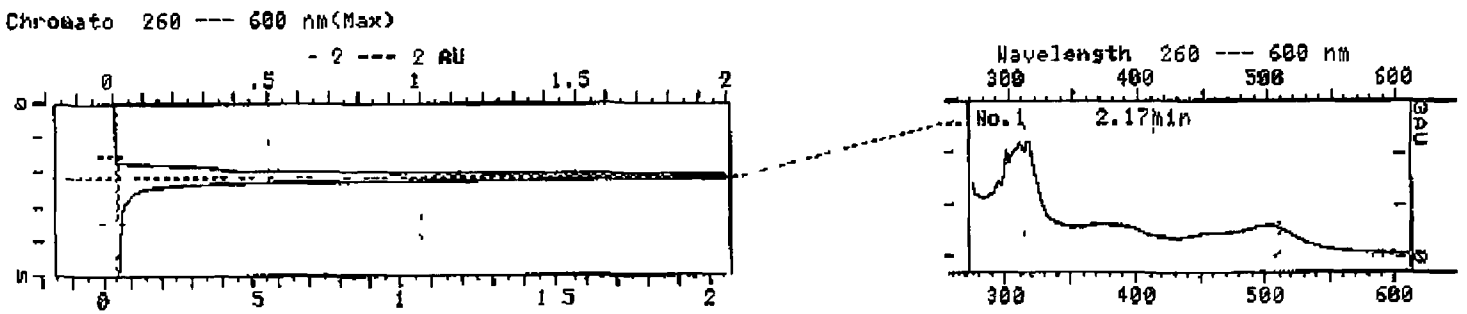

Figure 3 19, HPLC absorption spectrum of [Ru(dcbpy)$_2$(4-phenol-ptr)] from ester, final ppt, 2 6 21b

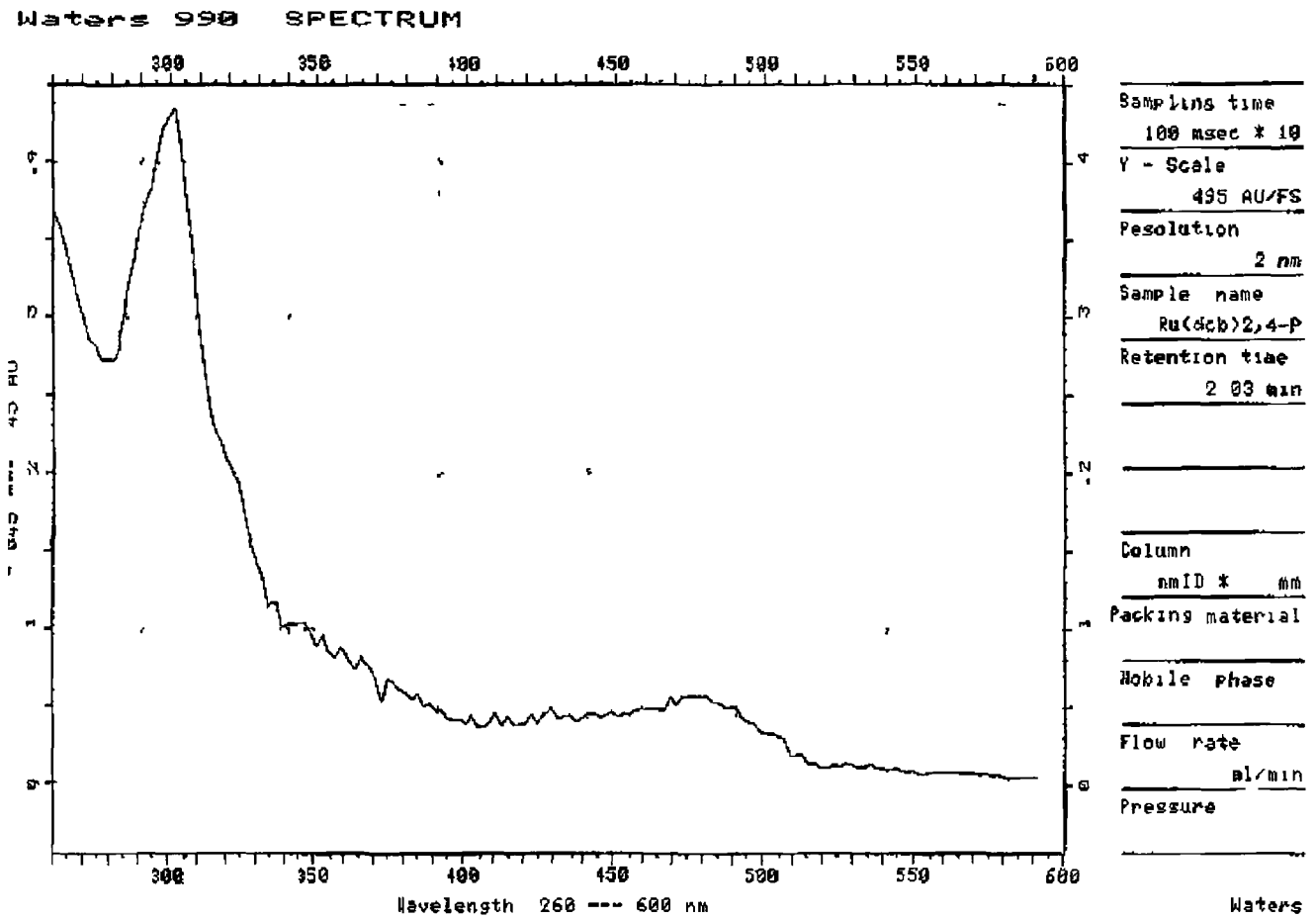

*Figure 3 20, HPLC chromatogram & absorption spectra of [Ru(dcbpy)$_2$(1-phenol-ptr)] from Ru(dcbpy)$_2$Cl$_2$, **2 6 18***

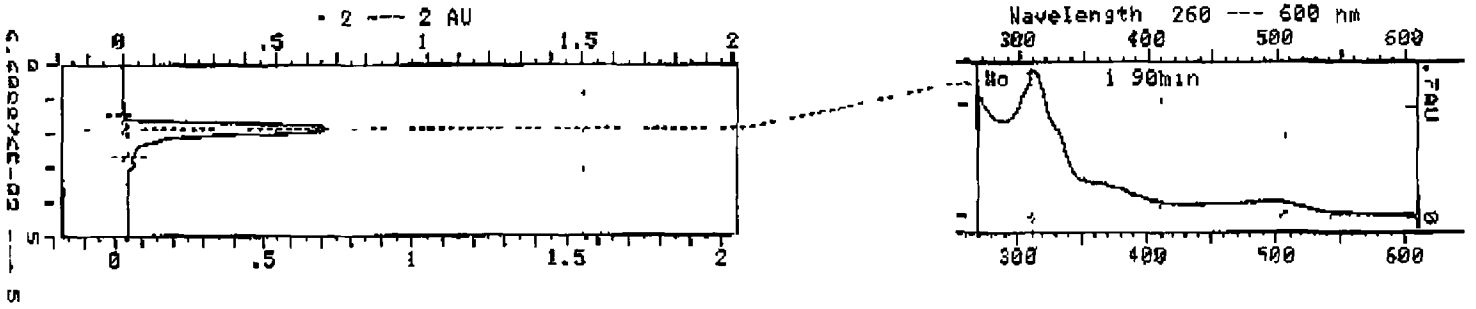

Figure 3 21, HPLC chromatogram & absorption spectra of [Ru(dcbpy)$_2$(1-phenol-ptr)] from ester, ppt 1, 2 6 22a

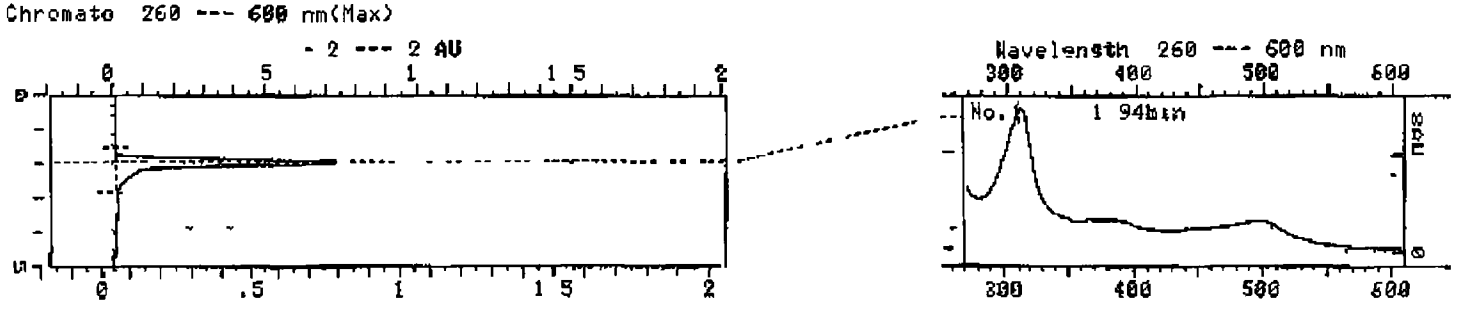

Figure 3 22, HPLC chromatogram & absorption spectra of [Ru(dcbpy)$_2$(1-phenol-ptr)] from ester, Final ppt, 2 6 22b

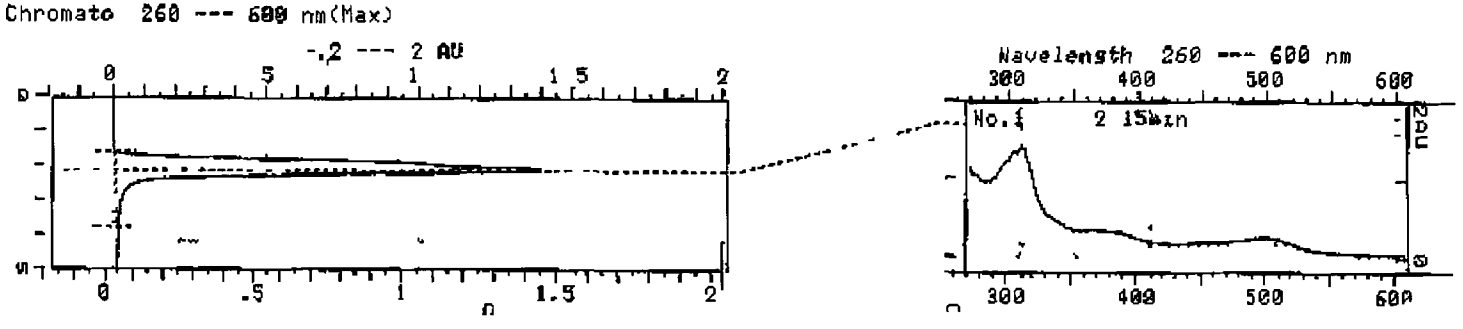

Figure 3 23, HPLC chromatogram & absorption spectra of [Ru(dcbpy)$_2$(phenyl-ptr)] from Ru(dcbpy)$_2$Cl$_2$, 2 6 20

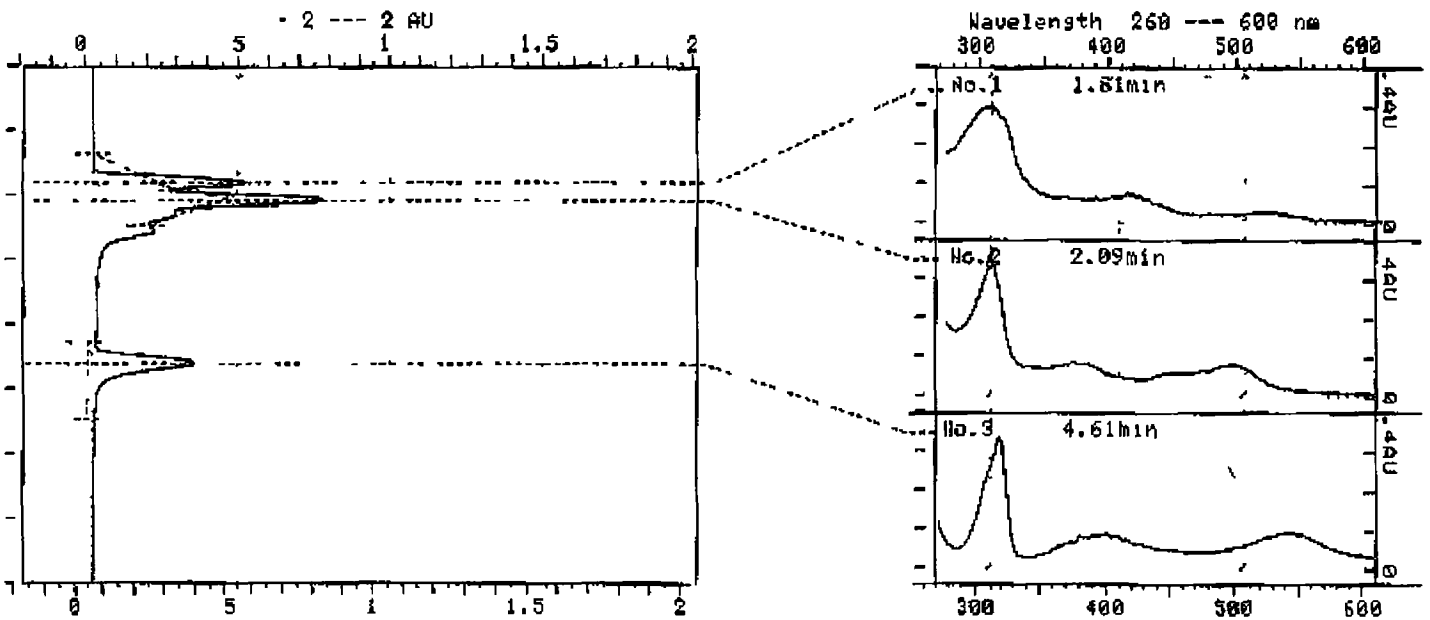

Figure 3 24, HPLC chromatogram & absorption spectra of [Ru(dcbpy)$_2$bptRu(bpy)$_2$], syn1, ppt 1, 2 6 23a

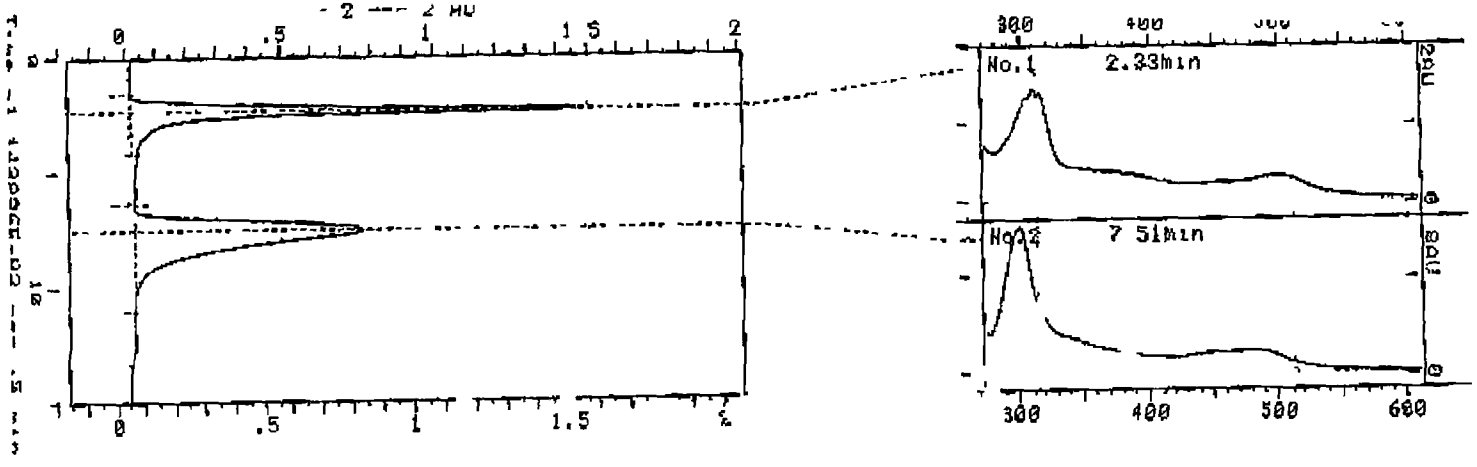

Figure 3 25, HPLC absorption spectrum of [Ru(dcbpy)$_2$bptRu(bpy)$_2$], syn1, ppt 1, 2 6 23a

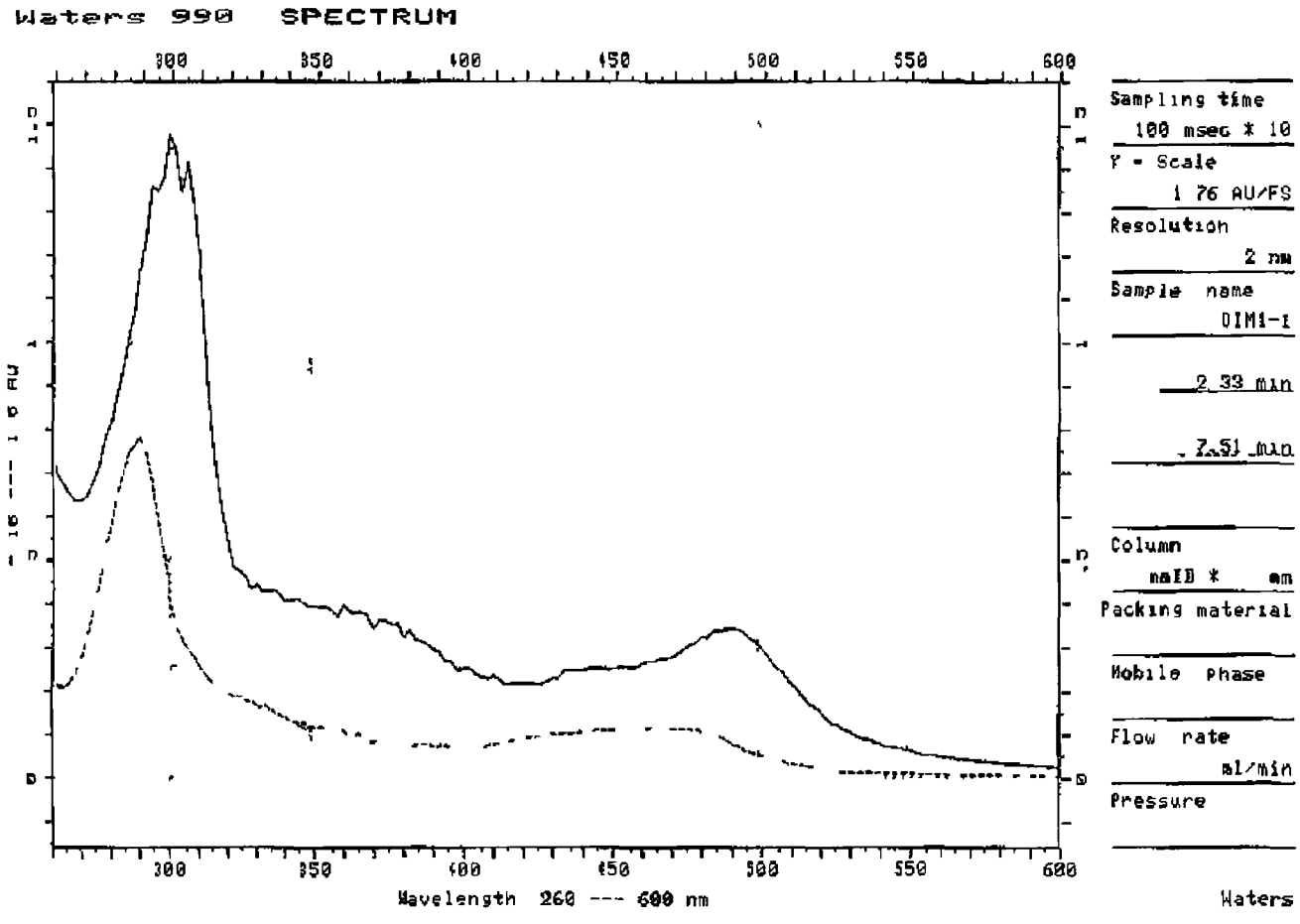

Figure 3 26, HPLC chromatogram & absorption spectra of [Ru(dcbpy)$_2$bptRu(bpy)$_2$], syn1, Final ppt, 2 6 23b

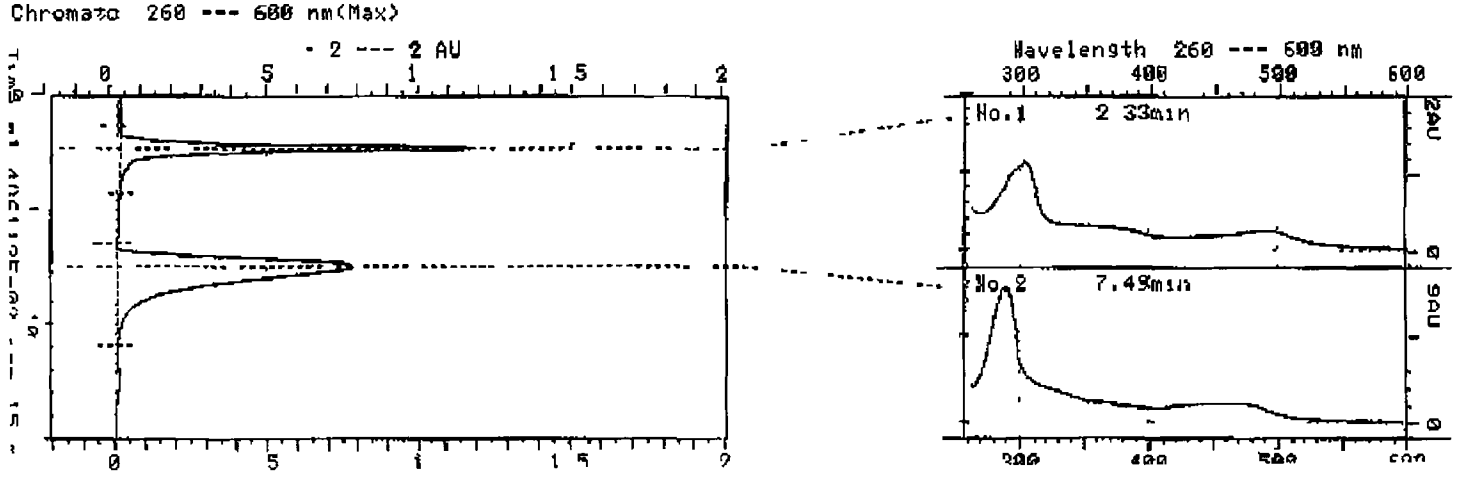

Figure 3 27, HPLC absorption spectrum of [Ru(dcbpy)$_2$bptRu(bpy)$_2$], syn1, Final ppt, 2 6 23b

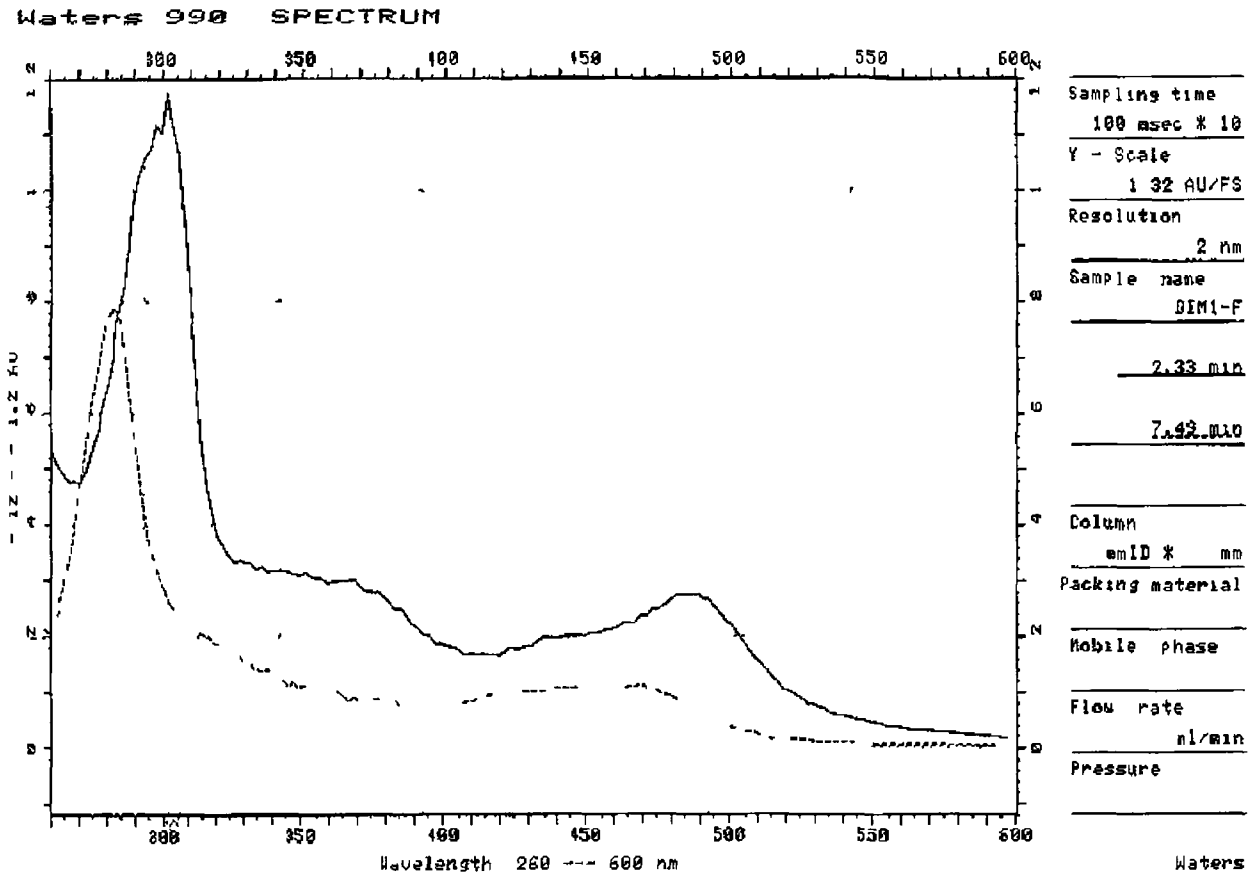

Figure 3 28, HPLC chromatogram & absorption spectra of [Ru(dcbpy)$_2$bptRu(bpy)$_2$], syn1, Final ppt , recrystallised from methanol/propanol, 2 6 23c

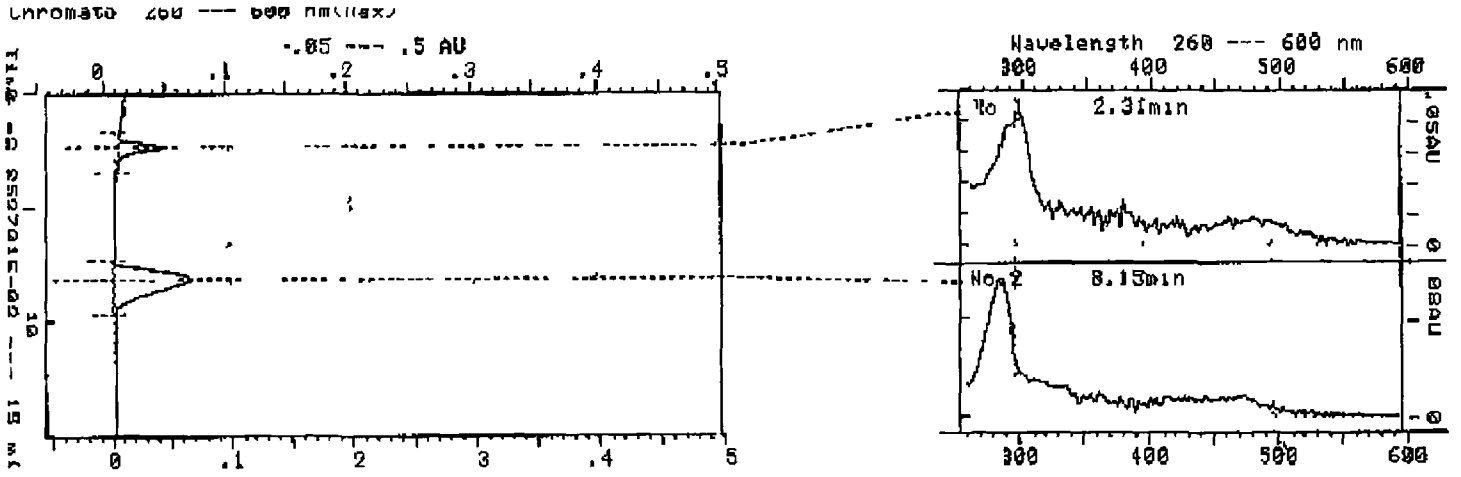

Figure 3 29, HPLC chromatogram & absorption spectra of [Ru(dcbpy)$_2$bptRu(bpy)$_2$], syn2, ppt 1, 2 6 23d

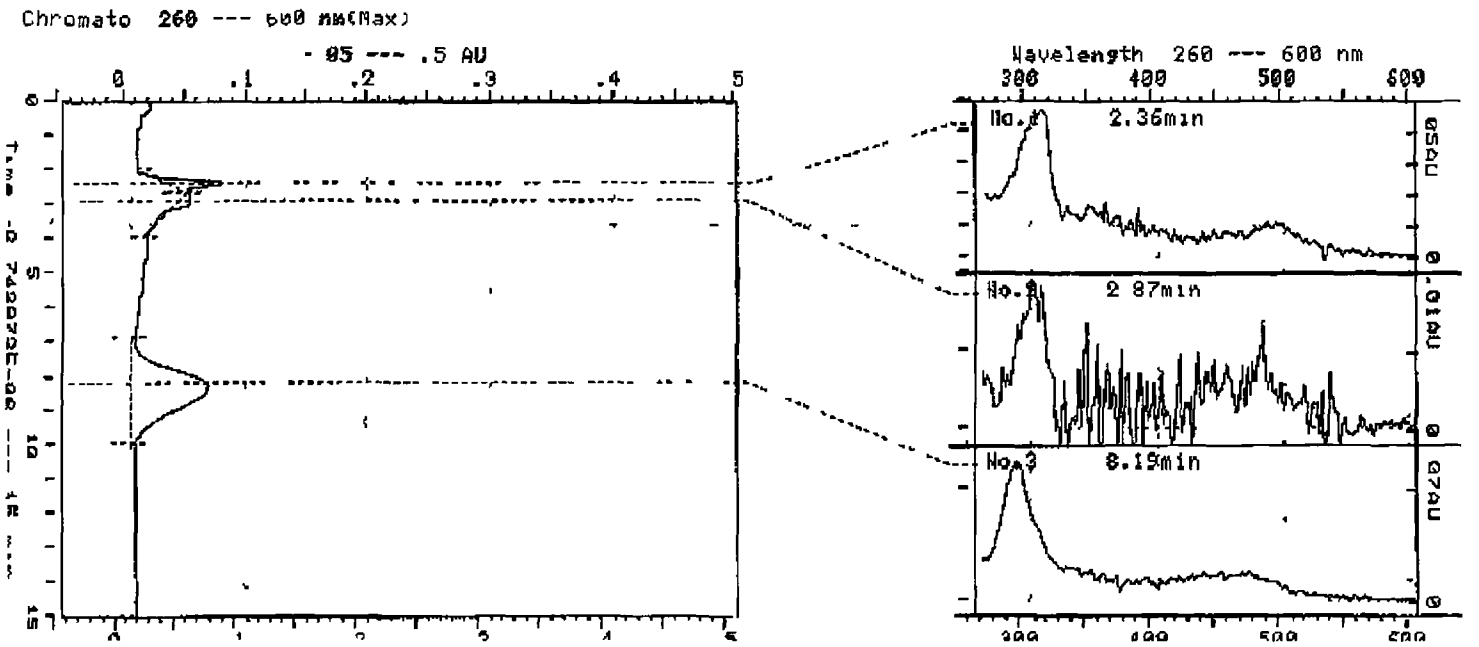

Figure 3 30, HPLC chromatogram & absorption spectra of [Ru(dcbpy)$_2$bptRu(bpy)$_2$], syn2, Final ppt, 2 6 23e

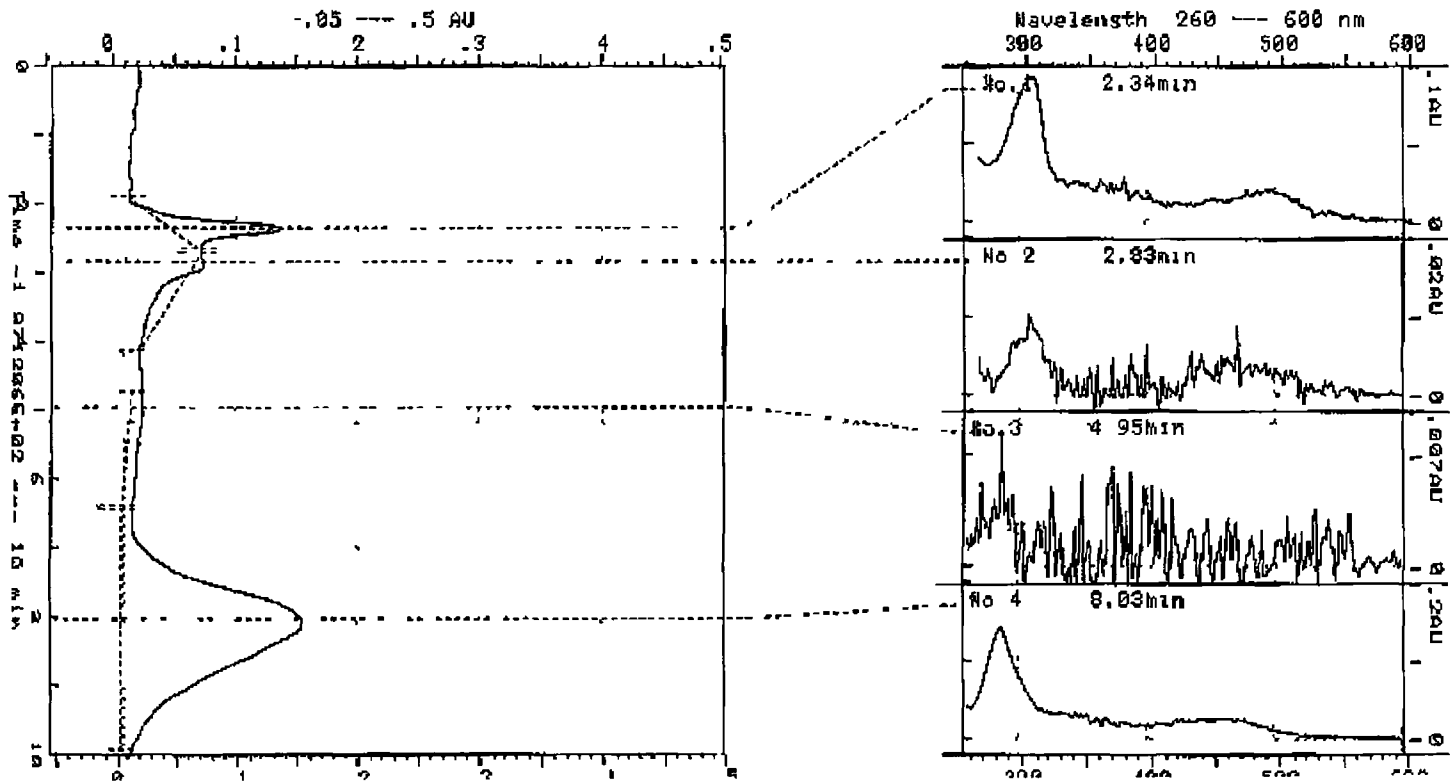

Figure 3 31, HPLC chromatogram & absorption spectra of [Ru(deut-bpy)$_2$(dcbpy)] , 2 6 15

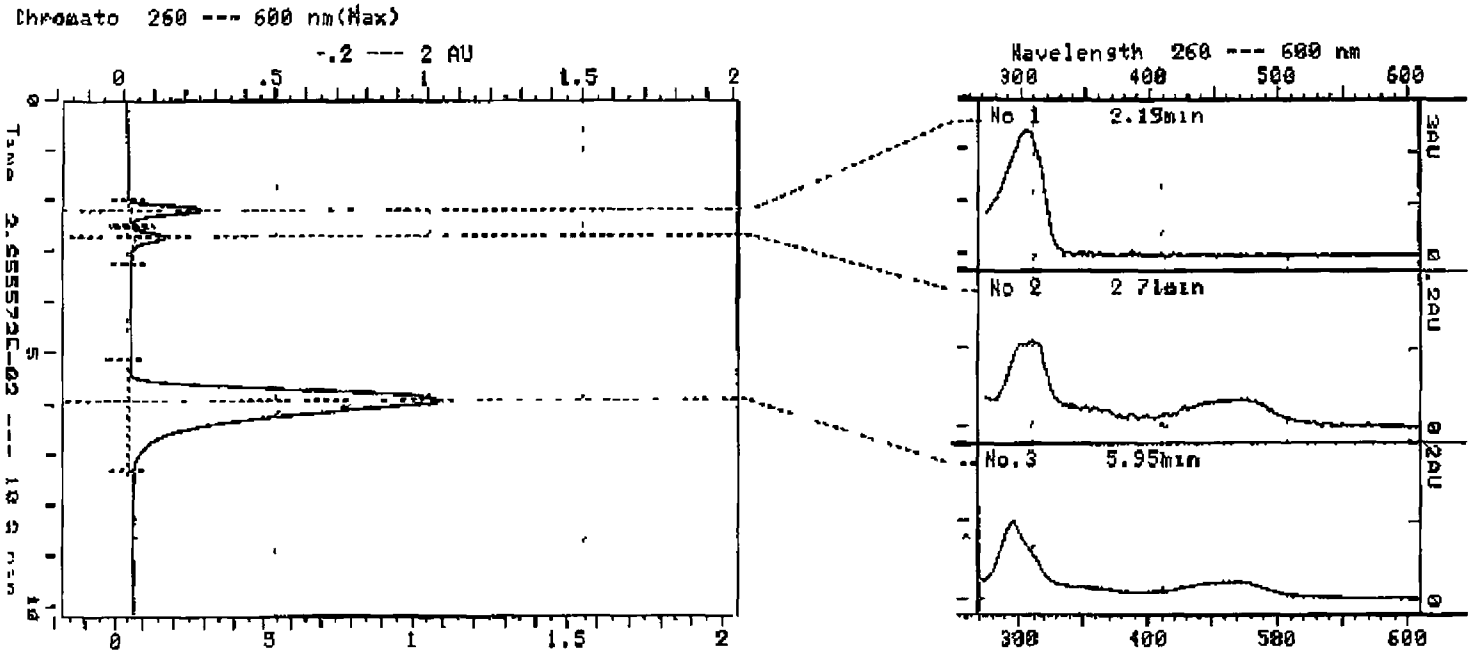

3 4 ^{1}H-NMR Spectroscopy

The complexes studied are all low spin d^6 systems that are diamagnetic which allows for their study using ^{1}H-NMR spectroscopy [28] When comparing the ^{1}H-NMR spectrum of $[Ru(bpy)_3]^{2+}$ with the spectrum of free bpy, a number of differences are apparent On co-ordination of the free bipyridine to the ruthenium metal the ligand adopts a cis configuration, whereas the free bpy (or substituted bpy) is presumed to have a trans structure [29] The steric crowding of the H^3 protons of the ligand gives rise to a strong Van der Waals interaction and a significant downfield shift is observed [30] Also in the complex the H^6 proton is directed over a pyridine of an adjacent bpy ligand This diamagnetic anisotropic effect causes a upfield shift [31] The metal ion also has an effect on the co-ordinated ligands Due to the σ-donation effect the electron density at the ligand atom diminishes and a general downfield shift is present

The effect of substituent groups on the bpy ligand will also have an effect on the position of the protons on the ^{1}H-NMR spectrum The protons on the bpy ring can be shifted upfield or downfield depending on whether the substituent groups are electron donating or withdrawing Other factors such as the type and position on the ring of the substituent group will effect the position of the bpy protons

For the complexes $[Ru(decb)_2(L)]^+$ **(2 6 11, 2 6 12, 2 6 13, 2 6 14)** containing pyridyl-triazole based ligands the ruthenium metal has to bind via one nitrogen of the pyridine ring and another nitrogen (either N^1 or N^4) of the triazole ring

Previous studies have shown that co-ordination is via the N^1 when the triazole has a substituent group in the C^3 position of the triazole ring for 3-Me-ptr or C^5 position of the

triazole ring for 4-phenol-ptr, 1-phenol-ptr, phenyl-ptr [8] Therefore the $-CH_3$ group in 3-Me-ptr will cause the ruthenium metal to bind to the ptr ligand via the N^1 position of the triazole ring only [8] If co-ordination occurs via N^4 the substituent in the C^5 position will be nearby an adjacent bpy ligand The ring current of the pyridine ring causes a large upfield shift for the protons in this position As mentioned above, co-ordination of all the complexes examined should be via the N^1 position due to the presence of a substituent group in the C^5 position and as a result this upfield shift should not be noted

The ^{1}H-NMR spectrum of the free 4,4'-diethylester-2,2'-bipyridine ligand (decb) **(Figure 3 32)** in solution indicates identical protons on each ring The $H^3H^{3'}$ protons are observed at 8 96, the $H^6H^{6'}$ protons at 8 88 and the $H^5H^{5'}$ protons at 7 93 ppm ($CDCl_3$) The $-CH_2$ of the ester group is observed as a quartet at 4 44 ppm and the $-CH_3$ of the ester group as a triplet at 1 44 ppm For the free dcbpy ligand H^3H^3 protons are observed as a singlet at 8 27 ppm, $H^6H^{6'}$ protons as a doublet at 8 64 ppm and $H^5H^{5'}$ protons as a doublet at 7 73 ppm ($NaOD/D_2O$) **(Figure 3 33)**

When the decb is complexed to the ruthenium in the $[Ru(decb)_2Cl_2]$ complex **(Figure 3 34)** the H^6 proton is shifted downfield to 10 47 ppm and $H^{6'}$ proton is shifted upfield to 8 15 ppm This upfield shift is typically observed in co-ordinated pyridine rings and is due to the fact that the H^6 proton of the pyridine ring feels the ring current of an adjacent decb ligand (magnetic anisotropic effect) and hence becomes shifted upfield [31, 32, 33] Both H^3 s will be sterically strained and are indicated at H^3 = 8 81 and $H^{3'}$ = 8 63 ppm The H^5 s are observed with an upfield shift to H^5 = 7 68 and $H^{5'}$ = 7 48 ppm

A similar effect is noted when the dicarboxybipyridine ligand is complexed with ruthenium For $[Ru(dcbpy)_2Cl_2]$ the H^6 proton is shifted downfield to 9.68ppm and the

$H^{6'}$ proton is shifted upfield to 7.82 ppm. The sterically strained H^3 protons are observed at H^3 = 8.65 and $H^{3'}$ = 8.48 ppm. The $H^{5'}$s are the least effected and indicate an upfield shift to H^5 = 7.35 and $H^{5'}$ = 7.09 ppm.

For all complexes **2.6.11, 2.6.12, 2.6.13, 2.6.14 (Section 2.6, Table 3.4)** the $H^{3'}$s of the decb ligands are noted the most downfield at approx 9 ppm. The next peaks noted upfield from this are the $H^{3'}$s of the ptr-ligand. As mentioned above the $H^{3'}$s are sterically strained when complexed with the ruthenium metal and will be shifted downfield on co-ordination with the metal. The next peaks noted are the H^6 of the pyridine ring of the pyridyl-triazole ligand. The H^6 of the pyridine ring is shifted approximately 0.40 ppm upfield, as mentioned above this is associated with the diamagnetic anisotropic magnetic interaction of the H^6 proton with an adjacent decb ligand. The $H^{6'}$ protons of the phenol and phenyl units are shifted upfield but a much smaller shift of approx. 0.04 ppm for 4-phenol-ptr and 1-phenol-ptr and 0.11 ppm for phenyl-ptr is observed which suggests that the hydroquinone or phenyl units are not involved in co-ordination.

For $[Ru(decb)_2(4\text{-phenol-ptr})]^+$ **(2.6.11, Table 3.4, Figure 3.35)** and $[Ru(decb)_2(1\text{-phenol-ptr})]^+$ **(2.6.12, Table 3.4, Figure 3.37)** the position of the –OH group effects the splitting and position of the peaks on the phenol ring. For **2.6.11** the doublets of the $H^{2'}$ and $H^{6'}$ on the phenol ring are noted at 8.44 and 7.85ppm respectively. The $H^{2'}$ is shifted downfield and the $H^{6'}$ remains unchanged in comparison to the free ligand **(Figure 3.36 & experimental section 2.6.11)**, indicating an interaction with the $H^{2'}$ and neighbouring ligands. The $H^{3'}$ and $H^{5'}$ doublets appear at the same position (6.87 ppm) indicating that both protons are in a similar environment i.e. one proton is not interacting with a neighbouring decb pyridine ring. Also both the $H^{3'}$ and $H^{5'}$ protons are noted in an upfield

position in comparison to the $H^{2'}$ and $H^{6'}$ on the same ring mainly due to the neighbouring electron donating hydroxyl group, which will shift protons ortho to it to a higher field [15] The distinctive two doublets (which are triplet in appearance) of H^4 (8 19 ppm) and H^5 (7 47 ppm) on the pyridyl ring are also noted In **2 6 12**, the $H^{6'}$ proton (6 98 ppm) is noted in a upfield position, with the distinctive two doublets of the $H^{4'}$ proton (6 92 ppm) noted slightly upfield from this As mentioned above the electron donating effect of the hydroxyl group will shift the protons ortho to it upfield The distinctive two doublets of the $H^{5'}$ proton is noted at 7 34 ppm And the two doublets of the H^5 proton (7 50 ppm) and H^4 proton (8 22 ppm) of the pyridine ring are also noted For both **2 6 11** and **2 6 12** the H^3 protons on the pyridine ring are observed downfield at 8 51 ppm (2 6 11) and 8 63 ppm (2 6 12) for the reasons described above, this is in comparison to the free ligand with the H^3 protons at 8 12 ppm **(2 6 11, Figure 3 36)** and 8 19 ppm **(2 6 12, Figure 3 38)**

The ^{1}H-NMR spectrum of [Ru(4,4'-dicarboxy-2,2'-bipyridine)$_2$(NCS)$_2$] **(2 6 8, Figure 3 39)** indicated a pure complex present One H^6 proton was at 9 68 ppm with the second $H^{6'}$ proton noted upfield at 8 43 ppm As mentioned earlier this is due to the interaction of the H^6 proton with a neighbouring dcbpy (in this case) ring The sterically strained H^3 protons were observed at H^3 = 9 17 ppm and $H^{3'}$= 9 01 ppm The doublets of the H^5 protons were observed at H^5 = 8 03 ppm and $H^{5'}$ = 7 67 ppm

^{1}H-NMR of the deuteriated complex [Ru(deut-2,2'-bipyridine)$_2$(4,4'-dicarboxy-2,2'-bipyridine)] indicated three peaks present which should be due to the H^3, H^5 & H^6 of the dcbpy ligand **(Fig. 3.40)** The singlet of the H^3 proton was observed at 8 75 ppm, the

doublet of the H^6 proton at 7 77 ppm and the doublet of the H^5 proton at 7 45 ppm Some small impurities were also noted as present that may be due to the presence of free dcbpy ligand, this is also indicated by the HPLC results **(Section 3.3 2, Figure 3 16)** The ^{1}H-NMR results show that the protons that are present from the dcbpy ligand in [Ru(2,2'-bipyridine)$_2$(4,4'-dicarboxy-2,2'-bipyridine)] can be identified more easily than in the unprotonated complex **2 6 8 9 (Figure 3 41)** This would indicate that deuteriation can be used in more complicated spectra to enable correct assignment of unknown protons

^{1}H-NMR spectra of the dimer complexes and the dcbpy complexes that were attempted to synthesise generally indicated several compounds present or as is the case with **Figure 3 42** the integration did not indicate the compound [Ru(4,4'-dicarboxy-2,2'-bipyridine)$_2$(3-(4-hydroxyphenyl)-5-(pyridin-2-yl)-1,2,4-triazole)] **(2 6 21)** that was desired Most of the dcbpy complexes produced ^{1}H-NMR spectra indicating so many peaks that integration of the peaks proved impossible Recent research has indicated that the dicarboxy complexes can precipitate as sodium salts [39] The amount of sodium incorporated is not always the same and may depend on the manner in which the materials are precipitated By elemental analysis and mass spectrometry the mononuclear complex Na_3[Ru(dcbpy)$_2$(bpt)] $3H_2O$ and dinuclear complex Na_4[Ru(dcbpy)$_2$bptRu(bpy)$_2$](PF$_6$)$_3$ $5H_20$ were identified [39] However the uncertainty of the complexes in the solid state does not affect the analysis of the complexes in solution as the pH can be controlled In the HPLC analysis of the dinuclear complexes **(2 6 23a, 2 6 23b, 2 6 23c, 2 6 23d, 2 6 23e Table 3 3)** more than one compound was noted indicating the need for further purification of the compounds Sodium was not used

in the synthesis of the mononuclear dicarboxy complexes 2 6 18, 2 6 19, 2 6 21, 2 6 22 so the presence of sodium salts of these complexes is not likely Also in order to assign the ^{1}H-NMR correctly a 2D-Cosy should be carried out or the complex should be synthesised with some of the ligands deuteriated (e g deuteriated dcbpy ligands) which would allow the remaining protons to be more easily assigned

Table 3 4, ^{1}H-NMR Data

Positions of protons of pyridyl-triazole based ligands

2 6 11 = $[Ru(decb)_2(4\text{-phenol-ptr})]^+$

2 6 12 = $[Ru(decb)_2(1\text{-phenol-ptr})]^+$

2 6 13 = $[Ru(decb)_2(phenyl\text{-ptr})]^+$

2 6 14 = $[Ru(decb)_2(3\text{-Me-ptr})]^+$

2 6 11 d_6 acetone	**H3** 8 51 (d)	**H4** 8 19 (dd)	**H5** 7 47 (dd)	**H6** 8 30 (d)	**H2'** 8 44 (d)	**H3'H5** 6 87 (d)		**H6'** 7 85 (d)
2 6.12 d_6-acetone	**H3** 8 63 (d)	**H4** 8 22 (dd)	**H5** 7 50 (dd)	**H6** 8 34 (d)	**H3'** 8 56 (d)	**H4'** 6 92 (dd)	**H5'** 7 34 (dd)	**H6'** 6 98 (m)
2 6.13 d_6-acetone	**H3** 8 39 (d)	**H4** 8 16 (dd)	**H5** 7 17 (dd)	**H6** 8 26 (d)	**H2'** 8 32 (d)	**H3', H5'** 6 76 (m)	**H4'** 7 12 (dd)	**H6'** 7 75 (d)
2.6.14 d_6-acetone	**H3** 8 63 (d)	**H4** 8 19 (dd)	**H5** 7 59 (dd)	**H6** 8 21 (d)	**-CH_3** 2 91 (s)			

^{1}H-NMR Spectra

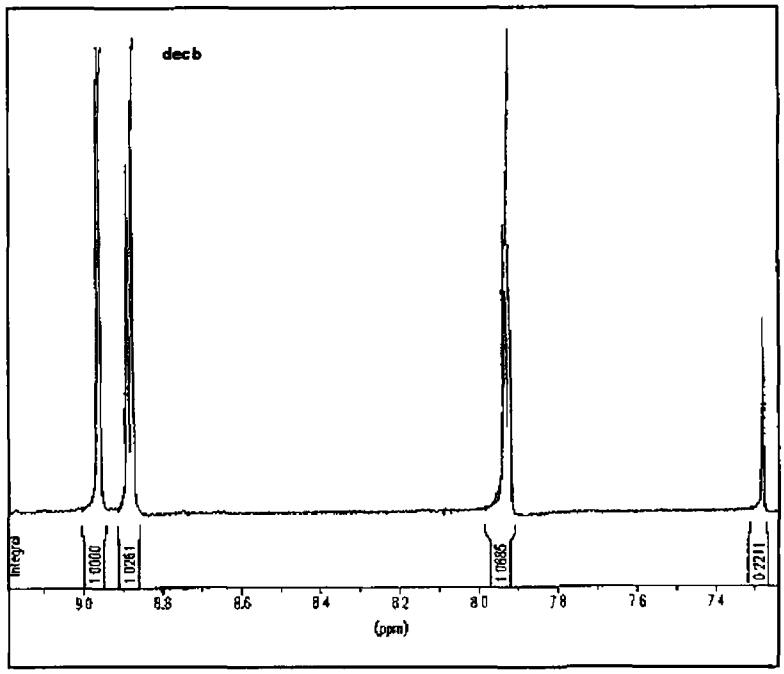

Fig 3 32, 4,4'-diethylester-2,2'-bipyridine, *($CDCl_3$), 2 6 3*

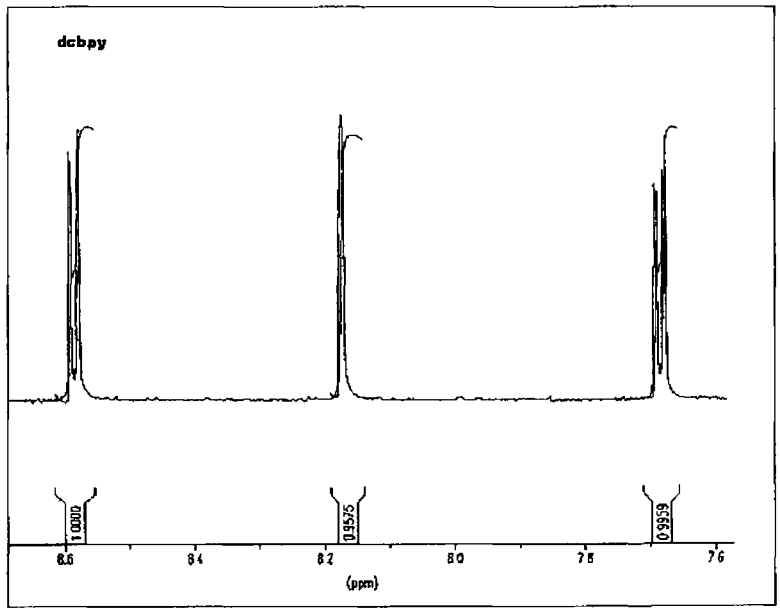

Fig 3 33, 4,4'-dicarboxy-2,2'-bipyridine, *($NaOD/D_2O$), 2 6 2*

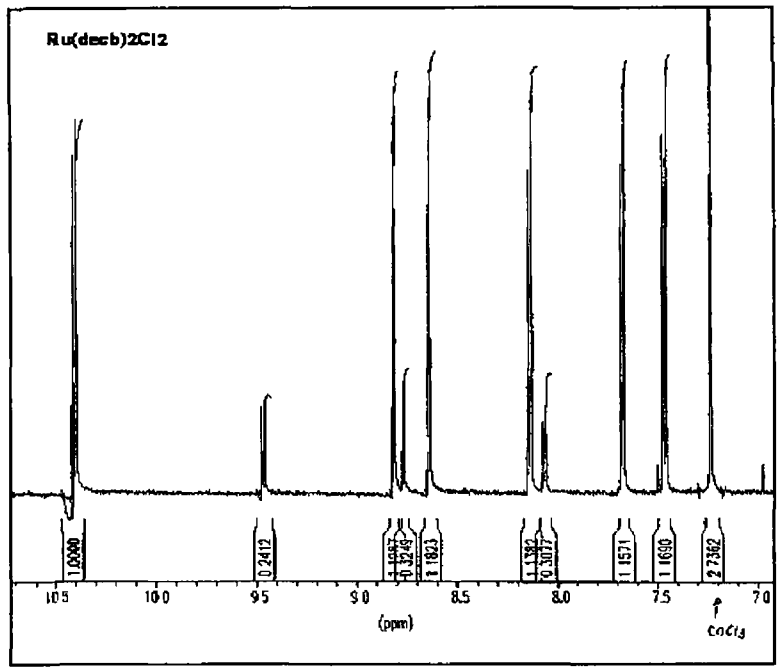

Fig 3 34, [Ru(4,4'-diethylester-2,2'-bipyridine)$_2$Cl$_2$], ($CDCl_3$), 2 6 16

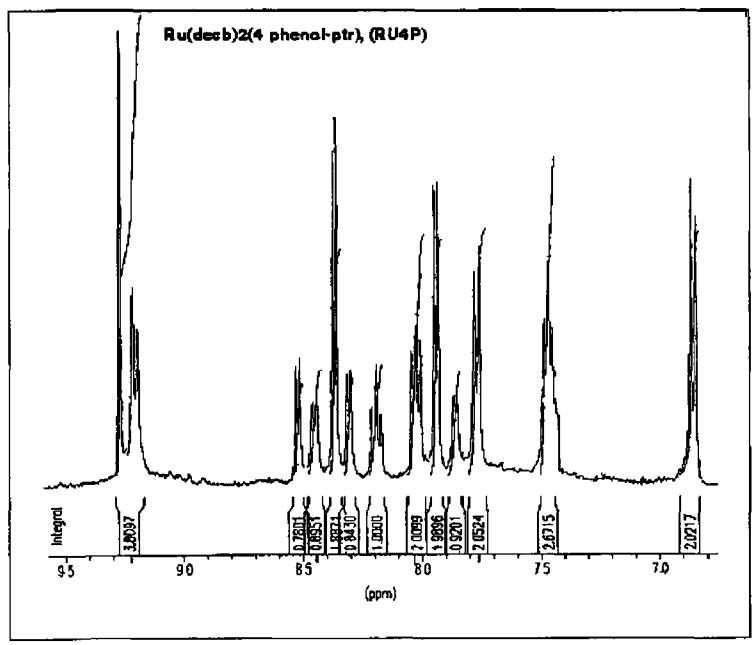

Fig 3 35, [Ru(4,4'-diethylester-2,2'-bipyridine)$_2$(3-(4-hydroxyphenyl)-5-(pyridin-2-yl)-1,2,4-triazole)]$^+$, (d_6-acetone), 2 6 11

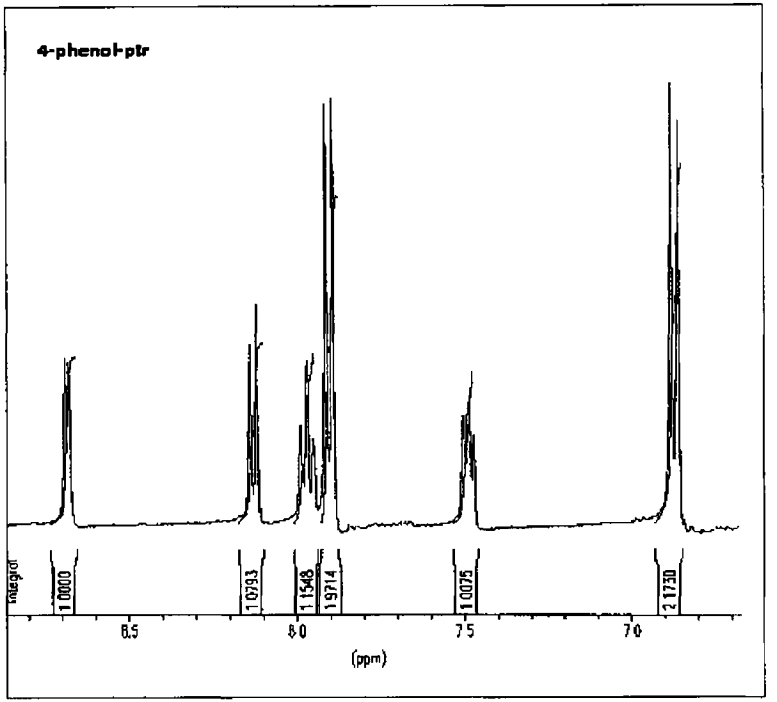

Fig 3 36, 3-(4-hydroxyphenyl)-5-(pyridin-2-yl)-1,2,4-triazole, *(d_6-DMSO)*

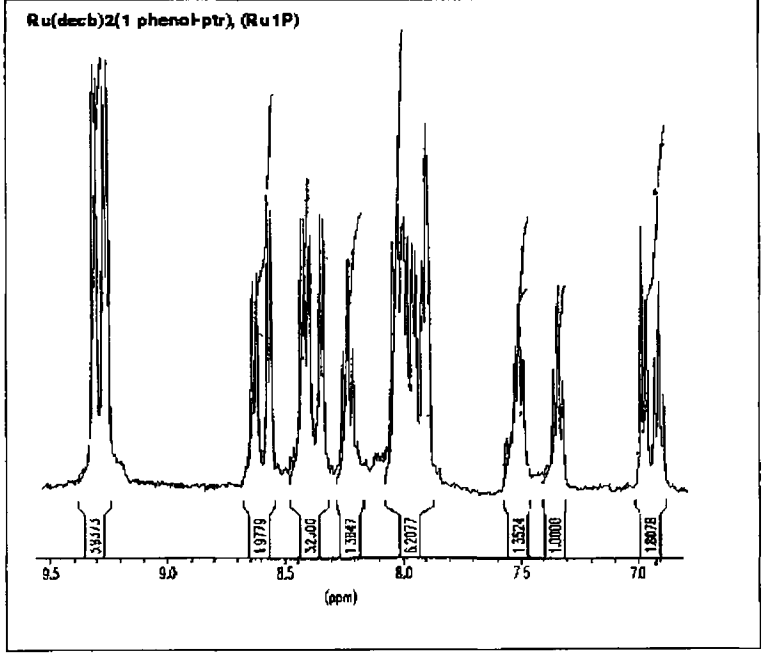

Fig 3 37, [Ru(4,4'-diethylester-2,2'-bipyridine)$_2$(3-(1-hydroxyphenyl)-5-(pyridin-2-yl)-1,2,4-triazole)]$^+$, *(d_6-acetone), 2 6 12*

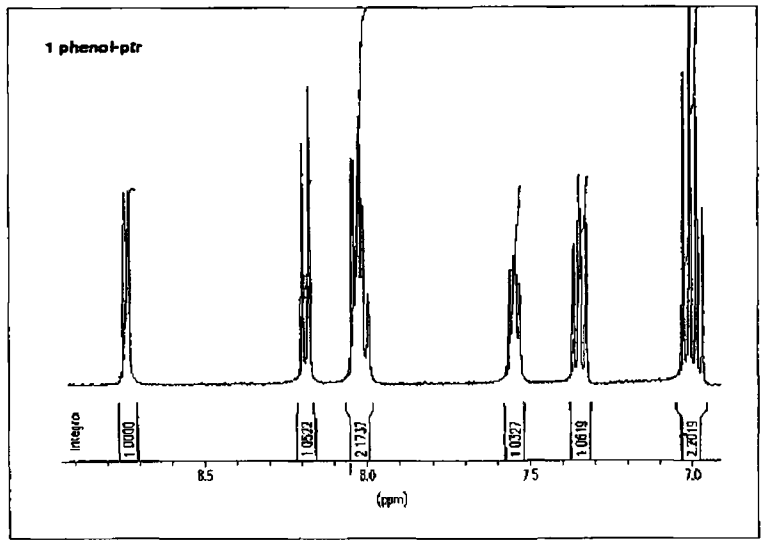

Fig 3 38, 3-(1-hydroxyphenyl)-5-(pyridin-2-yl)-1,2,4-triazole, (d_6-DMSO)

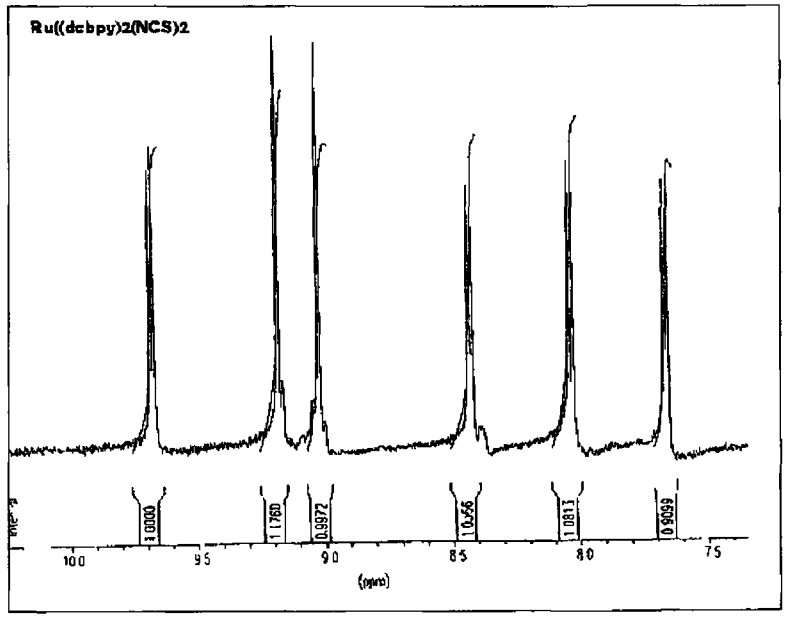

Fig 3 39 [Ru(4,4'-dicarboxy-2,2'-bipyridine)$_2$(NCS)$_2$], (NaOD/D_2O)

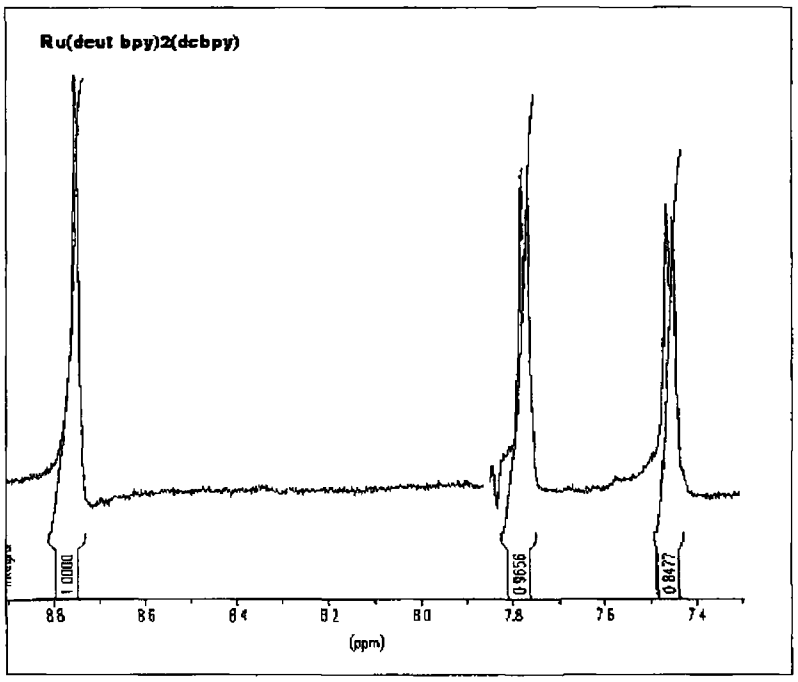

Fig 3 40, [Ru(deut-2,2'-bipyridine)$_2$(4,4'-dicarboxy-2,2'-bipyridine)], (NaOD/ D_2O), 2 6 15

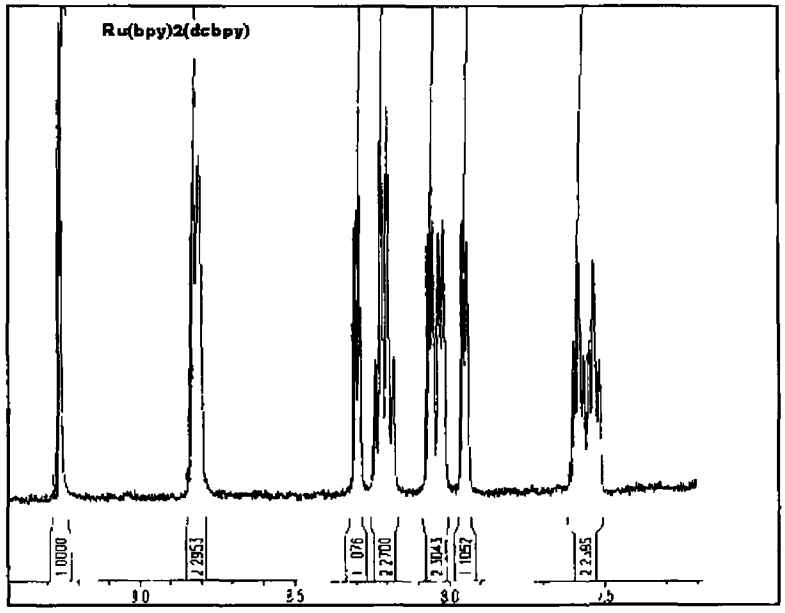

Fig 3 41, [Ru(2,2'-bipyridine)$_2$(4,4'-dicarboxy-2,2'-bipyridine)] (d_6-acetone +CF_3COOH), 2 6 8

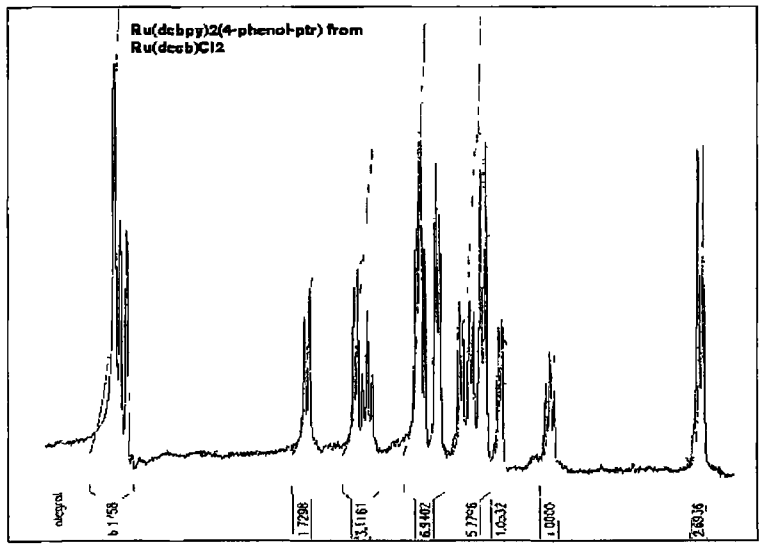

Fig 3 42, Impure [Ru(4,4'-dicarboxy-2,2'-bipyridine)$_2$(4-phenol-ptr)] (2 6 21), synthesised from [Ru(4,4'-diethylester-2,2'-bipyridine)$_2$(4-phenol-ptr)]$^+$, (NaOD/D_2O)

3 5 Electronic Properties

3 5 1 UV/vis Absorption Spectroscopy

The diester and diacid complexes, that were isolated in the pure form, were examined by UV-vis and fluorescence spectroscopy Acid-base properties of the triazolate ligand complexes were also examined In addition the influence of protonatable groups on the chromophore ligand and the possible hydrolysis of the ester groups on the ligands were examined

The addition of electron withdrawing substituents to the bpy ligand results in a lower electron density on the aromatic ring system and a lowering of the π^* orbital energy levels Therefore on complexation of the ligands with the ruthenium (II) metal the absorption spectra will be red shifted to lower energies in comparison to unsubstituted bpy complexes The UV absorption spectrum of $[Ru(decb)_2Cl_2]$ (**2 6 6**) shows absorption values into the red of the spectrum for the MLCT transitions from the filled $d\pi$(Ru(II)) levels to the low lying ligand π^* levels The first transition at lower energy with absorption at λ_{max} = 580 nm (MeOH) is assigned to the MLCT $d\pi \rightarrow \pi^*_1$ transition with the higher energy MLCT $d\pi \rightarrow \pi^*_2$ transition at λ_{max} = 421 nm in comparison to λ_{max} = 450 nm for $[Ru(bpy)_3]^{2+}$ (**2 6 9**) The higher energy absorption peak at λ_{max} = 315 nm is assigned to ligand based $\pi \rightarrow \pi^*$ transitions

The absorption spectrum for the $[Ru(dcbpy)_2Cl_2]$ (**2 6 7**) protonated complex has an MLCT λ_{max} of 554 nm (Britton–Robinson buffer) that is 26nm to the blue of the $[Ru(decb)_2Cl_2]$ but still to the red of the Ru to bpy transitions (MLCT λ_{max} of 520 nm for

$[Ru(bpy)_2Cl_2]$ in CH_2Cl_2) The similarities in the absorption energies indicate that the electron withdrawing effects are similar for both the carboxy groups and the diethyl ester groups However, the shift to the blue for the acid indicates that the LUMO on the dcbpy ligand is shifted to higher energies In the case of the dcbpy ligand the energy of the ligand π^* orbitals can also be altered by protonation/deprotonation of the dicarboxylic acid groups

At pH <1 0 both carboxy groups are protonated On raising the pH two deprotonation steps are seen for firstly the monoprotonated species and then the di-unprotonated species

$Ru(bpy\text{-}COOH)_2 \leftrightarrow Ru(bpy\text{-}COOH)(bpy\text{-}COO^-) \leftrightarrow Ru(bpy\text{-}COO^-)_2$ Equation 3 1

The first deprotonation step happens between pH 1 0 and 2 0 resulting in a blue shift in the absorption spectrum of the complex This is due to the formation of one negative charge on the carboxy moiety and the electron withdrawing effect of this group is subsequently reduced This results in a higher energy π^* orbital on the dcbpy ligand and the MLCT transition consequently shifts to a higher energy resulting in a blue shift in the absorption spectrum For $[Ru(bpy)_2(dcbpy)]$ **(2 6 8)** at low pH there is a blue shift of 5 nm from λ_{max} = 481 nm at pH = 0 87 to λ_{max} = 476 nm at pH = 1 68 due to a similar effect [33]

The second deprotonation step is seen between pH = 2 0 and 3 0 with a further blue shift of 8 nm in the spectrum from λ_{max} = 466 nm at pH = 2 34 to λ_{max} = 458 nm at pH = 9 65 and isosbestic points at 475 and 420 nm This blue shift is also due to the increased negative charge and subsequent decrease in the electron withdrawing capabilities of the carboxy substituent groups The higher electron density on the aromatic ring system

results in higher energy π^* orbitals and therefore a higher energy gap between the ruthenium $d\pi$ orbitals and the ligand π^* orbitals

The absorption spectra of the deteuriated [Ru($^2H_8$-bpy)$_2$(dcbpy)] **(2 6 15)** complex is the same as that for the undeuteriated complex with λ_{max} values as above **(Figures 3 42 & 3 43)** This would indicate that the absorption transitions are dcbpy based

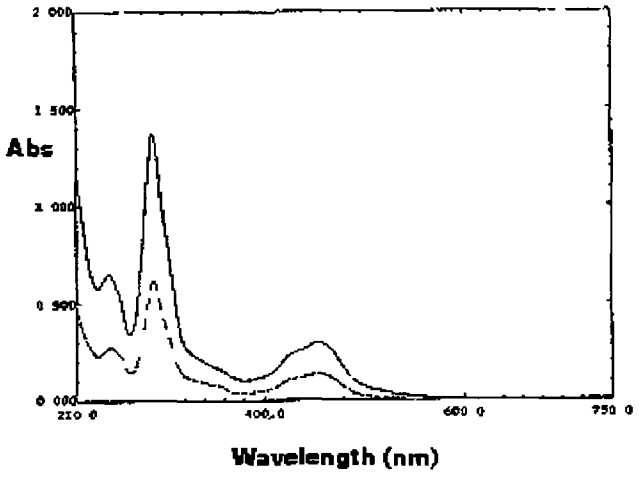

Figure 3 42
[Ru($^2H_8$-bpy)$_2$(dcbpy)], pH = 8 85 - top
[Ru(bpy)$_2$(dcbpy)], pH = 7 71 - bottom.

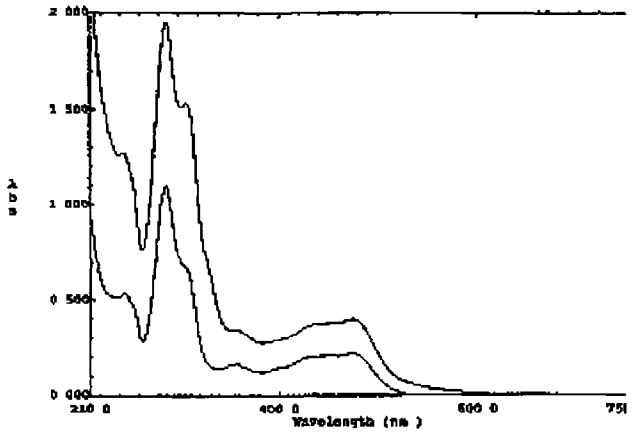

Figure 3.43
[Ru($^2H_8$-bpy)$_2$(dcbpy)], pH = 0.10 - top., [Ru(bpy)$_2$(dcbpy)], pH = 0.18 - bottom.

3 5 2 Acid-base behaviour

After deprotonation of the triazolate ligand, the ligand has a stronger σ-donating ability with its overall negative charge This causes an increase in electron density on the Ru metal which results in lower energy electronic transitions and a red-shift in the absorption spectrum with respect to the protonated form

Electron transitions, be they MLCT (d→π*) or LC (π→π*), are influenced by the σ-donor and π-acceptor properties of the ligands in a complex At low pH, from 1 0→7 0, $[Ru(decb)_2(1\text{-phenol-ptr})]^+$ **(2 6 12)** and $[Ru(decb)_2(4\text{-phenol-ptr})]^+$ **(2 6 11)** showed a significant red shift of 25 5 nm from λ_{max} = 479 nm at pH = 0 71 to λ_{max} = 504 nm at pH = 6 58 on deprotonation **(Figures 3 44 & 3.45)** Such a red shift was also noted in $[Ru(decb)_2(phenyl\text{-ptr})]^+$ **(2 6 13, Figure 3 46)** with a red shift of 24 nm between pH 1 0 and 7 0 and is most likely due to the deprotonation of the triazolate ligand

At high pH absorption spectra of $[Ru(decb)_2(1\text{-phenol-ptr})]^+$ and $[Ru(decb)_2(4\text{-phenol-ptr})]^+$ exhibit a lowering of absorption intensity and a minor red shift in absorption values of 5 nm from 507 nm at pH = 5 58 to 512 nm at pH = 11 43 **(Figure 3 47)** These changes are most likely due to deprotonation of the -OH group on the phenol ring A red shift at this pH was not seen with the $[Ru(decb)_2(phenyl\text{-ptr})]^+$ complex, which does not contain a phenol ligand linked to the triazole ligand The red shift in the spectra is due to a further increase (the σ-donating properties increased on deprotonation of the triazolate ligand) in the σ-donating properties of the ligand as a result of the presence of the negative charge on the phenol ligand This increased electron donating ability causes an

increase in electron density on the metal and therefore an increase in the energy of the highest occupied molecular orbit (HOMO) which results in lower energy transitions from the metal to the chromophore ligand - decb/dcbpy (MLCT) The red-shift in the spectrum with the deprotonation of the triazolate ligand (25 nm) is far greater and has a higher intensity than the red shift which is noted on deprotonation of the phenol ligand This is due to the close proximity of the triazole group to the ruthenium metal in comparison to the phenol group, (the ruthenium metal being attached to the ligand via the N^1 position triazole nitrogen and the pyridyl nitrogen [8]), thus the increase in the negative charge on the triazole ligand has a greater effect on the electron density on the ruthenium metal than the increase of negative charge on the phenol ligand

At even higher pH another shift in the absorption spectra is observed, this time to the blue of the spectrum This blue shift occurs in all decb complexes including $[Ru(decb)_2(phenyl\text{-}ptr)]^+$ and is most likely due to the base hydrolysis of the diethyl ester groups on the bpy ligands to form the unprotonated diacid (dicarboxy-bpy) Between pH 7 0 and 12 0 a 21 nm shift from 512 at pH = 7 36 to 491 nm at pH = 12 41 for $[Ru(decb)_2(1\text{-}phenol\text{-}ptr)]^+$ **(Figure 3 48, Table 3 4)** and a 16 nm shift from 505 nm at pH = 7 02 to 489 nm at pH = 10 69 for $[Ru(decb)_2(4\text{-}phenol\text{-}ptr)]^+$ **(Figure 3 49, Table 3 4)** was seen, with an increase in the intensity of the shoulder at 305 nm on increasing the pH This indicates instability of ester groups and prevents calculation of pka values for the complexes As a result of the ester instability there was problems with preparation and separation of these compounds The unprotonated acid can be acidified to convert firstly to the monoprotonated and then to the diprotonated diacid which results in a red shift in the spectrum The electronic effect of the acid substituents is comparable to the

electronic effect of the ester substituents (both are electron withdrawing) and therefore the resulting final spectrum of the protonated acid is practically identical to the spectrum of the ester complex at low pH This final base hydrolysis is the only acid/base condition of the diester complexes which directly involves the chromophore ligand as all the other protonation/deprotonation steps are effective only on the spectator pyridyl triazole based ligands

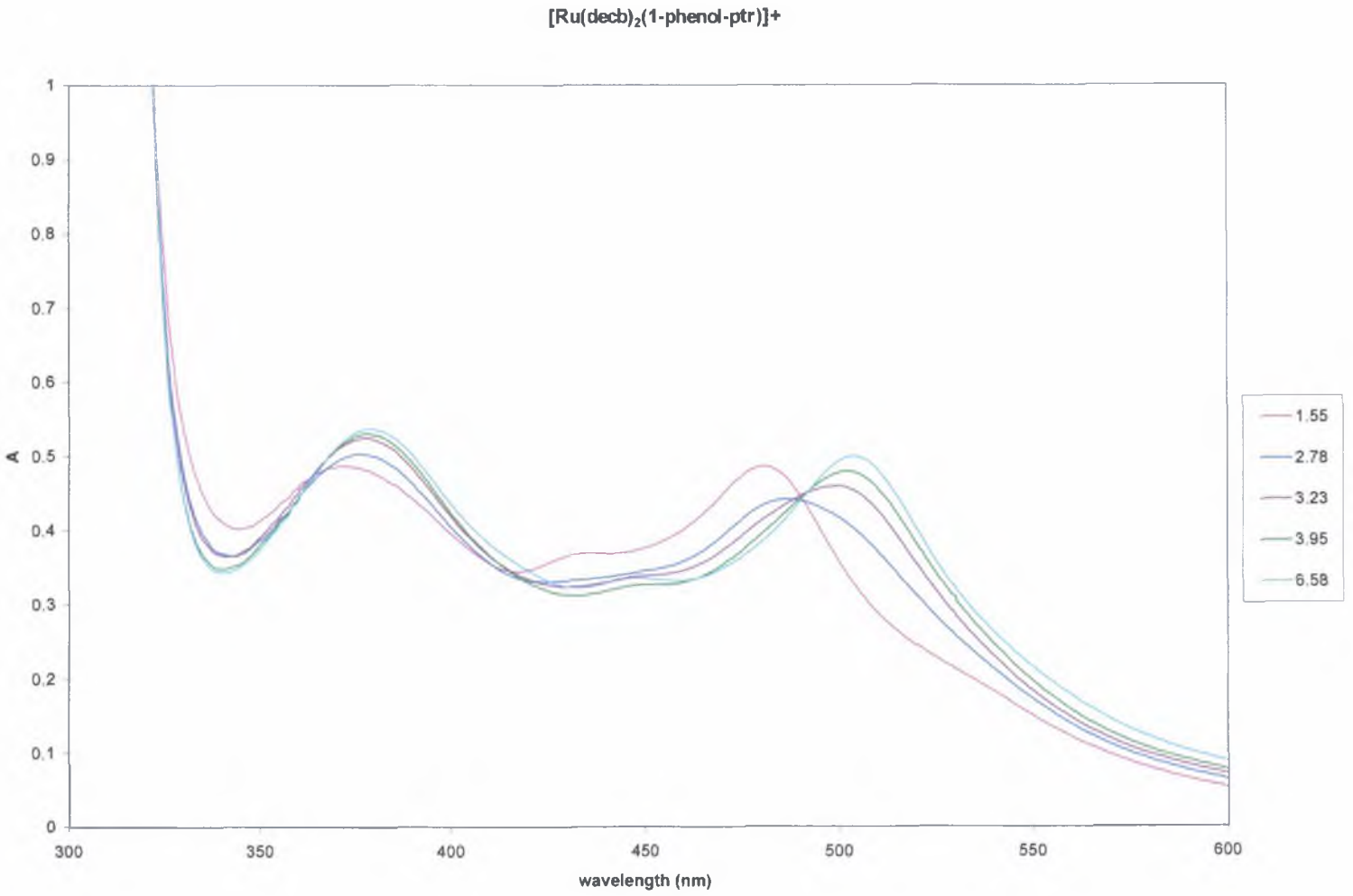

Figure 3.44, Dependence of $[Ru(decb)_2(1\text{-phenol-ptr})]^+$ (2.6.12) absorption spectrum on pH. From left to right pH = 1.55, 2.78, 3.23, 3.95, 6.58 (0.1 M Phosphate buffer).

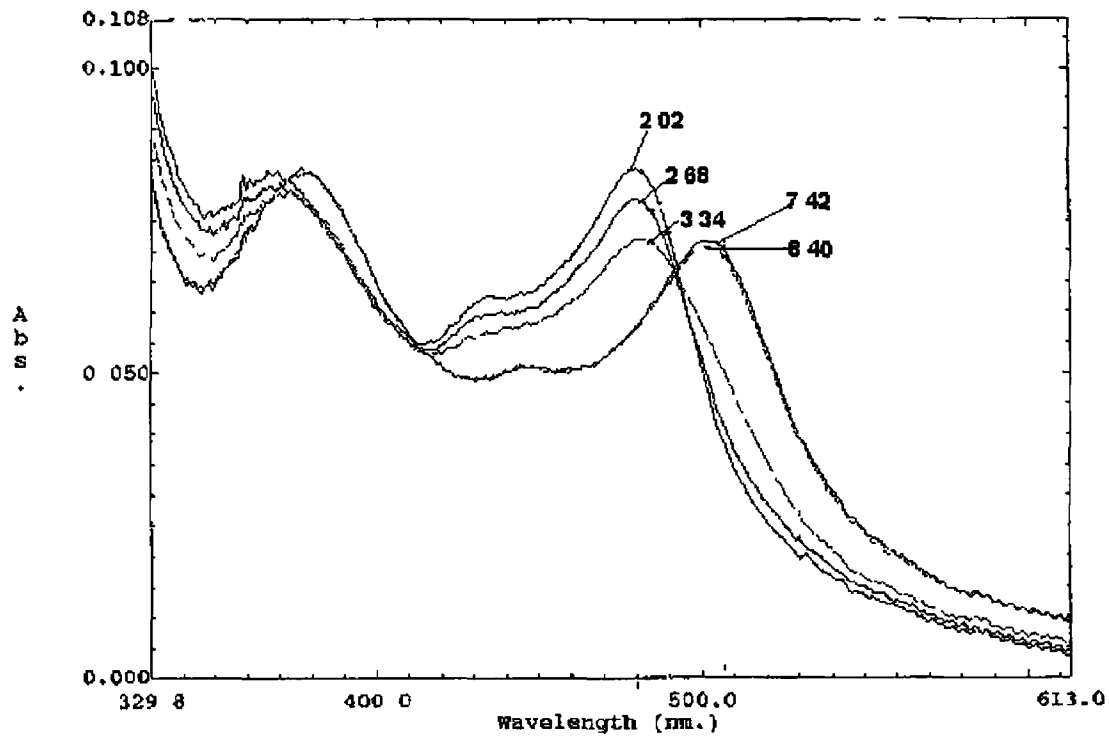

Figure 3 45, Dependence of $[Ru(decb)_2(4\text{-phenol-ptr})]^+$ (2 6 11) absorption spectrum on pH

From left to right pH = 2 02, 2 68, 3 34, 7 42, 8 40 (0 1 M Phosphate buffer)

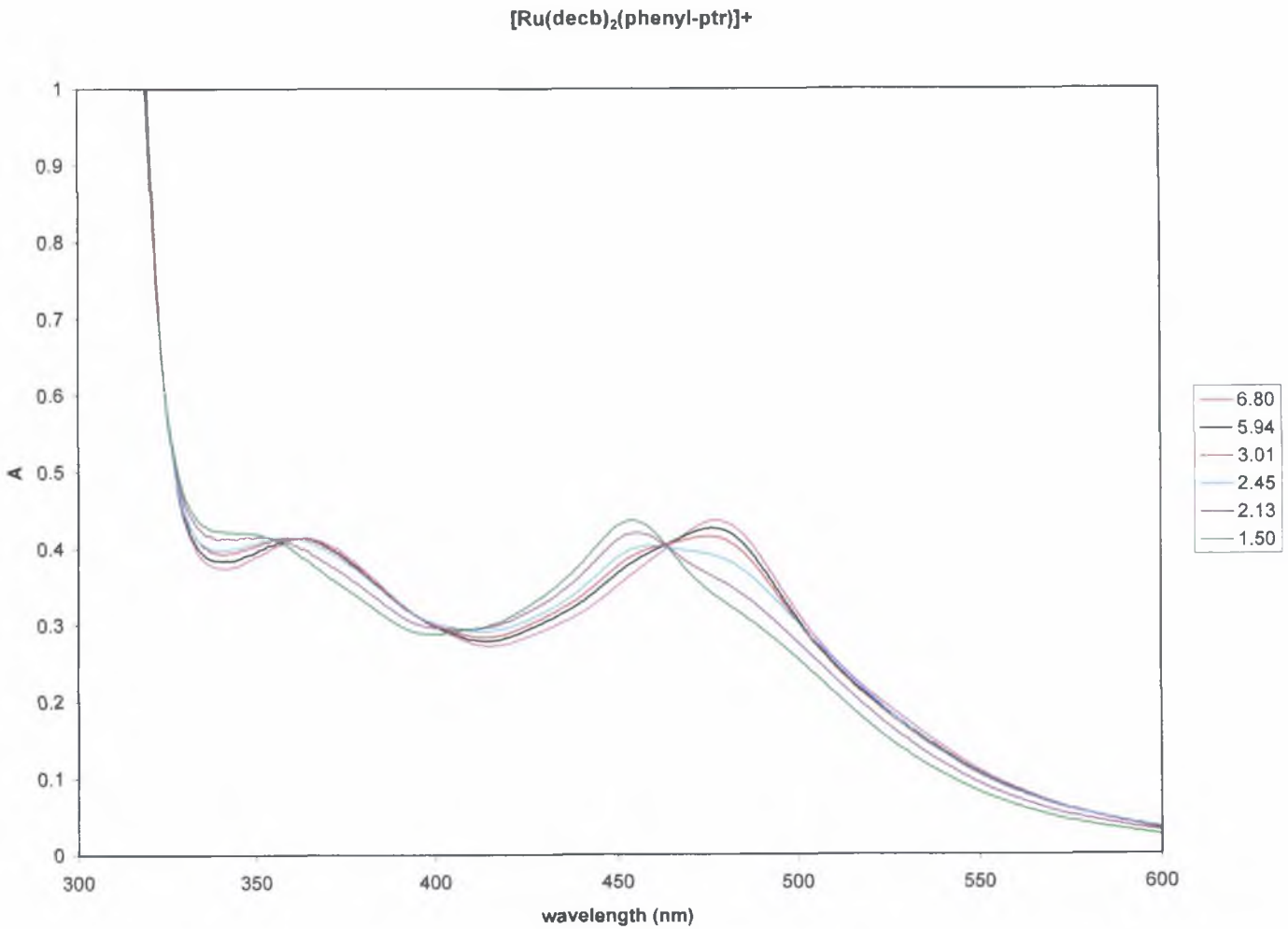

Figure 3.46, Dependence of [Ru(decb)$_2$(phenyl-ptr)]$^+$ (2.6.13) absorption spectrum on pH. From left to right pH = 1.50, 2.13, 2.45, 3.01, 5.94, 6.80 (0.1 M Phosphate buffer).

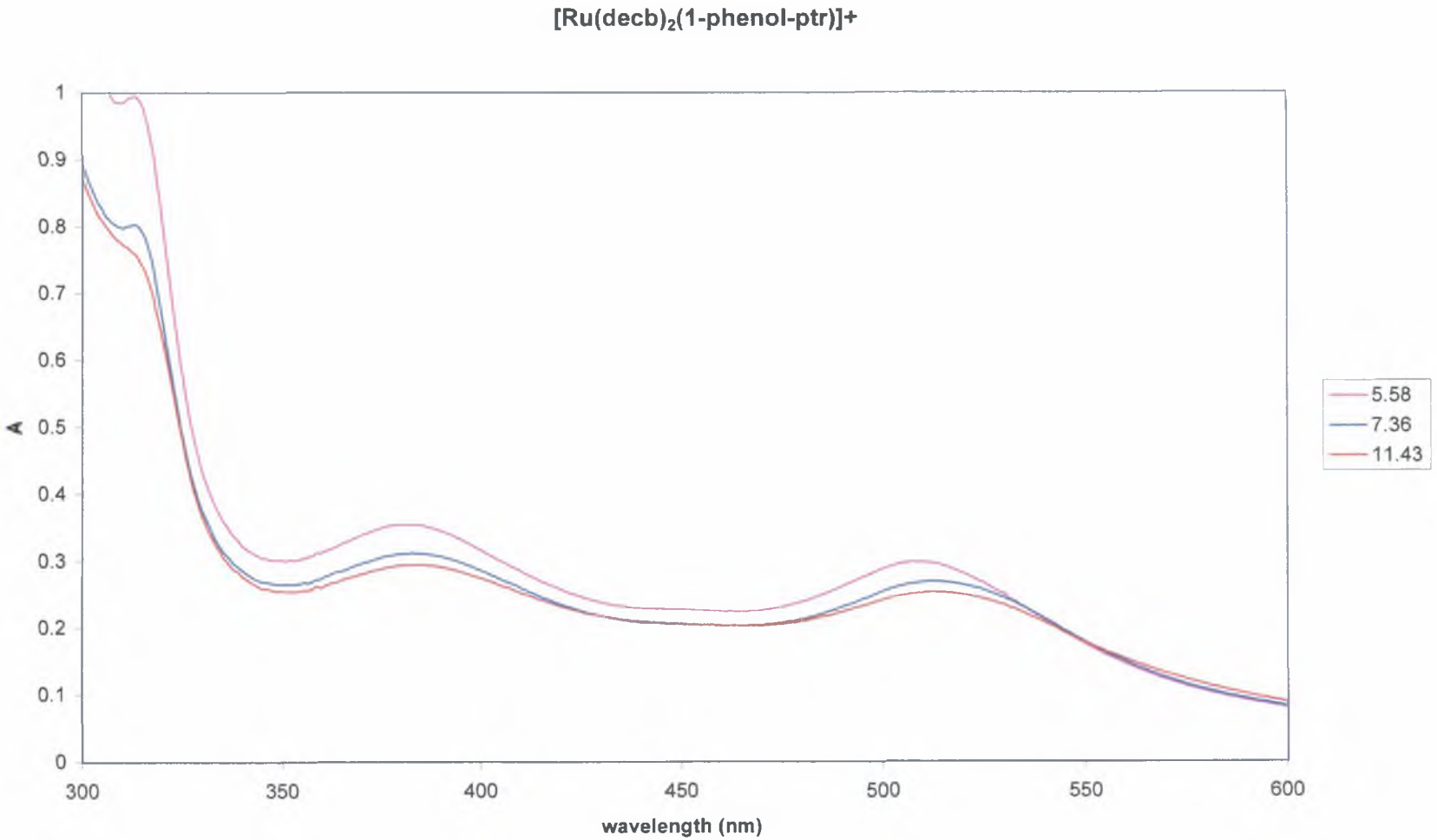

Figure 3.47, Dependence of [Ru(decb)$_2$(1-phenol-ptr)]$^+$ (2.6.12) absorption spectrum on pH. From top to bottom pH = 5.58, 7.36, 11.43 (0.1 M Phosphate Buffer).

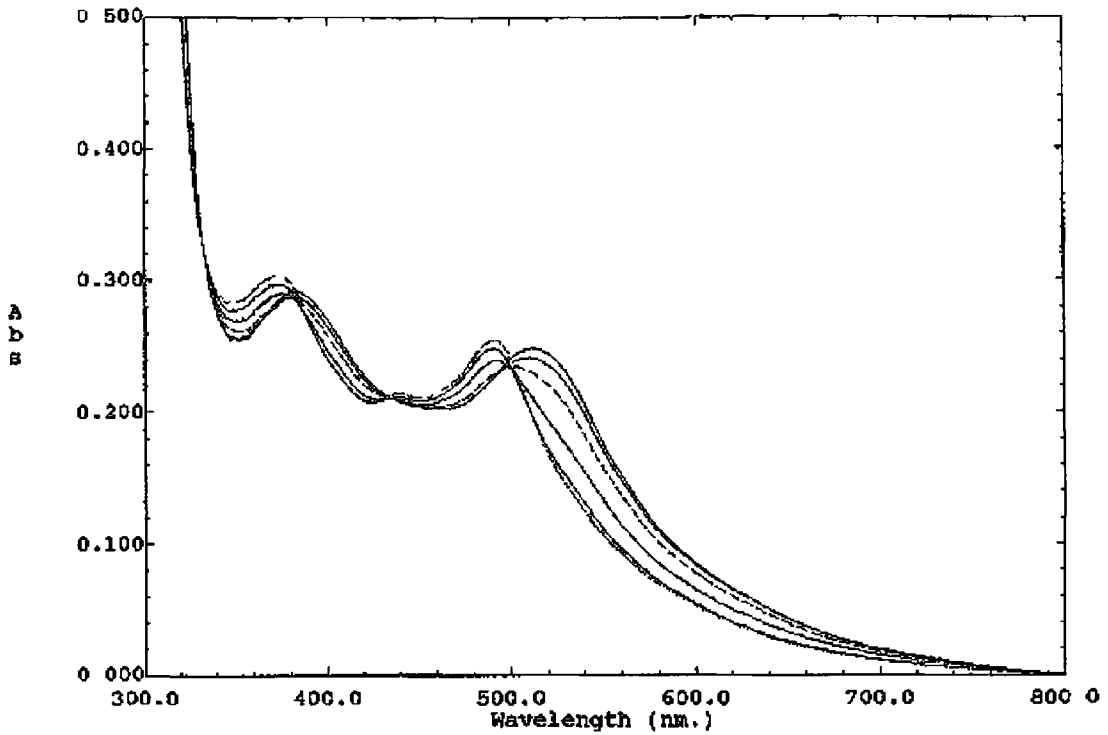

Figure 3 48, Dependence of [(Ru(decb)$_2$(1-phenol-ptr)]$^{+}$ (2 6 12) absorption spectrum on pH From left to right pH = 12 69, 12 41, 12 18, 11 89, 11 62, 11 13 (0 1 M Phosphate Buffer)

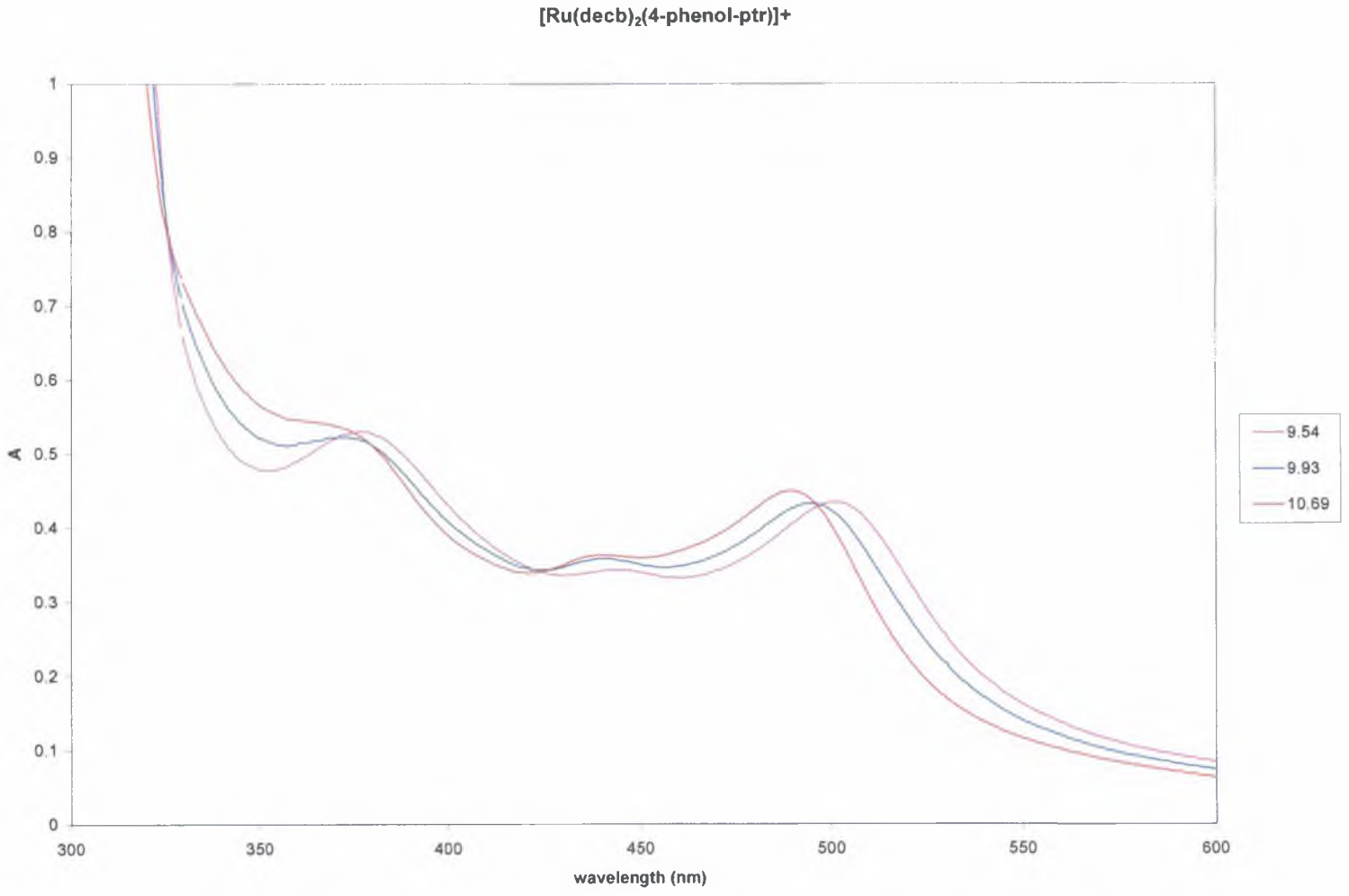

Figure 3.49, Dependence of [Ru(decb)$_2$(4-phenol-ptr)]$^+$ (2.6.11) absorption spectrum on pH. From left to right pH = 10.69, 9.93, 9.54 (0.1 M Phosphate Buffer).

For $[Ru(decb)_2(3\text{-Me-ptr})]^+$ **(2 6 14)** the absorption spectra is effected by the addition of the methyl substituent directly onto the azolate ring The CH_3- group has an electron donating effect and results in increased electron density on the triazole ligand This will in turn increase the σ-donor ability of the ptr ligand and will result in an increase in the electron density on the Ru(II) metal, which in turn will result in lower energy red-shifted transitions Because of the position of the methyl group on the triazolate ring the Ru(II) metal should bind to the triazolate ligand via the N^1 position only [8]

With $[Ru(decb)_2(3\text{-Me-ptr})]^+$ **(2 6 14)** protonation/deprotonation of the triazole ring occurs at low pH The 3-Me-ptr ligand is strongly σ-donating, increasing electron density on the Ru metal in the complex, thus as before deprotonation of the triazole moiety will lead to an increase in the σ-donating ability of the ligand A red shift of 28 nm was noted with the λ_{max} = 477 nm at pH = 2 08 and MLCT λ_{max} = 505 nm at pH = 6 77 **(Figure 3 50, Table3 4)**

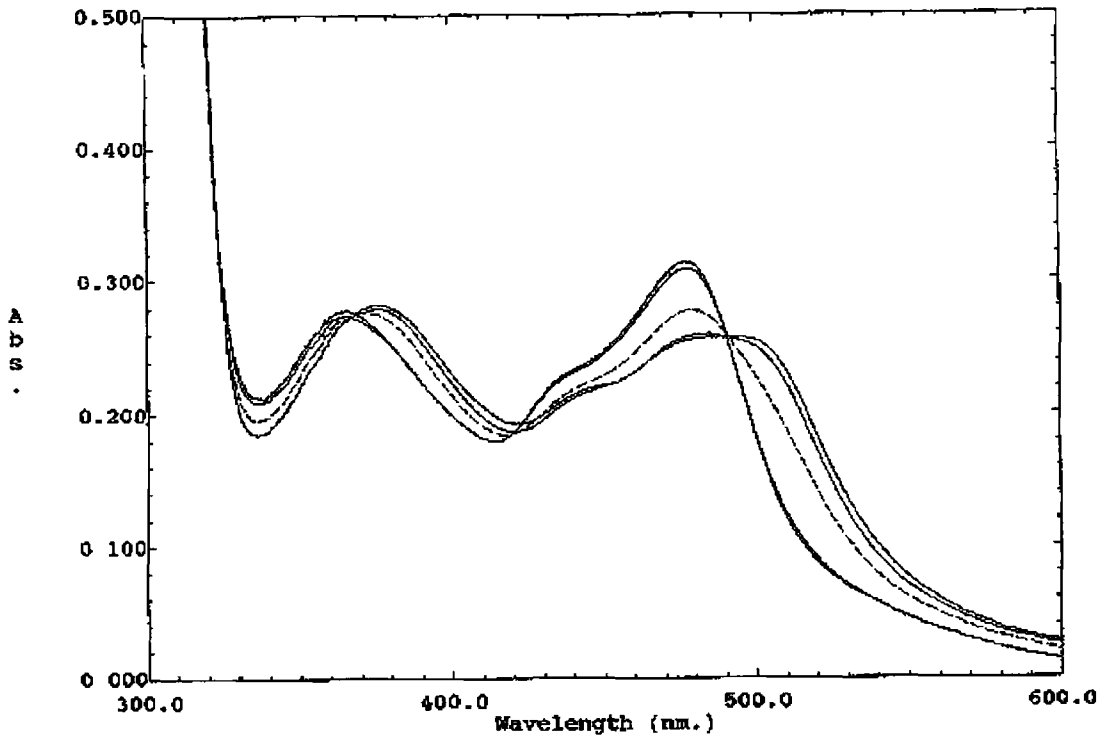

Figure 3 50, Dependence of [Ru(decb)$_2$(3-Me-ptr)]$^+$ (2 6 14) absorption spectrum on pH From left to right pH = 2 08, 2 34, 3 23, 4 75, 5 88, 6 77 (0 1 M Phosphate Buffer)

At higher pH no shift is seen initially in the absorption spectra between pH = 6 88 and pH = 10 35 **(Figure 3 51)** A solution of the complex was left overnight at pH = 6 88 with no change seen in the absorption spectrum which would indicate that the complex is stable at this pH

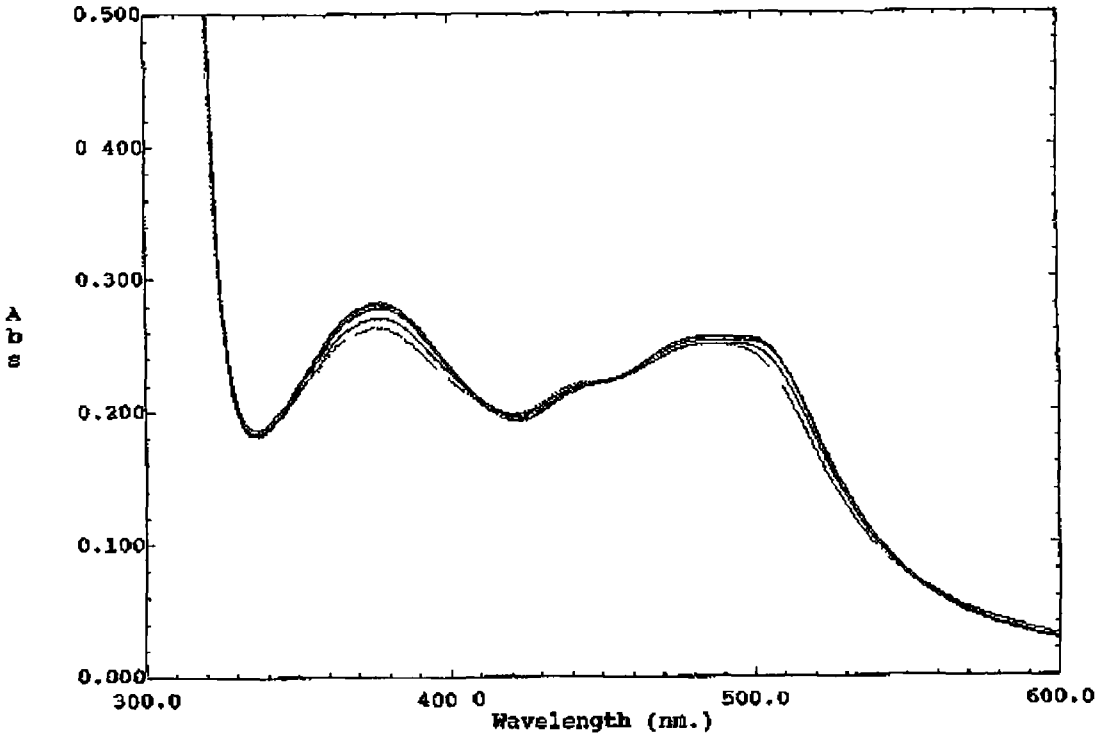

Figure 3 51, Dependence of [Ru(decb)$_2$(3-Me-ptr)]$^+$ (2 6 14) absorption spectrum on pH From top to bottom pH = 6 88, 7 26, 7 56, 8 28, 9 89, 10 35 (0 1 M Phosphate Buffer)

However, above pH = 10 and over time a blue shift of 29 nm is noted with λ_{max} = 505 nm at pH = 10 36 and λ_{max} = 476 nm at pH = 12 98 **(Figure 3 52, Table 3 4)**

As seen earlier this shift is probably due to the base hydrolysis of the diester groups

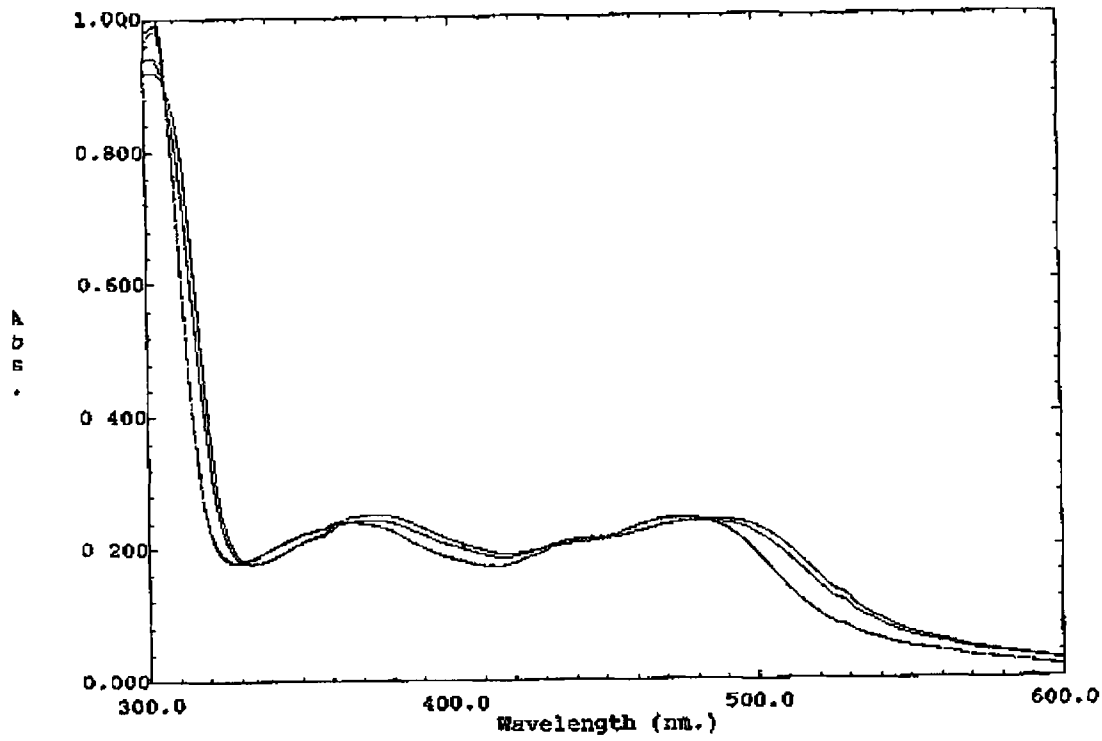

Figure 3 52, Dependence of [Ru(decb)$_2$(3-Me-ptr)]$^+$ (2 6 14) absorption spectrum on pH From left to right pH =11 84, 10 86, 10 36 (0 1 M Phosphate Buffer)

On lowering the pH for this newly formed species an absorption spectrum which may be due to the presence of a protonated dcbpy pyridyltriazole complex [Ru(dcbpy)$_2$(3-Me-ptr)]$^{2+}$ is seen with a λ_{max} = 474 nm at pH = 1 61 which is approximately 3 nm lower than the diester complex [Ru(decb)$_2$(3-Me-ptr)]$^+$ **(Table 3 4)** Both spectra should be similar at low pH, as the protonated diacid groups should have a similar electron withdrawing effect as the diethylester groups

Table 3 4

Visible λ_{max} (nm) values at different pH values for complexes 2 6 11, 2 6 12, 2 6 13, 2 6 14 ***(0 1 M Phosphate Buffer)***

	pH	λ_{max} (nm)
$[Ru(decb)_2(4\text{-phenol-ptr})]^+$ (2 6 11)		
	2 02	479 nm
	7 42	507 nm
	8 40	507 nm
	10 20	512 nm
Base hydrolysis	10 10	512 nm
	11 48	489 nm
$[Ru(decb)_2(1\text{-phenol-ptr})]^+$ (2 6 12)		
	0 71	479 nm
	6 58	504 nm
	5 58	507 nm
	11 43	512 nm
Base hydrolysis	11 43	512 nm
	12 41	491 nm
$[Ru(decb)_2(phenyl\text{-ptr})]^+$ (2 6 13)		
	1 50	454 nm
	6 80	478 nm
$[Ru(decb)_2(3\text{-Me-ptr})]^+$ (2 6 14)		
	2 08	477 nm
	6 77	505 nm
Base hydrolysis	10 36	505 nm
	12 98	476 nm

3 6 Luminescence

In mixed ligand complexes a number of electronic transitions may occur to each of the ligands, but rapid intramolecular transfer leads ultimately to a triplet MLCT state in which the excited state electron is localised on the lowest π*-acceptor orbital [34] In luminescent MLCT transition processes therefore, the excited state electron resides in the LUMO (Lowest Unoccupied Molecular Orbital) of the complex As mentioned earlier the ester and carboxy substituent groups lower the energy of the π* orbitals on the bpy ligands In the dcbpy/decb ruthenium(II) complexes with the ptr-based ligands emission is expected to originate from the decb/dcbpy ligands and not the ptr-based ligands with their high energy π* orbitals

The fluorescence spectrum for $[Ru(bpy)_2(dcbpy)]^{2+}$ **(2 6 8)** shows a blue shift of the emission maximum of 11 nm combined with a small increase in intensity from λ_{max} = 681 nm at pH = 1 23 to λ_{max} = 670 nm at pH = 2 84 **(Figure 3 53, Table 3 6)** Between pH 2 84 and 12 92 a blue shift of 25 nm is seen with the λ_{max} = 645 nm at pH = 12 92 and a three fold increase in the emission intensity of the deprotonated complex in comparison to the protonated **(Figure 3 53, Table 3 6)** The blue shift in the emission spectra may be as a result of the increased π* orbital energy levels on deprotonation increasing the MLCT energy gap with a subsequent increase in emission energy and intensity

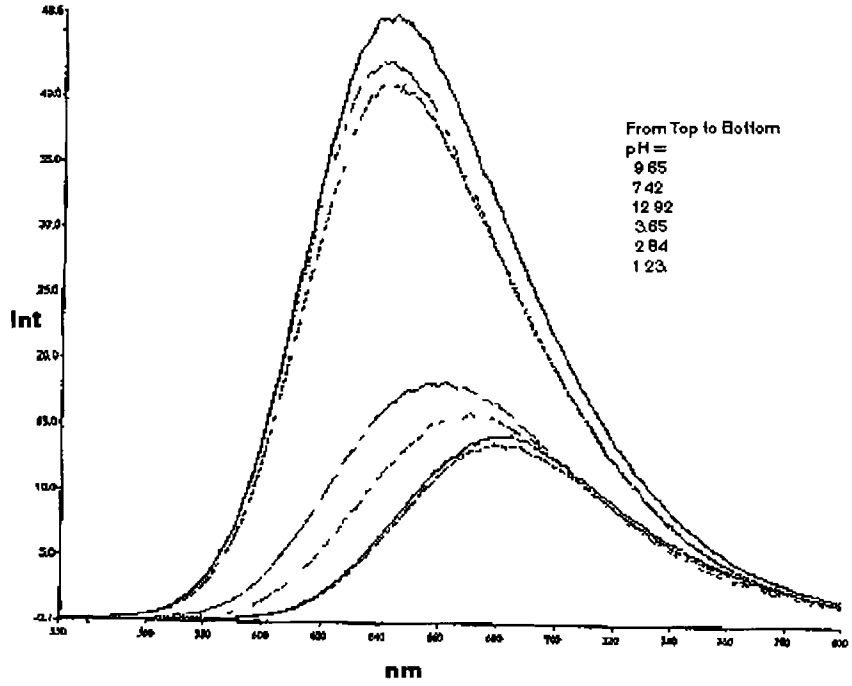

Figure 3 53, Dependence of [Ru(bpy)$_2$(dcbpy)]$^{2+}$ (2 6 8) fluorescence spectrum on pH From top to bottom pH = 9 65, 7 42, 12 92, 3 65, 2 84, 1 23 (Britton-Robinson buffer)

For the deuteriated complex [Ru(^{2}H$_8$-bpy)$_2$(dcbpy)]$^{2+}$ **(2 6 15, Figure 3 54, Table 3 6)** at pH = 1 00 the λ_{max} = 676 nm and 678 nm at pH = 2 3 This emission shift is probably due to the presence of the mono-protonated species at pH = 2 3 The protonated [Ru(^{2}H$_8$-bpy)$_2$(H$_2$-dcbpy)]$^{2+}$ indicated a blue shifted spectrum with λ_{max} = 643 nm at pH = 9 38 and as in the undeuteriated complex **(2 6 8)** an increase in the emission intensity was seen in comparison to the protonated complex Therefore the deuteriated complexes **(2 6 15)** indicated a 33nm shift on deprotonation in comparison to a 36 nm shift for the undeuteriated complex **(2 6 8)**

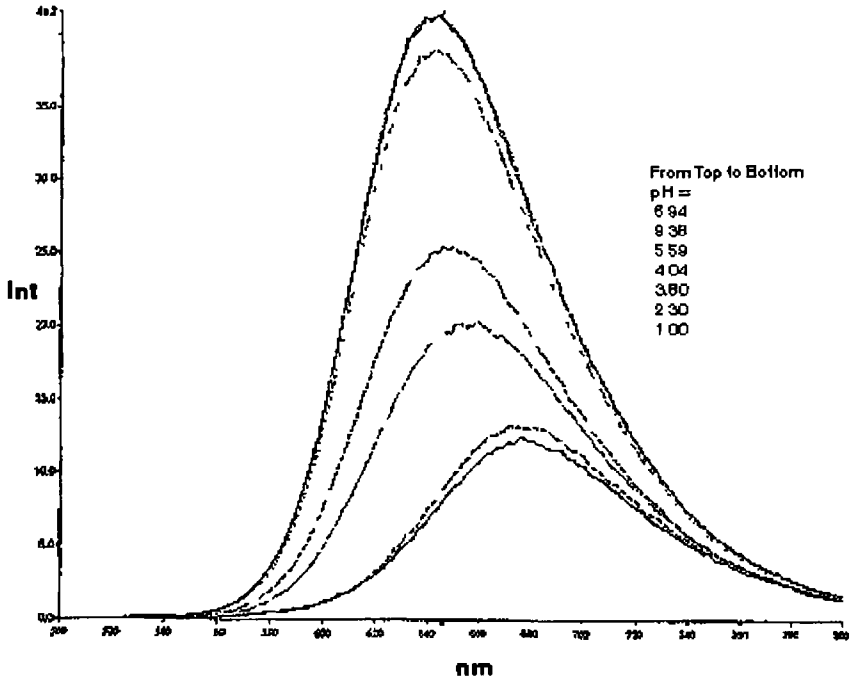

Figure 3 54, Dependence of [Ru($^2H_8$-bpy)$_2$(dcbpy)] fluorescence spectrum on pH From Top to bottom pH = 6 94, 9 38, 5 59, 4 04, 3 80, 2 30, 1 00 (Britton-Robinson buffer)

A difference in the excited state lifetimes for [Ru($^2H_8$-bpy)$_2$(dcbpy)] (**2 6 15**) and the [Ru(bpy)$_2$(dcbpy)] (**2 6.8**) was noted , see **Table 3 5** and **Appendix I**

Table 3 5
Luminescent Lifetimes were measured in deaerated acetonitrile + CF_3COOH/ Et_2NH at room temperature *The lifetime errors are estimated to be less than 10 %*

[Ru($^2H_8$-bpy)$_2$(dcbpy)] & [Ru(bpy)$_2$(dcbpy)] in protonated and unprotonated form	Lifetimes of complexes , τ (ns)
H COOH	588 ns
d COOH	673 ns
H COO^-	385 ns
d COO^-	564 ns

The difference in the laser lifetime results indicates that the emitting state is located on the dcbpy ligand with a lifetime change noted in both deuteriated and undeuteriated complexes on protonation of the complexes The longer lifetime values for the

deuteriated species is due to a slower relaxation process that takes place with the C-D relaxation in comparison to C-H relaxation According to Siebrand's theory of non-radiative transition [35, 36], high energy, anharmonic C-H stretching vibrations are important promotional modes in non-radiative decay This implies that, as found experimentally, excited-state lifetimes should increase upon deuteriation (Table 3 5 & Appendix I)

For both $[Ru(decb)_2(1\text{-phenol-ptr})]^+$ **(2 6 12, Table 3 6)** and $[Ru(decb)_2(4\text{-phenol-ptr})]^+$ **(2 6 11, Table 3 6)** a red shift is seen on going from the protonated with a λ_{max} = 661 nm for $[Ru(decb)_2(1\text{-phenol-ptr})]^+$ **(Figure 3 56)** and 669 nm for $[Ru(decb)_2(4\text{-phenol-ptr})]^+$ **(Figure 3 58)** to the unprotonated respective values of 743 nm **(Figure 3 55)** and 742 nm **(Figure 3 57)** These shifts in the emission maxima are most likely due to both the deprotonation of the azole ring and the -OH group of the phenol ring The change in the emission values is for the same reason as the absorption spectra change On protonation of the ptr based ligand it becomes a better π-acceptor and a weaker σ-donor compared to the deprotonated form As a consequence the t_{2g} orbitals are stabilised and the t_{2g} - ^{3}MLCT energy gap is increased resulting in higher energy emissions

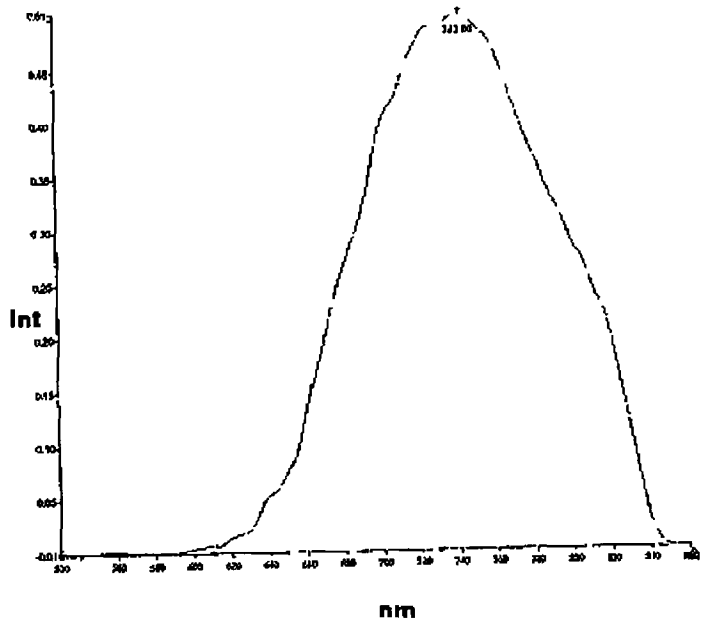

Figure 3 55, Fluorescence spectrum of $[Ru(decb)_2(1\text{-phenol-ptr})]^+$ (2 6 12) + NH_4OH (0 1 M Phosphate buffer)

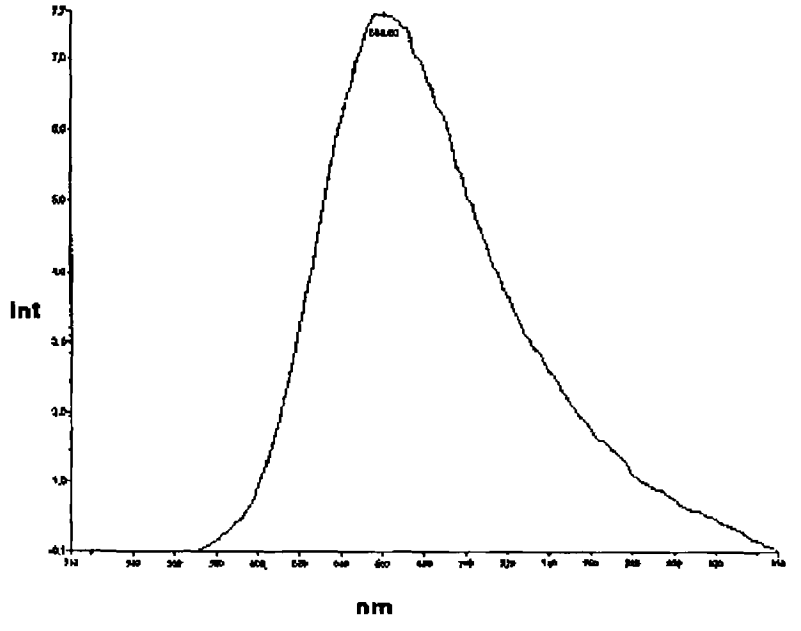

Figure 3 56, Fluorescence spectrum of $[Ru(decb)_2(1\text{-phenol-ptr})]^{2+}$ (2 6 12) + HCl (0 1 M Phosphate buffer)

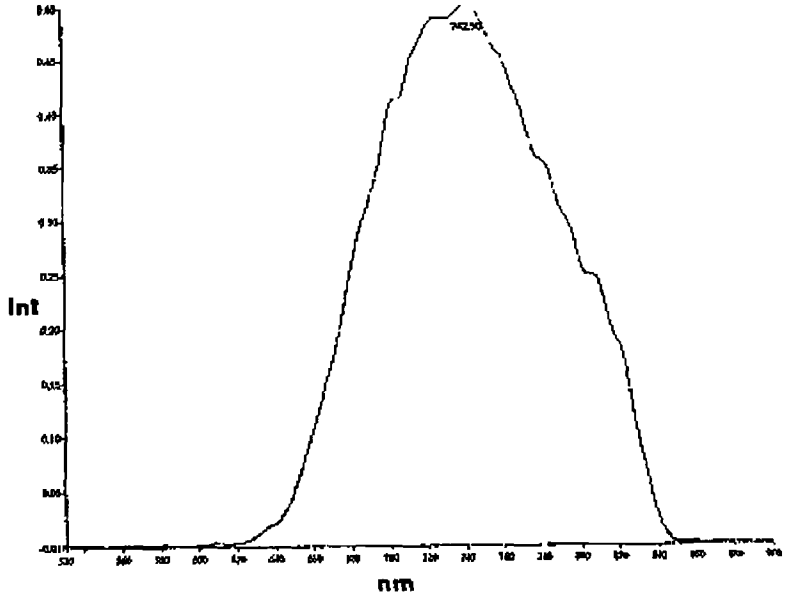

Figure 3 57, Fluorescence spectrum of [Ru(decb)$_2$(4-phenol-ptr)]$^+$ (2 6 11) + NH_4OH (0 1 M Phosphate buffer)

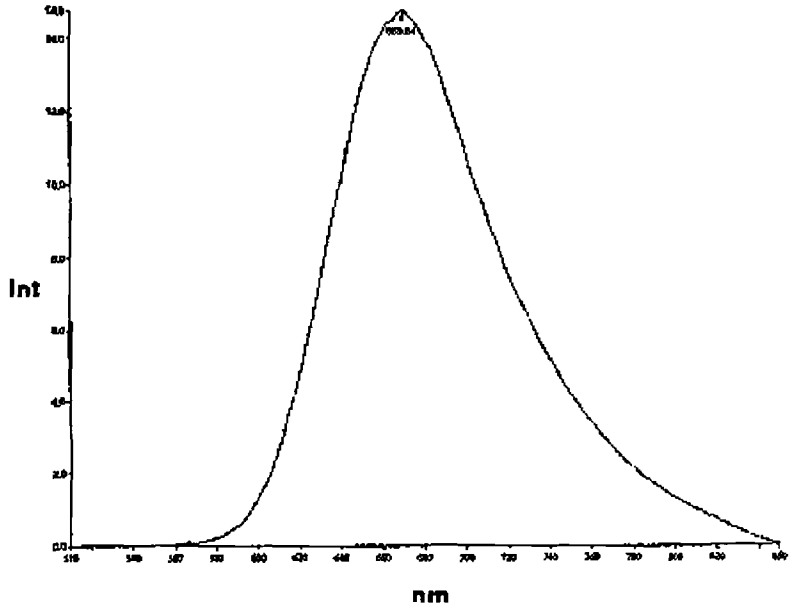

Figure 3 58, Fluorescence spectrum of [Ru(decb)$_2$(4-phenol-ptr)]$^{2+}$ (2 6 11) + HCl (0.1 M Phosphate buffer).

For the $[Ru(decb)_2(3\text{-}Me\text{-}ptr)]^+$ **(2 6 14, Figure 3 59, Table 3 6)** complex between pH=1 05 and 6 88 the λ_{max} = 635 nm with a decrease in intensity seen as the pH is increased and no change in the position of the λ_{max} value i e the energy at which the maximum emission occurs From pH 6 88 to 12 98 a 10 nm blue shift is seen in the spectrum with a λ_{max} = 625 nm at pH = 13 0 and a decrease in intensity also seen This blue shift may be due to the formation of unprotonated carboxy groups through base hydrolysis of the ester groups resulting in π^* levels at higher energy and a blue shift in the spectrum

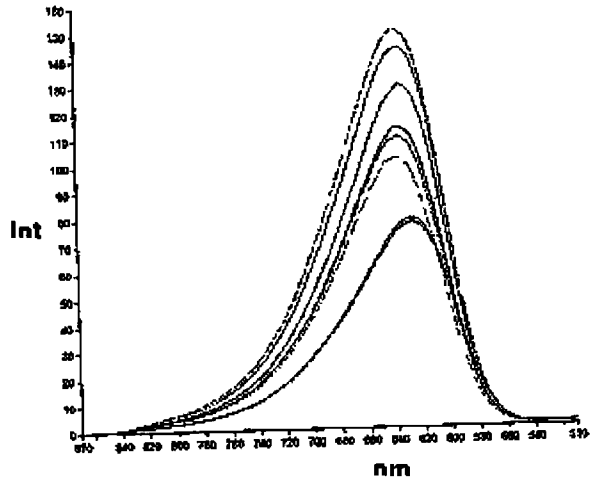

Figure 3 59, Dependence of $[Ru(decb)_2(3\text{-}Me\text{-}ptr)]^+$ (2 6 14) fluorescence spectrum on pH From top to bottom pH = 1 05, 1 34, 1 75, 2 66, 3 23, 6 88, 12 11, 12 13, 12 98 (0 1 M Phosphate buffer)

$[Ru(decb)_2(phenyl\text{-}ptr)]^+$ (2 6 13) did not indicate a shift in emission maxima at low pH with λ_{max} = 635 nm **(Table 3 6)** At high pH a blue shift of 5 nm to 630 nm was seen **(Table 3 6)** which may also be as a result of base hydrolysis of the ester groups as mentioned above

Table 3 6
Fluorescent emission values at different pH dcbpy complexes in Britton-Robinson buffer, decb complexes in 0 1 M Phosphate buffer pH adjusted by NH_4OH & HCl

	pH	**λ_{max}**
$[Ru(bpy)_2(dcbpy)]$ (2 6 8)	1 23	681 nm
	2 84	670 nm
	12 92	645 nm
$[Ru(^2H_8\text{-}bpy)_2(dcbpy)]$ (2 6 15)	1 00	676 nm
	2 30	678 nm
	9 38	643 nm
$[Ru(decb)_2(1\text{-}phenol\text{-}ptr)]^+$ (2 6 12)	Low pH conditions	661 nm
	High pH conditions	743 nm
$[Ru(decb)_2(4\text{-}phenol\text{-}ptr)]^+$ (2 6 11)	Low pH conditions	669 nm
	High pH conditions	742 nm
$[Ru(decb)_2(3\text{-}Me\text{-}ptr)]^+$ (2 6 14)	Low pH conditions	635 nm
Base hydrolysis	Very High pH conditions	625 nm
$[Ru(decb)_2(phenyl\text{-}ptr)]^+$ (2 6 13)	Low pH conditions	635 nm
Base hydrolysis	Very High pH conditions	630 nm

3 7 Elemental Analysis

Although the complexes examined by CHN **(2.6 11, 2 6 12, 2 6 13, 2 6 14)** were pure by HPLC and ^{1}H-NMR the CHN results did not always indicate the required values

Elemental analysis of the complexes should indicate a charge of 1^+ on the ester complexes analysed (2 6 11, 2 6 12, 2 6 13, 2 6 14) suggesting that the ligands 1-phenol-ptr, 4-phenol-ptr, 3-Me-ptr and phenyl-ptr have lost a proton and therefore there will be only one PF_6 group present However as previously reported by Hage et al [8] complexes formed by coordination of ruthenium with pyridyl triazole (ptr) containing ligands are very pH sensitive as the triazole can be in a protonated or deprotonated form On recrystallisation of the ptr based complexes Hage would have added a drop of basic solution in order to deprotonate the complex In recent studies [37] *ruthenium ptr type* complexes were not made basic on recrystallisation and the CHN analysis of the complexes showed that the compounds were obtained with different amounts of counter ions (PF_6) However in the case of recrystallisation of the esters the solutions cannot be made basic as this could lead to hydrolysis of the ester groups To accurately determine the number of counter ions present in the complexes a crystal structure analysis could be carried out

4 0 Concluding Remarks

The work carried out showed that the synthesis of pure ruthenium bis dicarboxybipyridine complexes proved difficult and on the whole unsuccessful As a result of the synthesis and purification problems associated with the dcbpy containing complexes the ester (decb) substituted complexes were synthesised and it was hoped that through hydrolysis of the pure ester ruthenium complexes that the dcbpy complexes could be obtained

However the ester complexes also proved difficult to synthesise and purify and hydrolysis did not lead to pure dcbpy complexes

Future work could involve the use of different types of column chromatography that were not used in the work in an attempt to purify the complexes such as size exclusion chromatography

Future work should also involve the comparison of the diacid and the diester complexes with the same spectator ligands synthesised either from the diacid dichloride or indirectly from base hydrolysis of the esters to allow for direct comparison between the two groups of complexes

The use of different substituent groups on the chromophore ligand is also an area of interest in the development of solar cells The disadvantages in the use of the dcbpy ligand for adsorbing onto semiconductor surfaces is that, as shown, the complex is pH dependant and will readily desorb from the surface at pH values greater than approximately pH = 5 The use of e g phosphonic groups ($-PO_3H$) which strongly adsorb onto TiO_2 films, provide sufficient coupling with the oxide to achieve light-induced charge separation, do not desorb in water and are stable over a large pH range ($0 \rightarrow 9$) is one area which is currently being researched into [38]

4 1 References

REFERENCE

[1] G Sprintschnik, H W Sprintschnik, P P Kirsch, D G Whitten, J Am Chem Soc 99, 1977, 4947

[2] P E Rosevear, W H F Sasse, J Heterocyclic Chem , 8, 1971, 483

[3] L D Ciana, W J Dressick, A von Zelewsky, J Heterocyclic Chem 27, 1990, 163

[4] A Launikonis, P A Lay, A W H Mau, A M Sargeson, W H F Sasse, Aust J Chem , 39, 1986, 1053

[5] F H Case, J Am Chem Soc , 68, 1946, 2574

[6] A R Oki, R J Morgen, Synthetic Communications, 25(24), 1995, 4093

[7] G Maerker, F H Case, J Am Chem Soc 80, 1958, 2745

[8] R Hage, Ph D Thesis, Leiden University, The Netherlands, 1990

[9] M K Nazeeruddin, A Kay, I Rodicio, R Humphry-Baker, E Muller, P Liska, N Vlachopoulos, M Gratzel, J Am Chem Soc , 115, 1993, 6382

[10] B P Sullivan, D J Salmon, T J Meyer, Inorg Chem ,17, 1978, 3334

[11] P Liska, N Vlachopoulos, M K Nazeerudin, P Comte, M Gratzel, J Am Chem Soc , 110, 1988, 3686

[12] T Shimidzu, T Iyoda, K Izaki, J Phys Chem , 89, 1985, 642

[13] G L Gaines, P E Behnken, S J Valenty, J Am Chem Soc , 100, 1978, 6549

[14] B E Buchanan, R Wang, J G Vos, R Hage, J G Haasnoot, J Reedijk, Inorg Chem , 29, 1990, 3263

[15] B Buchanan, E McGovern, P Harkin, J G Vos, Inorg Chim Acta , 154, 1988,1

[16] T E Keyes, F Weldon, E Mueller, P Pechy, M Gratzel, J G Vos, J Chem Soc Dalton Trans ,1995, 2705

[17] R Hage, J Haasnoot, D Stufkens, T Snoeck, J G Vos, J Reedijk, Inorg Chem , 28, 1989, 1413

[18] B Buchanan, J G Vos, M Kaneko, W van der Putten, J Kelly, R Hage, R de Graaf, R Prins, J Haasnoot, J Reedijk, J Che

[19] B Buchanan, H Hughes, J van Diemen, R Hage, J Haasnoot, J Reedijk, J G Vos, J Chem Soc , Chem Comm , 1991, 300

[20] R Wang, J G Vos, R Schmehl, R Hage, J Am Chem Soc , 114, 1992, 1964

[21] W F Wacholtz, R A Auerbach, R H Schmehl, Inorg Chem , 26, 1987, 2889

[22] R Hage, A H J Dijkhuis, J G Haasnoot, R Prins, J Reedijk, B E Buchanan, J G Vos, Inorg Chem , 27, 1988, 2185

[23] R Hage, R Prins, J G Haasnoot, J G Vos, J Chem Soc , Dalton Trans , 1987, 1389

[24] H A Nieuwenhuis, J G Haasnoot, R Hage, J Reedijk, T L Snoeck, D J Stufkens, J G Vos, Inorg Chem , 30, 1991, 48

[25] L de Cola, F Barigelletti, V Balzani, R Hage, J G Haasnoot, J Reedijk, J G Vos, Chem Phys Lett , 178, 1991, 491

[26] F Barigelletti, L de Cola, V Balzani, R Hage, J G Haasnoot, J Reedijk, J G Vos, Inorg Chem , 28, 1989, 4344

[27] O Kohle, S Ruile, M Gratzel, Inorg Chem 35, 1996, 4779

[28] P J Steel, F La House, D Lener, C Marzin, Inorg Chem , 22, 1983, 1488

[29] G M Bryant, J E Ferguson, Aust J Chem , 24, 1971, 441

[30] E C Constable, J Lewis, Inorg Chim Acta, 70, 1983, 251

[31] P Belser, A von Zelewsky, Helv Chim Acta, 63, 1980, 1675

[32] P Belser, A von Zelewsky, Helv Chim Acta, 57, 1971, 239

[33] J Ferguson, A Mau, W Sasse, Chem Phys Let , 68, 1979, 21

[34] R S Lumpkin, E M Kober, L Worl, Z Murtaza, T J Meyer, J Phys Chem , 94, 1990, 239

[35] W Siebrand, J Chem Phys , 46, 1967, 440

[36] W Siebrand, J Chem Phys , 55, 1971, 5843

[37] C O'Connor, Ph D Thesis, Dublin City University, Ireland, 1999

[38] P Pechy, F P Rotzinger, M K Nazeeruddin, O Kohle, S M Zakeeruddin, R Humphry-Baker, M Gratzel, J Chem Soc , Chem Commun , 1995, 65

[39] A C Lees, C J Kleverlaan, C A Bignozzi, J G Vos, Inorg Chem , 40, 2001, 5343

Appendix I

Laser Lifetime Results

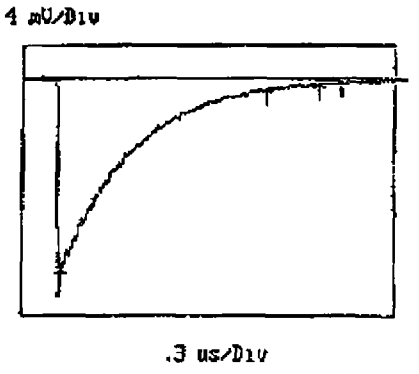

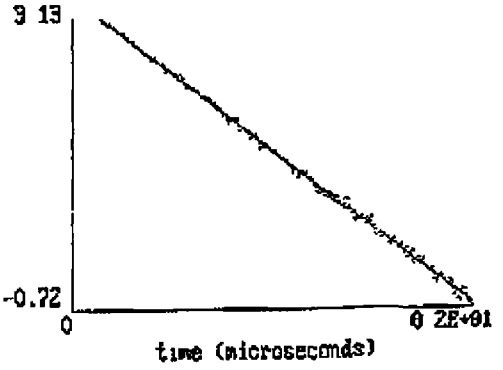

Figure (1)

Emission lifetime of protonated $[Ru(bpy)_2(dcbpy)]^{2+}$ (deaerated in acetonitrile + CF_3COOH)

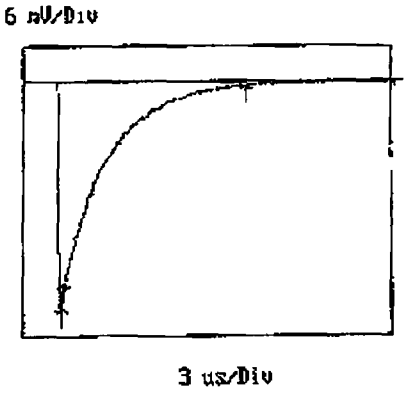

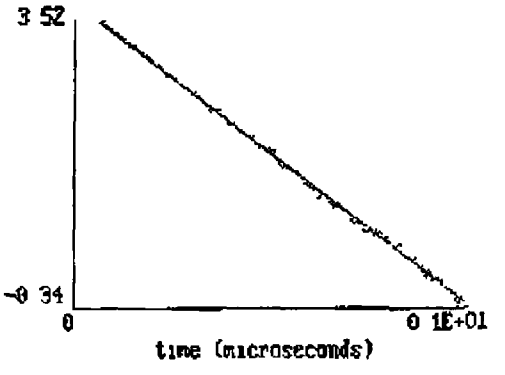

Figure (11)

Emission lifetime of unprotonated [Ru(bpy)$_2$(dcbpy)] (deaerated in acetonitrile + Et_2NH)

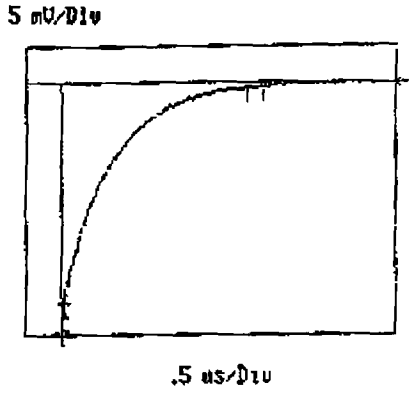

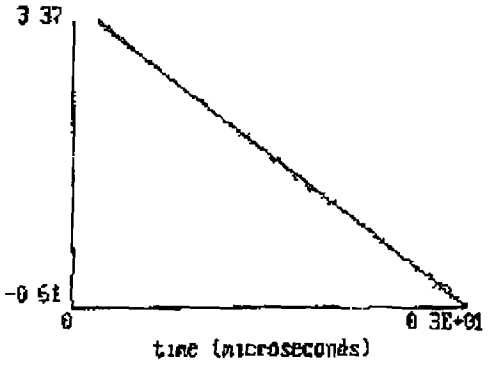

Figure (iii)

Emission lifetime of protonated $[Ru(^2H_8\text{-bpy})_2(dcbpy)]^{2+}$ (deaerated in acetonitrile + CF_3COOH)

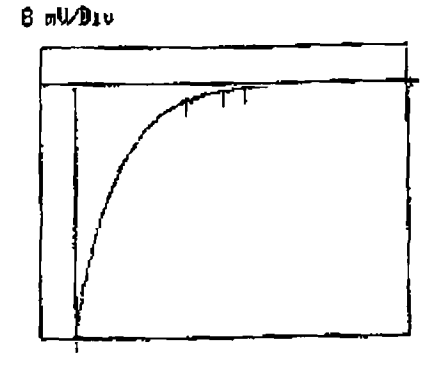

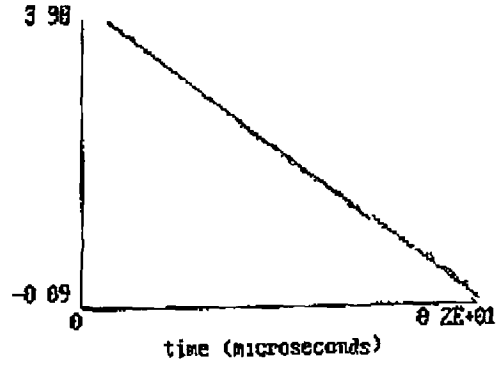

Figure (iv)

Emission lifetime of unprotonated [Ru($^2H_8$-bpy)$_2$(dcbpy)] (deaerated in acetonitrile + Et_2NH)